Durham E-Theses

Aspects of the cosmology of right-handed sneutrinos without lepton-number violation

Pagé, Véronique

Aspects of the Cosmology of Right-Handed Sneutrinos without Lepton-Number Violation

Véronique Pagé

A Thesis presented for the degree of

Doctor of Philosophy

Center for Particle Theory
Department of Mathematical Sciences
University of Durham
England

February 2008

1 2 JUN 2008

Aspects of the Cosmology of Right-Handed Sneutrinos without Lepton-Number Violation

Véronique Page

Submitted for the degree of Doctor of Philosophy

February 2008

Abstract

In this work we add a Dirac right-handed neutrino superfield to the Minimal Supersymmetric Standard Model (MSSM). We discuss the interactions of the right-handed (RH) sneutrino and its mixing with its left-handed counterpart. We study the possibility of this RH sneutrino to be the lightest supersymmetric particle (LSP). We obtain that this dark matter candidate is a non-thermal relic, and generally has a small relic density. This we argue makes it an interesting candidate for addressing the Ω_{DM}/Ω_b problem. We then discuss a lepton-number conserving leptogenesis scenario, in which an Affleck-Dine inspired mechanism generates a left-right asymmetry in the sneutrino sector. The left-handed part of this asymmetry eventually becomes the observed baryon density. This suggested leptogenesis is also a matter-genesis mechanism, as the right-handed part of the left-right asymmetry becomes the observed dark matter density.

Declaration

The work in this thesis is based on research carried out at the Center for Particle Theory, Department of Mathematical Sciences, Durham University. No part of this thesis has been submitted elsewhere for any other degree or qualification. This thesis contains solely my own work unless referenced otherwise in the text.

The results presented in this thesis have been published in [1] and in [2]. [1] has been written by both my supervisor Dr Steven Abel and I, and all calculations presented here and related to this paper have been made by myself under the supervision of Dr Abel. [2] has been written by myself, and all calculations presented here and related to this paper have been made by myself under the supervision of Dr Abel.

Acknowledgements

I would like to thank my supervisor Dr Steven Abel for his help throughout my PhD. I am very grateful for the many opportunities he has given me to travel through Europe for conferences and workshops, and for the freedom he has given me to develop my own ideas.

Also I would like to thank the office staff of the Maths Department for their patience in the many instances that I have needed their help, or in the many instances that I have not done as told!

Thanks as well to the members of the theory group at Université Libre de Bruxelles for welcoming me for these few weeks; thanks especially to Michel Tytgat and Jean-Marie Frère for their help.

I also would like to thank my co-PhD students Bina, James, John, Simon, Ryan for making this adventure much more fun and for helping me settle in this foreign country .

Thanks are also very much due to all my friends in my 'other home', Liz, Andreas, Dimi, Anne-Christine, Andrew, Paul, Rob, Alex. I am very grateful I had the chance of meeting you.

As the end of my PhD is also the end of my time in academia and physics, I would like to thank Mr Louis Lessard and Viktor Zacek of Université de Montréal for introducing me to dark matter almost ten years ago, and Mr David London, also of UdeM, for being such an example of passion for physics.

I also have to thank my partner Jean-François Mercure for a very large number of reasons, but especially for patiently fixing my laptop on the very day of the submission of this thesis.

Contents

List of Figures

List of Tables

Chapter 1

Introduction

The study of the interface of particle physics and cosmology has obtained a growing interest, and it is certainly now an exciting time for this field. Indeed the advent of precision cosmology experiments such as the Wilkinson Microwave Anisotropy Probe and the completion of the Large Hadron Collider at CERN mean that some of the most popular particle models related to dark matter, structure formation, inflation or the baryon asymmetry will be put under test. Certainly it is already well known that much can be learned by studying the cosmological aspects of a certain particle physics model, and conversely.

The question of the neutrino mass is one such subject where cosmology can shed an interesting light. Indeed this work is concerned with showing that the Dirac neutrino model, often seen as an underdog to its infamous counterpart, the see-saw or Majorana model, can have specific and interesting cosmological properties.

Leptogenesis, which aims at solving the question of the overwhelming abundance of baryons compared to anti-baryons in the Universe, necessitates the presence of a Majorana mass for the neutrino. This is sometimes taken as a strong argument against Dirac neutrinos. It is however very much a possibility to have leptogenesis without lepton number violation, and in this work we present a supersymmetry-specific model of leptogenesis, reminiscent of the Affleck-Dine mechanism, that also make use of the smallness of the Dirac neutrino Yukawa coupling. These results have been published in [1].

Moreover we wish to study the possible contribution of the Dirac neutrino model

to the question of dark matter. We will show that the superpartner of the Dirac right-handed neutrino, the right-handed sneutrino, could be a dark matter candidate if the possibility of mattergenesis is explored. Mattergenesis scenarios go a step further from leptogenesis scenarios by trying to produce both types of matter, baryonic and dark, through a common mechanism. We will observe that the leptogenesis scenario of [1] can indeed be such a mattergenesis scenario, with the right-handed sneutrino as dark matter. These results have been published in [2].

The outline of this work is as follow: we will first give an overview of the modern Standard Cosmological Model, introducing the basic ideas of an expanding Universe and particle dynamics within such a Universe. We will discuss recent cosmological observations from the WMAP collaboration related to the content of the Universe. We will briefly introduce the concepts of inflation and big-bang nucleosynthesis, before turning to discuss the baryon asymmetry of the Universe and the necessity for a baryogenesis (or leptogenesis) mechanism. We will then discuss dark matter and its properties, and explore the Ω_{DM}/Ω_b puzzle and the possibility of mattergenesis.

The following chapter is concerned with basics of supersymmetry, and the Minimal Supersymmetric Standard Model (MSSM), which is one of the building blocks of this work. We will introduce the MSSM and the necessary soft SUSY-breaking sector. We will then introduce the dark matter candidate of choice within the MSSM, the lightest supersymmetric particle, LSP, and will discuss again the possibility of mattergenesis within supersymmetry. We will then turn to discussing massive neutrinos, as this is again an important aspect of this work. We will mention the evidence for massive neutrinos, and explain why both the possibilities of Majorana and Dirac neutrinos are still open. We will then discuss some aspects of Dirac neutrinos mass models.

We begin the presentation of our results in chapter 5, where we introduce the lepton-number conserving model we are using to add Dirac (s)neutrinos to the MSSM. There we introduce the right-handed sneutrino, the superpartner of the Dirac right-handed neutrino, and discuss its interaction by studying its Lagrangian. We consider the possibility for this sneutrino to be the LSP, and study its potential for direct detection via the already existing dark matter detection experiments.

The following chapter discusses the behaviour of the right-handed sneutrino in the early Universe. We observe it is a non-thermal candidate, and then calculate its relic density, considering it is the LSP. Obtaining this to be generally small, we discuss the possibility of this particle being a dark matter candidate within matter-genesis models. Chapter 7 then presents our suggested leptogenesis model in the absence of lepton-number violation. We first introduce the idea of neutrinogenesis, then discuss how an Affleck-Dine-inspired mechanism can produce the necessary asymmetry between left- and right-handed sneutrinos. We study the dynamics of the Affleck-Dine fields, and obtain the size of the generated baryon asymmetry. We then discuss how this neutrinogenesis mechanism can be viewed as a mattergenesis mechanism in the light of the results obtained in the previous chapters.

Finally we conclude with an overview and a discussion of this work, and mention some potential additional work related to it.

Chapter 2

Modern Cosmology

2.1 Standard Cosmology and ΛCDM Model

Over the recent years a Standard Cosmological Model has emerged, and it is the
model we consider here as a basis for the rest of our work. Various works detail the
basics of modern cosmology; here we follow mainly the treatments available in [4–7]
and our notation is consistent with [4].

2.1.1 The expanding Universe

The Universe is described by Einstein's equation, which relates the geometry of the
Universe to its content. Under the assumption of homogeneity and isotropy, the
geometry of the Universe is best described by the Robertson-Walker metric,

$$\mathrm{d}s^2 = -\mathrm{d}t^2 + a^2(t) \left[\frac{\mathrm{d}r^2}{1 - kr^2} + r^2 \left(\mathrm{d}\theta^2 + \sin^2\theta \mathrm{d}\phi^2 \right) \right] \tag{2.1}$$

where $a(t)$ is the scale factor and k is the curvature factor. Using the Robertson-
Walker metric to solve the Einstein equation one obtains the Friedmann equation

$$\left(\frac{\dot{a}}{a} \right)^2 = \frac{8\pi G}{3} \rho - ka^{-2} , \tag{2.2}$$

G being the gravitational constant and ρ the total energy density of the Universe.
The Hubble constant, describing the expansion of the Universe is defined as

$$H(t) \equiv \frac{\dot{a}(t)}{a(t)} . \tag{2.3}$$

4

We should note right now that although H is usually called the Hubble 'constant', a term we will use frequently throughout, it is evidently not a constant in time, as evidenced by eq.(2.3)[1].

From eq.(2.2) we see that the Universe is flat ($k = 0$) if

$$\frac{8\pi G}{3}\rho = H^2 \tag{2.4}$$

or if the energy density respects

$$\rho = \frac{3H^2}{8\pi G} \equiv \rho_c \tag{2.5}$$

ρ_c being the critical density. Various energy density in the universe are commonly expressed in fractions of the critical energy density,

$$\Omega_i \equiv \frac{\rho_i}{\rho_c} . \tag{2.6}$$

Some more description of the content of the Universe is in order. The various possible components are described as perfect fluids. A perfect fluid in an isotropic Universe has an energy-momentum tensor $T_{\mu\nu}$ such that

$$T_{\mu\nu} = \begin{pmatrix} \rho & 0 & 0 & 0 \\ 0 & & & \\ 0 & & g_{ij}p & \\ 0 & & & \end{pmatrix}$$

where ρ is the energy density of the fluid and p is its pressure, and g_{ij} is the metric's spatial part. The energy density and pressure of the fluid are related via the equation of state

$$p = w\rho . \tag{2.7}$$

The zeroth component of the conservation of energy equation leads to[2]

$$\frac{\dot{\rho}}{\rho} = -3\left(1 + w\right)\frac{\dot{a}}{a} \tag{2.8}$$

---

[1]In general ρ is not a constant in time.

[2]Details of the calculation are found in [5].

which is equivalent to

$$\rho = a^{-3(1+w)} \ . \tag{2.9}$$

Friedmann's equation in a flat Universe, eq.(2.4), means that the scale factor and energy density are also related via

$$\left(\frac{\dot{a}}{a}\right)^2 \sim \rho \tag{2.10}$$

so that

$$a^{\frac{1}{2}(1+3w)}\mathrm{d}a \sim \mathrm{d}t \ . \tag{2.11}$$

In this work we shall be concerned with two types of energy densities: matter and radiation. Dust or non-relativistic matter has no pressure, meaning that $w_M = 0$; this in turn implies that in a matter-dominated Universe,

$$a_M \sim t^{\frac{2}{3}} \tag{2.12}$$

and in turn

$$H = \frac{2}{3}t^{-1} \ . \tag{2.13}$$

The equation of state for radiation is such that $w_R = 1/3$, so that in a radiation-dominated Universe

$$a_R \sim t^{\frac{1}{2}} \tag{2.14}$$

and in turn

$$H = \frac{1}{2}t^{-1} \ . \tag{2.15}$$

The third and last contribution to the energy density, dark energy, has an equation of state such that $w < 0$.

2.1.2 Particle dynamics

When considering a specific particle species, the particle number and energy densities are both of interest; they are defined as

$$n = \frac{g}{(2\pi)^3} \int f(\vec{p})d^3p$$

$$\rho = \frac{g}{(2\pi)^3} \int E(\vec{p})f(\vec{p})d^3p \tag{2.16}$$

where g is the number of internal degrees of freedom of the particle and $f(\vec{p})$ is its phase space distribution function. E is the energy of the species, $E^2 = |\vec{p}|^2 + m^2$. The number density of a species is evidently influenced by the various interactions it is allowed to have with other species present; the Boltzmann equation allows to calculate the number density of a species. Consider particle 1 with a number density n that can only be changed via the interaction 1+2 ↔ 3+4. The Boltzmann equation in an expanding Universe gives

$$
\begin{aligned}
\dot{n}_1 + 3Hn_1 = \quad & C \\
\equiv & \int \frac{d^3p_1}{(2\pi)^3 2E_1} \int \frac{d^3p_2}{(2\pi)^3 2E_2} \int \frac{d^3p_3}{(2\pi)^3 2E_3} \int \frac{d^3p_4}{(2\pi)^3 2E_4} \\
& \times (2\pi)^4 \delta^4 (p_1 + p_2 - p_3 - p_4) \\
& \times \left(|M_\leftarrow|^2 f_3 f_4 (1 \pm f_1)(1 \pm f_2) - |M_\rightarrow|^2 f_1 f_2 (1 \pm f_3)(1 \pm f_4) \right)
\end{aligned}
\tag{2.17}
$$

where $M_\leftarrow$ and $M_\rightarrow$ stand for the matrix element for the processes $1 + 2 \leftarrow 3 + 4$ and $1 + 2 \rightarrow 3 + 4$, respectively, and the f_i are distribution functions. The term involving the Hubble constant H takes into account the dilution of the number density coming from the Universe's expansion. Evidently in general many more interactions will contribute to the change in n_1; they can just be added on the right-hand side of the Boltzmann equation. We will come back more extensively to the Boltzmann equation in chapter 6.

To calculate the number density of a species we need to know what interactions should enter the Boltzmann equation. This is in general given by the model in which the particle is considered (eg. the SM or as in this thesis the Minimal Supersymmetric Standard Model) though one must consider the effect of the expansion of the Universe. Indeed as the Universe expands some interactions might become ineffective. The general criteria is that as long as the rate of an interaction Γ is smaller than the expansion rate, given by the Hubble constant, then this interaction does not happen at any significant rate [4]. When all interactions affecting the number density of a species become inefficient (and remain so) then the number density of this species remains constant (outside the dilution effect due to the Universe' expansion) and is then said to be frozen in. The $\Gamma < H$ criteria determines whether individual reactions are effective; it is also sometimes used as a rule of thumb to

approximate the freeze-out temperature of a species (by comparing one reaction rate to the Hubble constant), though the only precise way to determine the freeze-out temperature of a species is to use the Boltzmann equation in full.

From the Boltzmann equation it is obvious that even in the complete absence of number density-changing interactions, the number density is modified by the expansion of the Universe. A parameter of interest is thus the number density per comoving volume, $N \equiv n(t)R(t)^3$ (with $R(t)$ the scale factor), which is constant after number-changing interactions are switched off. It is most common to express the number density per comoving volume in terms of the total entropy density s. The entropy density is to a good approximation[3]

$$s = \frac{2\pi^2}{45} g_* T^3 \tag{2.18}$$

where g_* counts the number of degrees of freedom that are effectively massless and in equilibrium,

$$g_* = \sum_{i=bosons} g_i \left(\frac{T_i}{T}\right)^4 + \frac{7}{8} \sum_{i=fermions} g_i \left(\frac{T_i}{T}\right)^4 . \tag{2.19}$$

g_* is a function of temperature, as species cease being effectively massless when $T \lesssim m$. Within the SM the evolution of g_* is well known (see for example fig. 3.5 in [4]); of interest to us will be the time when all the SM particles are effectively massless $(T \gtrsim T_{ewpt})$ and no additional massless degrees of freedom are present. In such a situation g_* is $g_* = 106.75$. Now the number of massless degrees of freedom is $g_* = 3.36$

Two comment are in order here: first, strictly speaking the entropy is expressed in terms of g_{*S}, which has the same expression than g_* except that ratios of temperature are to the third power and not the fourth. During the history of the Universe g_* and g_{*S} only differ at very late times; for instance $g_{*,now} = 3.36$ while $g_{*S,now} = 3.91$. For our needs using g_* is sufficient. Moreover, g_* as expressed here is the one

---

[3]This is considering that only relativistic degrees of freedom contribute. Moreover using g_* instead of g_{*S}, as we will discuss shortly, amounts to considering that all contributing particle species have a common temperature, as explained in [4].

obtained within the SM, where there are three massless neutrinos; in this work we will be considering a model in which neutrinos are massive and the number of light neutrinos is necessarily higher. Thus within our model $g_{*,now}$ should be larger than 3.36, but smaller than double this amount. Here we will only use g_* to obtain order of magnitude approximation; for this reason we will use $g_{*,now} = 3.36$ ($g_{*S,now} = 3.91$) for definiteness.

Going back to the number density per comoving volume, we have that conservation of entropy means that $s \propto R^{-3}$, so that the number density per comoving volume, N is also given by

$$N = \frac{n}{s} \ . \tag{2.20}$$

In this work (and others) the term number density sometimes refer to the number density per comoving volume, especially when the number density is frozen in and N is constant. The distinction between the two (number density and number density per comoving volume) should be clear within the context.

We should mention that with the Friedmann equation (2.2) along with the definition of the Hubble constant (eq.(2.3)), the critical density (eq.(2.5)) and the expression for the energy density of a species (eq.(2.16)), we are in a position to calculate a wealth of interesting results in various limits. For example, considering the Universe to be radiation-dominated, we can model the energy density of the Universe as being given by eq.(2.16) in the case where most particles are relativistic species in thermal equilibrium. In terms of temperature the energy density then simplifies to

$$\rho_R = \frac{\pi^2}{30} g_* T^4 \tag{2.21}$$

with g_* as defined before. In turn we can use the Friedmann equation with the definition of the Hubble constant to obtain that in radiation domination (when g_* is approximately constant),

$$H = 1.66 g_*^{1/2} \frac{T^2}{M_P} \tag{2.22}$$

where M_P is the Planck mass.

2.1.3 Measured cosmological parameters

The Wilkinson Microwave Anisotropy Probe (WMAP) satellite [8] aims to measure the temperature anisotropy power spectrum of the cosmic microwave background (CMB) as a way of testing Standard Cosmology, determining cosmological parameters and studying structure formation processes. It is assumed that primordial fluctuations in the gravitational potential appear at the end of inflation as a result of quantum fluctuations in the inflaton field. These primordial fluctuations evolved into the temperature fluctuations in radiation that are observed at the moment when photons and baryons became decoupled. The way in which the primordial fluctuations evolved is highly dependent on the content of the Universe. In a similar way, the evolution of the CMB temperature fluctuations into today's large scale structure is also highly dependent on the content of the Universe. Thus observation of the CMB allows rather precise access to this information. Results released in 2003 [9] and in 2006 [10] agree exceptionally well with the picture of a flat, homogenous and isotropic Universe populated with matter and dark energy. The density of matter in the Universe accounts for approximately 25% of the critical density, while the remaining 75% are composed of a still mysterious dark energy.

The WMAP surveys have also obtained a value for the Hubble constant now, H_0; it is often expressed as

$$H_0 = 100h\frac{\text{km}}{\text{s}}\text{Mpc}^{-1} \tag{2.23}$$

which defines the parameter h, obtained by WMAP to be [10]

$$h = 0.732^{+0.031}_{-0.032} . \tag{2.24}$$

Moreover we will use as the current temperature of the Universe, T_{now} [4]

$$T_{now} = 2.75\text{K} . \tag{2.25}$$

As we have mentioned WMAP has obtained the amount of matter in the Universe, which is approximately 25% of the critical density. It has also obtained the amount of baryonic matter present in the Universe. Both quantities are far from

Parameter		Source
h	$= 0.732^{+0.031}_{-0.032}$	[10]
w_b	$= 0.02229 \pm 0.00073$	[10]
w_{DM}	$= 0.1054^{+0.0087}_{-0.0086}$	[10]
T_{now}	$= 2.75K$	[4]

Table 2.1: Values of cosmological parameters.

being equal. Indeed, [10]

$$w_b \equiv \Omega_b h^2 = 0.02229 \pm 0.00073$$
$$w_m \equiv \Omega_m h^2 = 0.1277^{+0.0080}_{-0.0079} \, . \tag{2.26}$$

where the baryon w_b and matter densities[4] w_m are expressed in terms of the h parameter as defined before. The amount of matter that is not baryonic is called dark matter, to which we will come back in section 2.3[5]. The quantity of dark matter in the Universe is thus

$$w_{DM} = 0.1054^{+0.0087}_{-0.0086} \, . \tag{2.27}$$

For convenience we give in table (2.2) the value of the various quantities we have listed up to now. We also include a table of the observed quantities that we will use. In this work we will work with units of powers of GeV to express any quantity, using $\hbar = c = k_B = 1$.

The present work is primarily concerned with dark and baryonic matter. By no means is WMAP the only source of information about the matter content of the Universe, or about the nature and distribution of dark matter; here we merely use the WMAP observations as our main source of cosmological information. Overviews of the various observations related to the baryon content of the Universe are found

---

[4]Unfortunately both the equation of state parameter and the densities as defined here are expressed by w; these two quantities are however unrelated.

[5]It also contains the neutrino density, which is much too small to account for such a difference; see section 2.3

Quantity		Value			
Planck mass	M_P	1.22	$\times$	10^{19}	GeV
Newton's constant	$G \quad = M_P^{-2}$	6.72	$\times$	10^{-39}	GeV^{-2}
Temperature now	$T_{now} = 2.75K$	2.43	$\times$	10^{-13}	GeV
Hubble constant now	$H_0 \quad = 100h\frac{km}{s}\mathrm{Mpc}^{-1}$	$2.13h$	$\times$	10^{-42}	GeV
Critical density now	$\rho_{now} \quad = \frac{3H_0^2}{8\pi G}$	$8.10h^2$	$\times$	10^{-47}	GeV^4
Entropy now	$s_{now} \quad = \frac{2\pi^2}{45}g_{*S,now}T_{now}^3$	2.46	$\times$	10^{-38}	GeV^3

Table 2.2: Various quantities expressed in powers of GeV.

in [4], and to dark matter, in [7,11]. We should mention that as dark energy is often expressed in terms of a cosmological constant, Λ, and most of the matter seems to consist of cold dark matter (as we have mentioned briefly), the present favoured cosmological model is often called the ΛCDM model.

2.1.4 Inflation

Although this work is not concerned with discussing inflation itself, it does refer to it and to some of its characteristics from time to time. For this reason we include a short description of inflation.

Inflation is the process by which the very early Universe expands in an exponentially accelerated way ($\ddot{a} > 0$, see section 2.1.1). This accelerated expansion is used to solve a number of cosmological 'problems': the large-scale smoothness problem, or the observation that the Universe is smooth on scales greater than causality permits; the spatial-flatness problem, or the observation that the curvature of the Universe is vanishing; and the unwanted relics problem, or the fact that some possible relics from the early Universe (such as monopoles) are not observed today. Although there exists a large number of inflation models, the information necessary for our work can be obtained by studying the basic general picture.

Inflation happens as a result of the slow-rolling of a new, weakly-interacting scalar field (generically the 'inflaton') along a potential generically described in figure (2.1). As the field rolls along the relatively flat part of the potential, the energy density

contained in the vacuum comes to dominate the energy density of the Universe, triggering the phase of accelerated expansion (see subsection 2.1.1). This inflation phase of the inflaton evolution is followed by a phase of coherent oscillations of the field around the minimum of the potential. During this phase the Universe is dominated by inflaton "matter" in the form of inflaton oscillations. Inflation ends with reheating, the process by which the energy stored in inflaton oscillations is transferred to decay products of the inflaton, that eventually thermalise. Immediately after reheating the Universe enters an era of radiation domination, as the energy density is dominated by the relativistic decay products of the inflaton.

Among the unwanted relics that can be erased by inflation is the gravitino, which we will discuss in chapter 3. In order to avoid disruption of the successful Big-Bang Nucleosynthesis (BBN), which we discuss next, the density of gravitinos needs be kept small, and this can be done through inflation if the reheating temperature is kept lower than $T_R \sim 10^9 \text{GeV}$ [12–14]. Although much can be said about inflation and the gravitino problem, as we have mentioned this is somewhat tangential to our work here. For this reason we shall use $T_R \lesssim 10^9 \text{GeV}$ as our benchmark for the reheating temperature.

2.1.5 Big-bang nucleosynthesis

As was the case with inflation, the subject of Big-Bang nucleosynthesis (BBN) is not central to our discussion, but we will refer to it several times in this work, and for this reason we include here a (very) short review of the subject.

BBN is the process by which the light elements present in the Universe are produced[6]. When the temperature of the Universe is higher than $T \sim 1 \text{MeV}$, nuclear statistical equilibrium is maintained, meaning that the various light elements are present in their (very small) equilibrium number and are coupled to the plasma. Shortly after this time, around $T \sim 0.3 \text{MeV}$, some of the nuclear interactions necessary to maintain nuclear statistical equilibrium become ineffective, and some light

---

[6]Heavier elements are produced in stars.
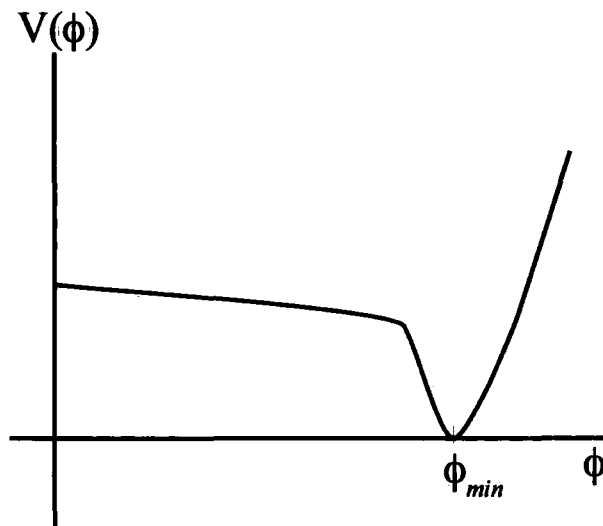
Figure 2.1: A generic inflation potential. The inflaton field first rolls down the relatively flat part of the potential, which causes vacuum energy domination. Its evolution ends with coherent oscillations around the minimum of the potential, until the inflaton decays.

elements see their number density depart from equilibrium. In turn the departure from equilibrium of a certain light element number density can modify a nuclear reaction rate necessary for maintaining the equilibrium of another species. A careful (numerical) analysis of this highly coupled system of Boltzmann equations allows one to obtain the number densities of, among others, deuterium, ^{3}He, ^{4}He and ^{7}Li.

Nucleosynthesis has a very long history; the idea was suggested in 1946 [15] and codes to calculate the abundances of various elements date as far back as the 1960's. Since then rather precise estimates of light elements abundances within the SM framework have been obtained and compared with information obtained

through observations[7]; the level of consistency between the number densities of D, ^{4}He and ^{7}Li as calculated and as inferred from observations is very high (see for example [16, 17]. For this reason, BBN is often used as a constraint on physics outside the SM: any new particle or new model must be such that it does not prevent successful BBN. This is the way in which we will be interested in BBN in this work.

A famous example of an exotic particle that can spoil BBN is the gravitino. The gravitino's interactions are very weak, leading it (if unstable) to be very long lived. Depending on the model, the gravitino lifetime can become so long that its decay happens after BBN; the decay products can then scatter off nuclei produced during BBN and, if abundant enough, alter the number densities of the light elements enough to make them inconsistent with observations. This is an example in which BBN comes as a constraint on model building for physics outside the SM. It has induced a constraint on the reheating temperature, as inflation is used as a means to render the number density of gravitinos small enough so that its decay cannot affect BBN sizeably[8]. Depending on the lifetime of the long-lived but unstable exotic particle under consideration, the abundances of different elements come as constraints on the amount of the particle involved. We will encounter such a situation in chapter 6.

2.2 The baryon asymmetry

As we have mentioned earlier the present baryon energy density of the Universe is by now well measured. A priori the baryonic energy density could be made up of either baryons, anti-baryons, or both. The evidence however excludes the existence of large amounts of anti-baryons in the Universe; the observed baryonic energy density comes from baryons only. In cosmic rays, for example, anti-protons are found in a

---

[7]It is unfortunately beyond the scope of this work to review the astrophysical observations leading to an experimental evaluation of light elements abundances.

[8]The abundance of gravitinos is proportional to the reheating temperature.

proportion of about 10^{-4} for each proton; this amount of anti-proton, however, is consistent with their secondary production as matter (as opposed to anti-matter) cosmic rays speed towards the Earth. This amount of anti-protons in cosmic rays is in fact consistent with the absence of anti-matter within our galaxy [4, 18]. On larger scales, it is expected that the existence of patches of anti-matter would lead to the occasional collision of matter and anti-matter patches, in turn leading to bursts of gamma rays. If anti-matter was as abundant as matter in the Universe, then these collisions would happen very frequently, leading to a diffuse gamma-ray background [4, 18]. This is not observed.

Starting with matter-anti-matter symmetric initial conditions, one can use Standard Cosmology and the SM to calculate the amount of baryons and anti-baryons that should be left in our contemporary Universe using the Boltzmann equation[9]. Performing such a calculation leads to values for baryon and anti-baryon numbers such that [4, 18]:

$$\frac{n_B}{s} = \frac{n_{\bar{B}}}{s} \simeq 7 \times 10^{-20} \; . \tag{2.28}$$

It is already evident that this calculation is unable to explain the observed baryon-anti-baryon asymmetry. The situation is however even stranger: considering the observed baryon energy density to be made of only baryons and no anti-baryons, we can translate the observed quantity into the baryon number of the Universe (using the necessary quantities from table (2.2)):

$$\frac{n_{B,observed}}{s} \simeq 10^{-10} \; . \tag{2.29}$$

The order of magnitude for the baryon number density obtained within the SM is definitely incompatible with observations. We are forced to conclude that there must be a novel mechanism at play that produces the observed baryon asymmetry. The idea of baryogenesis, and later leptogenesis, tackles this question: producing the correct amount of baryon and the correct baryon asymmetry through new physics. This section highlights the main aspects of these mechanisms and the main possibilities available. Throughout we use the discussions available in [4, 18, 19].

---

[9]This is without considering sphalerons, which we will discuss later.

2.2.1 Sakharov's conditions

Already in 1967, the necessary conditions for the production of a non-zero baryon asymmetry in the Universe (or a *baryogenesis*) were identified by Sakharov [20]. These three conditions are as follow.

- Baryon-number violation: in the absence of baryon-number violating interactions, no net baryon number can be created from a non-zero one; thus the observed baryon number would come directly from fixed initial conditions. This does not allow for an explanation of the observed baryon energy density, and for this reason the existence of baryon-number violating interactions is necessary.

- C and CP violation: the violation of charge (C) and charge-parity (CP) is necessary to obtain a Universe in which baryons and anti-baryons do not appear in the same numbers. As we have seen the observed baryon energy density is not made of equal (or even similar) numbers of baryons and anti-baryons; it is entirely constructed of baryons. Thus it translates directly to a net baryon number for the Universe. If there is no C and CP violation, then for any interaction producing a baryon there exist a conjugate interaction that produces an anti-baryon. Even if baryons and anti-baryons were somehow prevented to annihilate, the net result is a Universe with no net baryon number, or the existence of large patches of anti-matter, which is not what is observed.

- Departure from equilibrium conditions: in equilibrium, the number densities of baryons and anti-baryons are necessarily the same even when both above conditions are respected. Baryons and anti-baryons necessarily share the same mass; moreover in equilibrium the chemical potential of the phase space distribution function will be zero for baryons and anti-baryons[10]. Thus in equilibrium the distribution functions of baryons and anti-baryons will be the same,

---

[10]This is due to the fact that baryon number would not be conserved, and that in equilibrium entropy is maximal when the chemical potential associated with a non-conserved quantum number is zero [4].

leading to their number densities being the same as well. Putting it differently, supposing that B- violating and C and CP-violating interactions have created an instantaneous net baryon number, then assuming equilibrium necessarily implies the existence of interactions that rapidly reprocess this net number to zero.

Let us discuss possible known sources for each condition. Baryon-number violation seems especially problematic when one considers that the lifetime τ_p of the proton (which should be unstable would there be B-violating interactions) is much longer than the age of the Universe t_U: the Particle Data Group [21] lists

$$\tau_p > 2.1 \times 10^{29} yr \tag{2.30}$$

while WMAP obtained as their best-fit value [10]

$$t_U = \left(13.73^{+0.16}_{-0.15}\right) \times 10^9 yr. \tag{2.31}$$

Clearly baryon number is now very well conserved. But this needn't be the case in the early Universe. A baryon-number violating interaction might be highly suppressed at low temperature (as we have now) but effective at higher temperature. Indeed this is the case in the SM itself, as we will discuss in the next subsection. Within the SM baryon number is anomalous, which leads to the possibility of violating baryon number, but, in accordance with proton stability, this is exponentially suppressed at low temperature. Beyond the SM models such as Grand Unified Theories (GUTs) and supersymmetric models can also provide sources of baryon number violation.

The SM, it is already well known, also possesses C- and CP-violation. C is violated by the weak interaction (as left- and right-handed fermions couple differently). CP is also violated by the weak interaction; CP violation was discovered in 1964 in the kaon system [22], and since then has also been observed in the B system [23, 24]. Thus the SM readily provides a source of C and CP violation. CP violation in the SM is however a very small effect. Indeed, although the baryon asymmetry of the Universe seems maximal, it has been noted that the CP violation of the SM is not [25]; moreover the SM CP violation effect can be parameterised

by a dimensionless constant which is of order 10^{-22} [26, 27], and this appears to be too small to lead to successful models that would use only this as a source of CP violation [28]. Models of baryogenesis that use only the SM CP violation are up to now unsuccessful. Again supersymmetric theories can provide additional sources of CP violation, and it is possible to include some CP violation in GUTs as well.

Turning last to the departure from equilibrium condition, it is worth remembering that as the Universe expands, various processes naturally fall out of equilibrium as their rates fall below the expansion rate. A priori, thus, the expansion of the Universe could itself provide the necessary out-of-equilibrium environment.

Before going to explore the various ways in which baryogenesis might be achieved, let us first describe the baryon number violating effects that exist within the SM: the sphalerons.

2.2.2 Sphalerons

In the SM, baryon number is not conserved despite the fact that the classical Lagrangian does not violate baryon number: in other words, baryon number is anomalous. This reflects the result obtained by Adler, Bell and Jackiw [29, 30] that the axial current of a gauge coupled Dirac fermion is anomalous. Deriving the various results related to the B non-conservation in the SM that are of importance here is outside the scope of this work; we will simply list them and explain some of their consequences. [28, 31] present in-depth analysis.

Considering the baryon (resp. lepton) current,

$$
\begin{aligned}
j_B^\mu &= \frac{1}{2}\bar{q}\gamma^\mu q \\
j_L^\mu &= \frac{1}{2}\bar{l}\gamma^\mu l
\end{aligned}
\tag{2.32}
$$

we have that the divergence of this current is non-zero:

$$
\partial_\mu j_B^\mu = \partial_\mu j_L^\mu = n_f \left(\frac{g^2}{32\pi^2} W_{\mu\nu}^a \tilde{W}^{a\mu\nu} - \frac{g'^2}{32\pi^2} F_{\mu\nu} \tilde{F}^{\mu\nu} \right)
\tag{2.33}
$$

where $W_{\mu\nu}^a$ and $F_{\mu\nu}$ are the $SU(2)$ and $U(1)$ gauge field strengths (and their dual comes with a tilde), g and g' are $SU(2)$ and $U(1)$ gauge couplings, and $n_f = 3$ is the

number of families. The total baryon number is related to the baryon current via

$$B = \int d^3x j_b^0 \qquad (2.34)$$

and so considering the change in B from $t = 0$ to an arbitrary time t (and considering the average of the field strength to start and end at zero; see later) we obtain that

$$\Delta B = n_f \left(N_{CS}(t) - N_{CS}(0) \right) \qquad (2.35)$$

where N_{CS} is the Chern-Simons number,

$$N_{CS} = \frac{g^2}{32\pi^2} \int d^3x \epsilon^{ijk} \mathrm{Tr} \left(A_i \partial_j A_k + \frac{2}{3} ig A_i A_j A_k \right) \qquad (2.36)$$

with the A_i the $SU(2)$ gauge fields. For $SU(2)$ the Chern-Simons numbers (in a vacuum) are integers, and so baryon number can change by multiples of the number of families.

To better understand the baryon number violation we need to discuss the vacuum structure of the electroweak theory. In the space of the Higgs and $SU(2)$ gauge fields, there exist an array of vacua separated by energy barriers, as is depicted in figure (2.2). From one vacuum to the other the Chern-Simons number changes by one, meaning in turn that the baryon number changes by three. Thus if somehow it is possible to go from one vacuum to the other, the baryon number can be changed.

Before we turn to determining the rate at which baryon number can be violated in this way, a few remarks are in order. Although we have focused our discussion on the violation of baryon number, it is clear from equations (2.32) and (2.33) that we could as well have discussed the violation of lepton number. What is also clear from eq.(2.33) however is that if L and B are both violated, $B - L$ is not. This will be of importance when discussing leptogenesis. Moreover, although we have mentioned that the Adler-Bell-Jackiw anomaly applies to gauge-coupled Dirac fermions, it is only the $SU(2)$ gauge group that plays a role in the baryon number variation, as can be seen from eqs.(2.35, 2.36). As right-handed quarks and leptons in the SM are $SU(2)$ gauge-singlet, we have that anomalous baryon-number violation in the SM affects only the left-handed sector of the theory. This is a major ingredient

$$V(A,\phi)$$
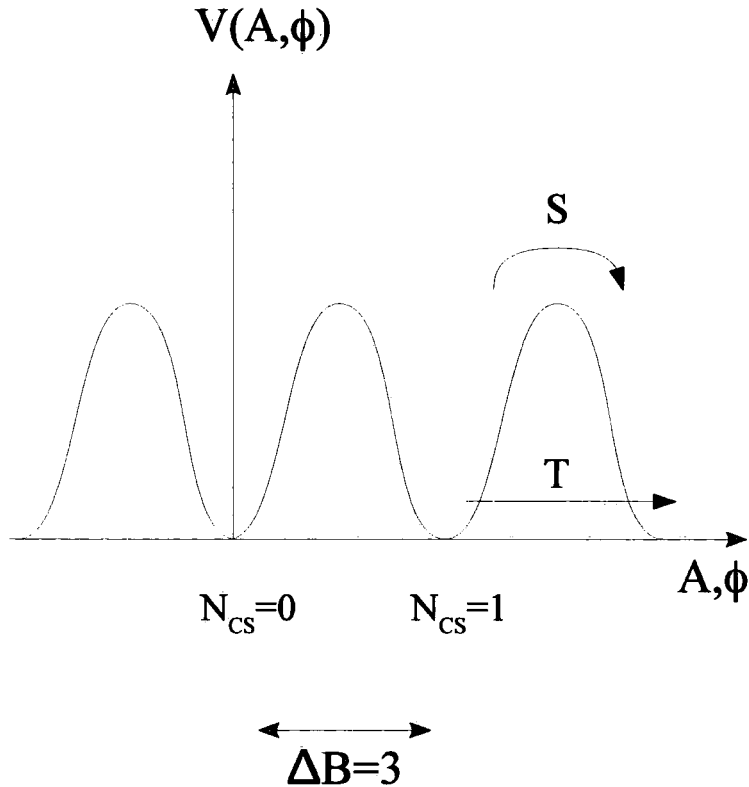
Figure 2.2: Different vacua of the SM in a certain direction of the SU(2) gauge fields (A) and Higgs field (ϕ). The baryon number changes by three (the number of families) from one vacuum to the other. We have also shown tunneling through the barrier that separates vacua (T) and the sphaleron transition (S), which effectively allows for passing over the barrier. The sphaleron is an unstable field configuration where fields stand atop the barrier.

in neutrinogenesis, or lepton-number conserving leptogenesis, as we will discuss in section 2.2.3 and later in chapter 7.

The rate of baryon number violation depends then on the rate of transition from

one vacuum to another. At zero temperature transitions between vacua go through tunneling through the barrier that separates vacua. Unsurprisingly (considering the stability of the proton), the rate of tunneling is exponentially suppressed by a factor

$$e^{-\frac{4\pi}{\alpha_w}} \tag{2.37}$$

where $\alpha_w = g^2/4\pi$. Remembering that $g \sim O(10^{-1})$, it is clear that this factor is essentially zero. This is good news as far as the stability of the proton is concerned, but for baryogenesis this rate needs to become much larger at high temperature. This is indeed the case, as was first noted by [32]; at finite temperature, the transition from one vacuum to another needn't go through tunneling, but can happen by jumping over a $B + L$-violating field configuration known as a sphaleron, as the energy available in the system can be large enough. The height of the energy barrier is given by the sphaleron mass. The rate at which $B + L$-violating processes occur have been studied extensively (see for example [19] or more recently [18] for overviews). The most important result of these calculations for our work here is that at temperatures roughly larger than the electroweak phase transition, sphaleron transitions occur at a rate faster than the expansion rate of the Universe, while at lower temperature the suppression factor is large enough to render them inefficient.

2.2.3 Baryogenesis and Leptogenesis

Let us now turn to some possible baryogenesis models. Although the three Sakharov's conditions can be respected within the SM, as we have mentioned the CP violating effect is generally too small, so models that don't venture outside of the SM are not successful. Electroweak baryogenesis aims at using sphalerons as the necessary source of baryon number violation; CP violation is provided by a beyond-the-SM effect such as additional Higgses. The main difficulty encountered by these models is that at temperatures around the electroweak phase transition, where sphalerons are active, departure from equilibrium is very small, as SM interactions are fast. Thus departure from equilibrium has to be provided by the phase transition itself [32]. It has been obtained already that within the SM it is unlikely that the electroweak phase transition is a strong enough source of departure from equilibrium

[33]; electroweak baryogenesis might however still be possible in supersymmetric extension of the SM (see [34] for an overview).

GUT baryogenesis might be in a more comfortable position. GUTs can very naturally include baryon number violation, as the unifying gauge group G of GUTs generally has quarks and lepton in the same representation, meaning that new GUT interactions might well mix fermions with different baryon numbers. Additional CP violation is also easily found. The decay of new, heavy particles can lead to the observed baryon asymmetry, and these decays will eventually freeze-out due to the expansion of the Universe, which provides the necessary departure from equilibrium. One difficulty of these models is the fact that although sphalerons are not used as the source of baryon number violation, they are still present, and their effect will alter the baryon number produced by GUT baryogenesis. In fact sphalerons can even completely erase (or wash-out) a previous baryon asymmetry. As sphalerons conserve $B - L$, a solution to this problem is to use GUTs to generate a net $B - L$ number, which then sphalerons will not erase. Generation of $B - L$ might also be achieved within GUTs. [18] gives an overview of the successes and difficulties of GUT baryogenesis models.

A third type of models, to which our work is very much related, is leptogenesis, as introduced by [35]. Since sphalerons conserve $B - L$ but do not conserve $B + L$, when they are rapid they can convert a net lepton number to a net baryon number. Indeed a careful analysis of the SM particles' chemical potentials under rapid sphaleron transition lead to the following relations between B, L and $B - L$ [36]:

$$B = \frac{8N + 4m}{22N + 13m} (B - L)$$
$$L = -\frac{14N + 9m}{22N + 13m} (B - L). \qquad (2.38)$$

where N is the number of generations and m is the number of Higgs doublets. Once the sphalerons have switched off these relations turn to

$$B = \frac{8N + 4(m + 2)}{24N + 13(m + 2)} (B - L)$$
$$L = -\frac{16N + 9(m + 2)}{24N + 13(m + 2)} (B - L) \qquad (2.39)$$

What is needed then is a source of lepton number violation, so that sphalerons can

transfer part of the created lepton asymmetry to baryons. Extending the SM so as to provide a mass for the neutrino can in fact provide a source of lepton number violation. Indeed, as we will discuss in chapter 4 the now observed fact that neutrinos have mass requires physics outside the SM, and one in one class of neutrino mass models (Majorana neutrinos) the neutrino is its own anti-particle. As neutrinos do carry lepton number, this amounts to introducing a source of lepton number violation. We will see in chapter 4 why neutrinos being their own anti-particle is a possibility, but let us assume for now that a new, right-handed heavy neutrino has been added to the SM, and that its decay can violate lepton number, as neutrinos are now taken to be their own anti-particle. If CP violation is also present, then there exist net lepton-number violating processes that are not fully compensated by their CP-conjugated processes. The new heavy right-handed neutrino would be in equilibrium in the very early Universe, and would then freeze-out, holding a net lepton number. Its out-of-equilibrium decay would transfer this lepton number to SM leptons, and considering these events to occur before the electroweak phase transition, sphalerons would quickly transfer part of this lepton number to a net baryon number, which after sphaleron freeze-out would remain as the net baryon number of the Universe. This is the general picture of leptogenesis, as first suggested by Fukugita and Yanagida [35]. Since then much work has been done to study leptogenesis in different (Majorana) neutrino models or within wider contexts such as supersymmetry, and to try and understand further the source of CP violation within the neutrino mass matrix or outside of it. Evidently any leptogenesis scenario necessitates the presence of lepton number violation, which, as we have mentioned, only occurs in the case of Majorana neutrinos. Part of this work is concerned with discussing a possibility of leptogenesis within the class of neutrino mass models that do not allow for lepton number violation.

2.3 Dark matter

Here we briefly overview the necessary properties of dark matter candidates and discuss the possibility of mattergenesis. We delay part of the discussion of dark matter

to the chapter introducing supersymmetry, as in this work we are interested in dark matter candidates that arise within these models. Throughout we use discussions available in dark matter reviews [7, 11], as well as WMAP papers [8, 10] and more general comments available in [4].

2.3.1 Dark matter candidates

As we have seen WMAP confirms the existence of a large amount of non-baryonic dark matter in the Universe on the cosmological scale. On smaller scales, however, evidence of dark matter has been gathering for over seventy years. In 1933, Zwicky observed the rotation of galaxies within the Coma cluster and obtained that the distribution of their velocities could not be explained if the only matter present was the one directly observed through its radiation [37]. In other words, considering Einstein's general relativity to hold, he inferred that the cluster must contain a large amount of unseen, or dark, matter. The evidence for dark matter at the scale of clusters of galaxies is now strong (see [7, 11] for an overview, and for a review of dark matter evidence at various scales). Similarly, it is observed that the rotation curves of stars within galaxies require the presence of matter that is not seen via radiation.

Up to now dark matter evidence is only indirect; indeed no detection of a dark matter particle as yet been made. Much effort is being put in direct detection; we will describe direct detection experiments in chapter 5, as we will be concerned with discussing whether direct detection of our dark matter candidate is possible.

Dark matter has to be non-baryonic so as to explain WMAP's results; moreover it does not radiate, or it would be observable directly via its radiation and not solely via its gravitational effects. Moreover, it needs have zero electric charge and zero colour, otherwise it would have interacted with baryons and produced heavy isotopes, which is not observed [7]. Massive neutrinos might have all the necessary properties, and as it has now been established that neutrinos have mass (see chapter 4), it is tempting to conclude that dark matter simply is neutrinos. Within certain models of neutrino mass heavy sterile neutrinos might possibly be the dark matter [38]. The left-handed neutrinos of the SM, when added a mass, come however in too short a number to

account for dark matter. Moreover (left-handed, light) neutrino dark matter would be relativistic, which is not what is favoured by structure formation models.

Supersymmetry (SUSY), which we will discuss in chapter 3, was first studied for reasons unrelated to dark matter, but it was soon noticed that it naturally provided a dark matter candidate in the form of the lightest supersymmetric particle (LSP) [39, 40]. Within the Minimal Supersymmetric Standard Model (MSSM), the LSP can have both the necessary properties of dark matter as we have listed and the right relic density to account for WMAP's observations. Although the LSP is not the sole potential candidate for dark matter (see for example [7]), it is a widely popular one and it is the only possibility we will be considering in this thesis. As we will see in chapter 3, supersymmetry should soon be tested, and for this reason supersymmetric dark matter is certainly at the moment of special interest. We will delay our discussion of LSP dark matter to chapter 3, where we will introduce SUSY in more details.

We should mention that although dark matter is generally considered to be cold (to have decoupled while non-relativistic) due to structure formation constraints, models in which dark matter is produced non-thermally [41] and might be warm [42] are not ruled out. In this work we shall consider a dark matter candidate that never reaches thermal equilibrium. Unfortunately structure formation within our model is outside the scope of this work.

2.3.2 The possibility of mattergenesis

As we have mentioned earlier, the presence of the observed amount of baryonic matter necessitates the existence of a baryogenesis mechanism[11] This is because the relic density of baryons as can be calculated in the Standard Model does not correspond

---

[11]Here we use the term *baryogenesis* in a generic way, meaning any mechanism that would have as a result the creation of a sizeable amount of baryonic matter, be it GUT baryogenesis or leptogenesis à la Fukugita and Yanagida [35], or any other mechanism. We will use the term *mattergenesis* also in a generic way to describe any baryogenesis mechanism that also produces a sizeable amount of dark matter.

to the observed baryonic density. From this it is concluded that the baryons we observe today are not simply relics of the big-bang, but were instead produced at some point in the history of the Universe by some baryogenesis mechanism. Evidently perhaps, the fact that the SM baryonic relic density does not correspond to the observed one has not been taken as grounds that the SM does not accurately describe baryons, or that BBN should be completely reviewed; this is simply because the case for the SM is strong enough for other, independent reasons, and also because possible baryogenesis mechanisms have been found that do not necessitate such drastic departure from known physics.

The situation for dark matter is fairly different. On the one hand the very nature of dark matter is evidently much less obvious than the nature of baryonic matter; although we have gathered much information on the properties a dark matter candidate should have, it is clear that no particle already observed possesses these properties. In the search for a dark matter candidate in possible extensions of the SM, a criterion generally used is the relic density of this candidate within the extended model (see for example [11]): if the relic density of the candidate is too high, then overclosure of the Universe forbids this candidate, and if the relic density is too low, then the candidate is considered not to be the main source of dark matter. As we have just seen, however, such a reasoning in the baryonic case would have lead us to 'rule out baryons as baryonic matter candidates', or else to start seriously questioning the SM itself, two avenues physicists haven't followed. As we have said, the SM has other strong arguments in its favour; one could argue that a certain dark matter candidate (among many others) in a certain SM extension (among many others as well) that does not have the necessary relic density is not in such a good position, and can be abandoned readily. Whether we are missing out on some potentially interesting candidates in this way is debatable, and certainly in this thesis we outline that indeed it could be the case. One reason to study alternative production methods for dark matter, therefore, is simply the fact that the relic density of dark matter particles could be as irrelevant to their observed density as the relic density of baryons is to their observed density.

Once this is said, however, it becomes interesting to wonder whether it would

be possible for baryogenesis and 'dark-matter-genesis' to be united in a single *mattergenesis* mechanism that would simply create all matter, baryonic and dark, at once. If such a mechanism existed, it would perhaps also allow one to explain the observed ratio of dark-to-baryonic matter. Comparing eq.(2.26) and eq.(2.27), we have that

$$\frac{\Omega_{DM}}{\Omega_b} \sim 4.7 \ . \tag{2.40}$$

If we take the origins of both types of matter to be completely different (baryons coming from baryogenesis, dark matter density being given by its relic density), there is certainly no reason to expect their final density to be similar in any way. Yet the ratio of their densities is order one. The unexplained resemblance of the observed densities of dark and baryonic matter, sometimes called the 'Ω_{DM}/Ω_b problem', has been studied first in [43], and has received increasing attention [44–54]. Explaining the 'Ω_{DM}/Ω_b puzzle' is another argument to justify looking for mattergenesis mechanisms.

Some general characteristics of mattergenesis mechanisms can be obtained. It has been suggested before [47,54]) that candidates for mattergenesis-induced DM should generally have weak or even super-weak interactions with the 'visible' sector. If the candidate never thermalises, the asymmetry created by mattergenesis will not be erased or reprocessed at later times. In this case, the smallness of the couplings would act as a built-in protection of the DM asymmetry. Having such a constraint means that we would be able to estimate a correct amount for the dark matter density directly from the suggested mattergenesis mechanism even without owning detailed information about its interactions. A condition that other possible sources of DM stay small need also added, for in the opposite case mattergenesis is not the leading source of dark matter. We should mention that another mechanism to 'protect' the created dark matter asymmetry has been suggested in [46], where this time the candidate is thermal in the early Universe but freezes-out at some temperature $T \sim m_{DM}/20$, creating a low relic density. The observed DM density (and baryon density) is created after freeze-out by the decay of a heavier particle which couples to both dark and baryonic matter. For this reason the mechanism has been called the 'late decay' scenario. In both cases (of late-decay and non-thermal

candidate), the DM asymmetry is created at a time when the DM candidate is out of thermal equilibrium with the plasma, and will remain so.

In this work we suggest the right-handed Dirac sneutrino as a dark matter candidate that could have been produced within a mattergenesis mechanism, and part of our work will be concerned with discussing whether it has properties specifically interesting for mattergenesis.

Chapter 3

The Minimal Supersymmetric Standard Model

The popularity of supersymmetric theories, and of the Minimal Supersymmetric Standard Model (MSSM) in particular, has been unwavering for over twenty-five years. Soon the LHC should be able to determine whether low energy broken supersymmetry (SUSY) is indeed an accurate description of Nature. Although as yet no experimental signals of SUSY have been seen, there are a number of reasons why it has generated so much interest. The MSSM offers a solution to the hierarchy problem of the SM, which put simply is the fact that the Higgs mass is sensitive to new physics that would enter at scales much higher than the electroweak scale. It also permits the unification of gauge couplings. And although it was not constructed for this reason, it naturally provides a candidate for dark matter. As we have mentioned earlier, both the observed amount of baryonic matter in the Universe and the existence of large quantities of dark matter necessitate physics outside the SM. In this work we take the MSSM as the basic beyond-the-SM ingredient to tackle these two questions.

This chapter is concerned with giving basics of SUSY and the MSSM that are necessary for the completeness of this work. In the next section we give some essential basics of SUSY; we then go on to present the MSSM and its particle content, along with the description of their interactions. In section 3.2 we will discuss the phenomenon of soft SUSY breaking and different models that can implement it. Last

we discuss the MSSM dark matter candidate. Throughout we keep the emphasis very much on the aspects of SUSY and the MSSM most relevant to this work. Various reviews of SUSY basics deal with SUSY and the MSSM in more details (see for instance [55] and references therein). In this chapter we mainly follow the treatment of [55] and [56] for basics of the MSSM, and we additionally use [27] for SUSY-breaking issues, and [7,11,57] for phenomenology questions.

3.1 SUSY basics and MSSM

We introduce the SUSY algebra, followed by the particle content of the MSSM, its superpotential, scalar interactions and gauge interactions. We do not explain how to obtain the MSSM Lagrangian from first principles; this can be found in [55].

As we have mentioned, one of the leading reasons for introducing SUSY is the existence of the hierarchy problem. The Higgs mass, within the SM, is related to the scale of electroweak symmetry breaking, and experimental constraints are already in place that force it to be above 114.4GeV [21]. The Higgs mass however receives corrections from any particle it couples to, even in the case where the coupling appears only at higher orders. This in turns means that if there is any physics at energies higher than the electroweak scale, the Higgs mass could be dramatically affected. As the energy gap between the electroweak scale and the Planck scale is so wide, postulating that there exists no new physics in it seems rather constrained. This is in very short terms the hierarchy problem. Supersymmetry, which is a symmetry that relates boson and fermions, offers a solution to the hierarchy problem by assuring that for all fermionic contribution there exist a bosonic one that exactly cancels it (up to logarithmic contributions). Indeed at 1 loop level the corrections arising from an additional fermion and scalar cancel exactly (up to logarithmic contributions); within SUSY, the cancellation of fermionic and scalar contributions is kept even when all higher order corrections are included.

3.1.1 SUSY algebra

The generators of supersymmetry, Q, transform bosons into fermions and vice-versa; as such they are are fermionic generators. They respect the following algebra:

$$\{Q_\alpha, Q_{\dot{\alpha}}^\dagger\} = 2\sigma_{\alpha\dot{\alpha}}^\mu P_\mu \tag{3.1}$$

$$\{Q_\alpha, Q_\beta\} = \{Q_{\dot{\alpha}}^\dagger, Q_{\dot{\beta}}^\dagger\} = 0 \tag{3.2}$$

$$[Q_\alpha, P^\mu] = [Q_{\dot{\alpha}}, P^\mu] = 0 \tag{3.3}$$

where P^μ is the spacetime momentum operator, $P = (H, P^i)$, with H the Hamiltonian and P^i the 3-momentum operator, $\sigma^\mu = (1, \vec{\sigma})$ are the Pauli matrices, the μ index runs on spacetime coordinates and the α, $\dot{\alpha}$ indices are spin indices that run from 1 to 2. SUSY generators can be constructed by considering the SUSY Lagrangian for a fermion and a scalar; using Noether's procedure, we can construct from it the conserved supercurrent, and in turn obtain the supercharges, which are the SUSY generators.

A first interesting result (and which will be of importance to us in chapter 7) comes from considering the zeroth component of eq.(3.1). Let us try and obtain the Hamiltonian operator in terms of the SUSY operators; we have from eq.(3.1)

$$Q_1 Q_1^\dagger + Q_1^\dagger Q_1 = 2P_0 + 2P_3$$
$$Q_2 Q_2^\dagger + Q_2^\dagger Q_2 = 2P_0 - 2P_3 \tag{3.4}$$

so that

$$H = \frac{1}{4}\left(Q_1 Q_1^\dagger + Q_1^\dagger Q_1 + Q_2 Q_2^\dagger + Q_2^\dagger Q_2\right). \tag{3.5}$$

If in the vacuum SUSY is unbroken, then

$$Q_\alpha|0\rangle = 0, Q_{\dot{\alpha}}^\dagger|0\rangle = 0 \tag{3.6}$$

and the vacuum energy is zero. Conversely, it must imply that if the vacuum energy is positive, then SUSY is broken in the vacuum. Indeed if the vacuum is not invariant under SUSY, then

$$Q_\alpha|0\rangle \neq 0, Q_{\dot{\alpha}}^\dagger|0\rangle \neq 0 \tag{3.7}$$

so that the vacuum energy is

$$\langle 0|H|0\rangle = |Q_1^\dagger|0\rangle|^2 + |Q_1|0\rangle|^2 + |Q_2^\dagger|0\rangle|^2 + |Q_2|0\rangle|^2 > 0 . \tag{3.8}$$

In chapter 7 we will mention that the non-zero vacuum potential present during inflation necessarily leads to SUSY breaking [58].

3.1.2 Fermions within the MSSM

SUSY generators transform fermions into bosons, so the minimal supersymmetric extension of the SM, the MSSM, must include for each SM fermion a new scalar superpartner. In the MSSM each SM fermion and superpartner (or sparticle) pair is included in a chiral supermultiplet[1]. Matter fields and their superpartners are described by chiral superfields; the fact that matter superfields need be chiral is related to the fact that the SM treats left-handed and right-handed particles differently. The Higgs boson is also part of a chiral supermultiplet with its fermionic superpartner, the higgsino, though for reasons that we will explain shortly, the MSSM needs to contain two higgs superfields, the up-type higgs $\mathbf{H_u}$ and the down-type Higgs $\mathbf{H_d}$. Each higgs boson shares its chiral supermultiplet with its corresponding higgsino.

We denote a superfield in general by the bold character $\mathbf{\Phi}$; the fermionic (resp. scalar) component of a chiral superfield we denote by ψ (resp. ϕ). When describing a specific fermion-scalar pair, we use the usual SM symbol for the fermion and add a tilde for the scalar partner; for instance the lepton doublet superfield is

$$\mathbf{L} = \left(l, \tilde{l} \right) \tag{3.9}$$

which includes the lepton doublet

$$l = \begin{pmatrix} \nu \\ e \end{pmatrix}$$

and the slepton doublet,

$$\tilde{l} = \begin{pmatrix} \tilde{\nu} \\ \tilde{e} \end{pmatrix} .$$

---

[1]Chiral supermultiplets also include the F auxiliary field, which we will mention briefly shortly.

The up-type and down-type Higgs are the following superfields:

$$\mathbf{H_u} = \left(\tilde{H}_u, h_u \right) \tag{3.10}$$

$$\mathbf{H_d} = \left(\tilde{H}_d, h_d \right) \tag{3.11}$$

which include the higgsino $SU(2)$ doublets

$$\tilde{H}_u = \left(\begin{array}{c} \tilde{H}_u^+ \\ \tilde{H}_u^0 \end{array} \right), \tilde{H}_d = \left(\begin{array}{c} \tilde{H}_d^0 \\ \tilde{H}_d^- \end{array} \right) ,$$

and the Higgs doublets

$$h_u = \left(\begin{array}{c} h_u^+ \\ h_u^0 \end{array} \right), h_d = \left(\begin{array}{c} h_d^0 \\ h_d^- \end{array} \right) .$$

Each chiral supermultiplet also contains a complex scalar auxiliary field F. The auxiliary field's kinetic term in the Lagrangian is

$$\mathcal{L}_{aux} = F^* F . \tag{3.12}$$

This field serves to ensure that the SUSY algebra closes off-shell.

We should mention briefly what happens with electroweak symmetry breaking now that we have added a Higgs field. Following [55] we denote the Higgses vacuum expectation values (vev's) upon electroweak breaking as

$$\langle h_u \rangle = v_u$$

$$\langle h_d \rangle = v_d \tag{3.13}$$

and these must be related to the usual electroweak breaking scale[2] $v \simeq 174\text{GeV}$ via

$$v_u^2 + v_d^2 = v^2 . \tag{3.14}$$

Traditionally both vev's are related by their ratio, which is defined by

$$\tan\beta \equiv \frac{v_u}{v_d} . \tag{3.15}$$

---

[2]We have $v \simeq 174$ so that the top Yukawa coupling λ_t is $\lambda_t \simeq 1$

In this work we shall be using $\tan\beta \gg 1$, or $v_u \simeq v$ as a simplifying assumption.

The interactions of superfields that do not involve gauge interactions are contained within a single, analytic function of the scalar components of the various superfields of the theory, the superpotential. The most general superpotential that leads to a renormalizable, gauge-invariant and SUSY-conserving Lagrangian[3] is given by

$$W = \frac{1}{2}M^{ij}\phi_i\phi_j + \frac{1}{6}y^{ijk}\phi_i\phi_j\phi_k \tag{3.16}$$

where M^{ij} is a symmetric mass matrix and y^{ijk} is totally symmetric under the exchange of i, j, k. The Lagrangian is obtained from the superpotential in the following way:

$$\mathcal{L} = \mathcal{L}_{kin} - \left[\sum_{j,k}\frac{\partial^2 W}{\partial\phi_j\partial\phi_k}\psi_j\psi_k + h.c.\right] + \sum_j \frac{\partial W}{\partial\phi_j}F_j + h.c. \tag{3.17}$$

with

$$\mathcal{L}_{kin} = -\partial^\mu\phi^{*i}\partial_\mu\phi_i - i\psi^\dagger\bar{\sigma}^\mu\partial_\mu\psi_i + F^*F . \tag{3.18}$$

Using the equation of motion of the auxiliary field,

$$\frac{\partial\mathcal{L}}{\partial F} = 0$$
$$\Rightarrow F^* = -\frac{\partial W}{\partial\phi_j} \tag{3.19}$$

we can eliminate the F-field contribution to the interaction Lagrangian to obtain

$$\mathcal{L} = \mathcal{L}_{kin} + \mathcal{L}_{int} \tag{3.20}$$

with

$$\mathcal{L}_{int} = -\sum_j \left|\frac{\partial W}{\partial\phi_j}\right|^2 - \left[\sum_{j,k}\frac{\partial^2 W}{\partial\phi_j\partial\phi_k}\psi_j\psi_k + h.c.\right] . \tag{3.21}$$

---

[3]An additional linear term $k^i\phi_i$ is allowed in the case where there exists a gauge singlet in the theory, which is not the case in the MSSM. Here we will introduce such a gauge singlet but will not consider adding a linear term to the theory.

The first term of $\mathcal{L}_{int}$ is generally called *F-terms* for obvious reasons and is a purely scalar contribution, while the second term mixes fermions and scalars.

The MSSM superpotential is given by

$$W_{MSSM} = \lambda_{\mathbf{u}}\tilde{Q}h_u\tilde{u}_R^c - \lambda_{\mathbf{d}}\tilde{Q}h_d\tilde{d}_R^c - \lambda_e\tilde{L}h_d\tilde{e}_R^c + \mu h_u h_d \qquad (3.22)$$

where $\lambda_{\mathbf{u}}, \lambda_{\mathbf{d}}, \lambda_{\mathbf{e}}$ are the Yukawa matrices that give rise to the fermion masses in the usual way and the μ term gives rise to the Higgses masses. Since the superpotential needs to be analytic, it is not possible to use the conjugate of one of the Higgs fields to play the role of h_d, as is done in the SM; thus it is necessary to have two different Higgses, one for the up-type quarks and one for the down-type quarks. Moreover two Higgses (or rather two higgsinos of opposite charge) are necessary to maintain the cancellation of gauge anomalies[4]. The usual Yukawa terms for SM fermions will stem from interactions of the type given by the second term of eq.(3.21).

3.1.3 Gauge interactions of matter fields

Gauge fields appear as components of vector superfields, which also include the fermionic superpartners of the gauge bosons, the gauginos, and an auxiliary field D. The gauge boson part of the vector superfield we denote in general by A^μ and the fermionic part by λ. When describing a specific gauge boson-gaugino pair we use the usual SM symbol for the gauge boson and add a tilde for the fermionic partner.

The Lagrangian for gauge interactions with chiral superfields is composed of various parts. Once the auxiliary D fields are eliminated from the interaction Lagrangian we obtain a contribution to the scalar Langrangian, which we will call D-terms:

$$\mathcal{L}_D = \frac{1}{2}\sum_a g_a^2\left(\phi^* T^a \phi\right)^2 \qquad (3.23)$$

---

[4]Considering the hypercharge Y and the third component of isospin, T_3 (with the electric charge $Q_e = Y + T_3$), the gauge anomalies cancellation conditions include $Tr(YT_3^2) = Tr(Y) = 0$, with the trace running over all left-handed fermions. As this condition is respected within the SM, when adding a higgsino we need to add another one of opposite hypercharge so both contributions can cancel.

where a is a gauge index, g is the gauge coupling, T^a are the gauge generators and ϕ is the scalar part of the chiral superfield. The coupling of gauge bosons with either fermions or their scalar partners is given, as in the SM, by the replacements of ordinary derivatives by covariant derivatives in the kinetic term for the fermions and scalars:

$$\mathcal{L}_{kin} = -D^\mu \phi^{*i} D_\mu \phi_i - i\psi^\dagger \bar{\sigma}^\mu D_\mu \psi_i \qquad (3.24)$$

where the covariant derivative is such that

$$D_\mu \phi_i = \partial_\mu \phi_i - ig A_\mu^a \left(T^a \phi \right)_i$$
$$D_\mu \phi^{*i} = \partial_\mu \phi^{*i} + ig A_\mu^a \left(\phi^* T^a \right)^i$$
$$D_\mu \psi_i = \partial_\mu \psi_i - ig A_\mu^a \left(T^a \psi \right)_i \ . \qquad (3.25)$$

Finally interactions of gauginos with matter are given by new SUSY terms:

$$\mathcal{L}_{gauginos} = -\sqrt{2} g \left(\phi^* T^a \psi \right) \lambda^a - \sqrt{2} g \lambda^{\dagger a} \left(\psi^\dagger T^a \phi \right) \ . \qquad (3.26)$$

This completes the set of interactions of matter fields.

3.1.4 R parity

SM particles and their superpartners are differentiated by a new multiplicative, conserved quantum number, R parity. For each MSSM particle R parity is defined as

$$P_R = (-1)^{3(B-L)+2s} \qquad (3.27)$$

with B (resp. L) the baryon (resp. lepton) number of the particle and s its spin. With this definition each SM particle has R parity $+1$ and each of their superpartners has R parity -1.

Within the MSSM R-parity is included to forbid renormalizable B or L violating terms from appearing in the superpotential. If such terms were allowed, fast proton decay, for example, would have been observed unless the size of these new couplings were fine-tuned to be extremely tiny. In the SM there is no need to add a symmetry

to forbid B or L violating terms in the perturbative theory; gauge symmetry does this[5].

The consequences of the conservation of R parity reach far beyond forbidding fast proton decay. R parity conservation implies that superpartners are only produced in pairs, which is an important observation for direct searches for SUSY at the LHC, for example. Of even more importance for the present work is the fact that R-parity conservation renders the lightest superymmetric particle (LSP) stable. This is the crucial element of the MSSM that allows the possibility of a dark matter candidate, as we will discuss further in section 3.3.

3.2 Soft SUSY breaking

3.2.1 Soft Lagrangian

It is clear from experiment that supersymmetry, if indeed an accurate description of Nature, must be a broken symmetry. However one of the main advantages of unbroken SUSY is to offer a solution to the hierarchy problem, and for this reason it is expected that SUSY should be broken in a way that does not bring back large (quadratic) quantum contributions to the Higgs mass. The usual way of obtaining this is to include all SUSY-breaking contributions in a *soft* Lagrangian, $\mathcal{L}_{soft}$, such that the overall effective MSSM Lagrangian is written as

$$\mathcal{L}_{MSSM} = \mathcal{L}_{SUSY} + \mathcal{L}_{soft} . \tag{3.28}$$

No new fields are added in $\mathcal{L}_{soft}$ and all new couplings have positive mass dimension, such that $\mathcal{L}_{soft} \to 0$ when the SUSY-breaking coupling(s), say m_{soft}, goes to zero. Because of this, the additional corrections to the Higgs mass brought about by the terms in $\mathcal{L}_{soft}$ must also vanish in the limit $m_{soft} \to 0$[6]. This in turns forces them

---

[5]Although evidently gauge symmetry does not forbid a L-violating Majorana mass for the right-handed neutrino, which we will discuss in the next chapter. The same is true here as a Majorana mass can be added for the right-handed neutrino to the superpotential even in the presence of R parity conservation.

[6]Since we already know $\mathcal{L}_{SUSY}$ not to generate large quantum corrections to the Higgs mass.

to be at most logarithmic in the cut-off scale. The possible soft-terms are in general (see [27] for a discussion of why these and no other terms are indeed soft)

$$\mathcal{L}_{soft} = A^{ijk}\phi_i\phi_j\phi_k + (m^2)^i_j\phi_i\phi^j + M_a\lambda^a\lambda^a + b^{ij}\phi_i\phi_j \qquad (3.29)$$

where A^{ijk} are called trilinear terms, $(m^2)^i_j$ are SUSY-breaking mass terms for scalar superpartners and M_a terms are mass terms for fermionic superpartners. Within the MSSM only terms for which there exists a corresponding term in the non-SUSY breaking Lagrangian are allowed by gauge symmetries: trilinear terms for which there exist corresponding Yukawa terms, superpartners masses from either m or M terms, and a b term that mixes the up and down Higgses.

As written above $\mathcal{L}_{soft}$ contains a very large number of parameters. A simplified version of it is generally assumed in the vast majority of models that have been analysed. One of these simplifying assumption, sometimes called the minimal flavour violation scenario, MFV, assumes that SUSY-breaking squark and slepton masses are diagonal in flavour space,

$$(m^2)^{i,j}_{Q,U,D,L,E} = \delta^{ij}(m^2)_{Q,U,D,L,E} \qquad (3.30)$$

and trilinear terms are proportional to their corresponding Yukawa terms,

$$A^{i,j,k}_{U,D,E} = a_{U,D,E}\lambda^{i,j,k}_{U,D,E} \ . \qquad (3.31)$$

With this scenario the SM Yukawa couplings are the only source of flavour violation. Within the SM the GIM mechanism [59] offers an effective explanation of why flavour-changing neutral currents, FCNC's, are suppressed; within the MSSM suppressed FCNC can be difficult to obtain due to the potentially large contributions from soft terms. The MFV assumption makes it easier to ensure the accordance of broken SUSY with the known constraints on FCNC[7]. In this work we assume soft parameters follow eq.(3.30) and (3.31). Although we shall not be concerned with flavour effects, MFV is a popular assumption in the literature and a large number of models attempting to explain the origin of SUSY-breaking use it.

---

[7]Soft Lagrangians that respect FCNC constraints without this simplification are also possible.

We can gain one more piece of information on the soft Lagrangian by noting that although large quantum corrections are avoided by our choice of SUSY-breaking terms, this is only true up to the point that the scale of these terms is itself not too large. Indeed, since the quantum corrections on the Higgs mass are logarithmic, for dimensional reasons they must be proportional to m_{soft}^2. Explicitly, the logarithmic correction from the soft terms is [55]

$$\Delta m_{Higgs}^2 = m_{soft}^2 \left(\frac{\lambda^2}{16\pi^2} \log\left(\Lambda_{UV}/m_{soft}\right) \right) . \tag{3.32}$$

where m_{soft} stands for any SUSY-breaking mass or trilinear coupling in eq.(3.30) or (3.31), λ is a generic dimensionless coupling such as the Yukawas in eq.(3.31), and Λ_{UV} is the cut-off scale. Considering a cut-off scale of order the Planck mass, a Yukawa $\lambda \sim 1$ and a Higgs mass of roughly 100GeV, then the soft-breaking scale is $m_{soft} \sim 100 - 1000$GeV. This result we also use as a guideline throughout this work.

3.2.2 The hidden sector framework

As it was introduced here, $\mathcal{L}_{soft}$ explicitly breaks SUSY but gives no explanation of the origin of the various terms it contains. To this end we must first ask whether SUSY can be broken without the introduction of new fields and/or new energy scales. This does not seem to be the case. SUSY is broken if the vacuum energy is positive, eq.(3.8); thus if it is possible for all values of fields to produce either a non-zero D- or F-term in the scalar potential, SUSY must be broken. The Fayet-Iliopoulos mechanism [60] creates a non-zero D-term by introducing in the Lagrangian a term linear in the auxiliary field of a gauge symmetry. This is only possible if the gauge symmetry is $U(1)$. Implementing the Fayet-Iliopoulos mechanism with the $U(1)_Y$ of the SM does not lead to acceptable phenomenology. The O'Raifeartaigh mechanism [61] instead breaks SUSY via a non-zero F-term. This requires the presence of a gauge-singlet chiral superfield for which there could be a linear term in the Lagrangian. Such a gauge singlet is not present in the MSSM. Thus neither D- nor F-term SUSY breaking appears possible within the MSSM only. This remains true in general even when one allows for the inclusion of new fields at the m_{soft} scale (as

obtained from eq.(3.32))[8].

This situation has led to the development of the hidden sector approach, where SUSY-breaking occurs in an higher-energy sector that has suppressed interactions with the MSSM sector, or visible sector. Various hidden sector models differ principally by their choice of the interactions that mediate the breaking of SUSY from the hidden to the visible sector. Two popular choices of mediating interactions are SM gauge interactions and gravity. In gravity-mediated SUSY breaking, the hidden and visible sectors only share gravitational interactions. Some F-term is generated in the hidden sector, and the soft term scale appears as

$$m_{soft} \sim \frac{\langle F \rangle}{M_{Pl}} \tag{3.33}$$

and hence vanishes either when SUSY is unbroken ($\langle F \rangle \to 0$) or gravity is not considered ($M_{Pl} \to \infty$). To obtain an $m_{soft} \sim 10^2 \text{GeV}$, the scale of SUSY-breaking needs to be $\sqrt{\langle F \rangle} \sim 10^{11} \text{GeV}$. We will discuss gravity mediation further in the next section. In gauge-mediated SUSY breaking a new messenger sector is added; it shares gauge interactions with the visible sector and couples to the SUSY-breaking F-term of the hidden sector. In the visible sector diagrams involving gauge and gaugino fields can now include messenger loops, leading to the effective appearance of the soft terms. The soft term scale is thus, on dimensional grounds,

$$m_{soft} \sim \frac{g^2}{(4\pi)^2} \frac{\langle F \rangle}{m_{mess}} \tag{3.34}$$

where the first term is a loop factor (with gauge coupling $g \sim O(1)$) and m_{mess} is the messenger sector mass scale. Here the scale of SUSY-breaking can be much lower than in the gravity-mediation case; for instance for a messenger mass of $m_{mess} \sim 10^{10} \text{GeV}$, a SUSY-breaking scale of $\sqrt{\langle F \rangle} \sim 10^7 \text{GeV}$ is obtained.

---

[8]This is due to the existence of sum rules that link various masses of the MSSM and that are valid if only renormalisable tree-level SUSY breaking is present. Were these sum rules valid, some sleptons or squarks would have to have masses much smaller than m_{soft}, and would have been discovered already.

3.2.3   Supergravity and the gravitino

Although somewhat tangential to the subject of this work, we wish for completeness to briefly describe the idea of supergravity, or SUGRA. Taking SUSY as a local symmetry instead of global one leads to the inclusion of gravitational effects[9], though the obtained Lagrangian is non-renormalisable. Within SUGRA the spin-2 graviton is accompanied by its superpartner the spin-3/2 gravitino. Global SUSY breaking implies the existence of a massless goldstino, the fermionic equivalent of the more usual Goldstone boson[10]. In a manner reminiscent of the Higgs mechanism, upon local SUSY breaking the gravitino 'eats' the goldstino to become massive. This is the so-called super-Higgs mechanism. In the case of F-term breaking the gravitino mass, $m_{3/2}$, is given by

$$m_{3/2} \sim \frac{\langle F \rangle}{M_{Pl}} \,, \tag{3.35}$$

which vanishes when SUSY is restored or when gravity effects are ignored. In gravity-mediated SUSY breaking, the gravitino mass and the soft scale are the same, and so the gravitino has mass similar to the other superpartners. In such a case the gravitino being the LSP is a possibility, although it is not in a different position than any other superpartner. In gauge-mediated SUSY-breaking, the gravitino mass can be much smaller than the soft scale, depending on the size of the messenger scale. For the example given above with a messenger scale of $m_{mess} \sim 10^{10}$GeV, the gravitino mass would be as low as $m_{3/2} \sim 10^{-5}$GeV. In such a case, the gravitino is most likely to be the LSP. In this work we shall use $m_{soft} = m_{3/2}$ as a rule of thumb, and assume the gravitino not to be the LSP of the MSSM.

---

[9] A hint of this phenomenon can be obtained by recalling that the SUSY algebra, eq.(3.1), contains the spacetime operator. When considering local SUSY transformations we should be led to consider local spacetime transformations, and thus general relativity.

[10] The 'Goldstone field' needs to be a fermion because the SUSY generators are themselves fermionic.

3.3   Lightest supersymmetric particle dark matter

Although SUSY was not originally introduced to address the question of dark matter, it was soon realised that the MSSM naturally contains a dark matter candidate [40]. As we have mentioned, within the MSSM R-parity ensures that the lightest supersymmetric particle is stable; if moreover this particle has no electric charge or colour (see our discussion in section 2.3) and is not produced in such quantities that it overcloses the Universe, then it is a good dark matter candidate.

The MSSM indeed contains a neutral, colourless massive particle: it is the neutralino. We have not yet mentioned the neutralino explicitly, although we have all the necessary ingredients to discuss it. Looking back at eq.(3.26) we see it includes the possibility of a gaugino-higgsino-higgs coupling; once the higgs has acquired its *vev* then this terms becomes a mixing term between a gaugino and a higgsino. Hence the overall gaugino-higgsino mass matrix needs to be diagonalised to obtain the mass eigenstates. The charged states are generally called charginos, C_i's and the neutral states, neutralinos, χ_i's. The neutralinos' only gauge interactions are $SU(2)$ interactions and their mass stems from SUSY-breaking terms, as we have discussed. If the lightest of the four neutralinos is also the LSP, then it is a dark matter candidate. As we have mentioned, none of the aspects of the MSSM that lead to the existence of the neutralino were introduced to allow for a dark matter candidate: it instead appears as a 'bonus' of the model. The only assumption is that the neutralino is the LSP. Supposing the MSSM to be an appropriate description of nature, then if the neutralino is indeed the LSP, there is now the possibility of the neutralinos being the main source of dark matter, but also of an overclosure of the Universe due to an over-abundance of neutralinos. The first evaluation of the neutralino relic density was obtained in [40] and helped establish the LSP as the very popular dark matter candidate it is now. Let us review the argument. We follow the treatment of [11]

We recall from chapter 2 that the number density of a particle is given by eq.(2.16),

$$n = \frac{g}{(2\pi)^3} \int f(\vec{p}) d^3 p \ . \tag{3.36}$$

The neutralino has strong enough interactions to be kept in thermal equilibrium, which means its number density is described by the above expression with the Fermi-Dirac distribution as its distribution function,

$$f(\vec{p}) = \frac{1}{e^{E(\vec{p})/T} + 1} \, .$$ (3.37)

At early times, when $T \gg m$, the equilibrium number density follows $n^{eq} \sim T^3$, while at later times, $T \ll m$, it instead follows

$$n^{eq} \sim g \left(\frac{mT}{2\pi} \right)^{3/2} e^{(-m/T)}$$ (3.38)

meaning it decreases exponentially. As we have seen however, due to the expansion of the Universe we expect the annihilation and creation processes to eventually freeze-out, leaving the number density per comoving volume fixed at the equilibrium amount at freeze-out[11].

In the case of a relic X in equilibrium until the time of freeze-out and for which there is no sizeable particle-antiparticle asymmetry, the Boltzmann equation (eq. 2.17) can be rewritten as

$$\dot{n}_X + 3Hn_X = -\langle \sigma_A v \rangle \left[(n_X)^2 - (n_X^{eq})^2 \right]$$ (3.39)

where n_X is the number density of X, $\langle \sigma_A v \rangle$ is the thermally averaged total annihilation cross-section for X and the rate of annihilation is given by $\Gamma_A = \langle \sigma_A v \rangle n_X$. Freeze-out occurs when $H = \Gamma_A$. We have $H = 1.66 g_*^{1/2} T^2 / M_{Pl}$ (eq. (2.22)), so that freeze-out happens when

$$\frac{1.66 g_{*,F}^{1/2} T_F^2}{M_P} = \langle \sigma_A v \rangle n_{X,F}$$ (3.40)

which implies

$$n_{X,F} = \frac{1.66 g_{*,F}^{1/2} T_F^2}{M_P \langle \sigma_A v \rangle}$$ (3.41)

---

[11]See figure 4 of [11].

where the index F stands for freeze-out. After freeze-out the relic number density per comoving volume is conserved,

$$\frac{n_X}{s}\bigg|_{now} = \frac{n_X}{s}\bigg|_F$$
$$\simeq \frac{3.8}{g_{*,F}^{1/2} M_P \langle \sigma_A v \rangle T_F} \tag{3.42}$$

where we have used $s = \frac{2\pi^2}{45} g_* T^3$, eq.(2.18). The freeze-out temperature also depends on the annihilation rate. Let us relate this number density to a quantity more amenable to comparison with the observed dark matter density (eq.(2.27)); we define

$$w_X \equiv \frac{\rho_X h^2}{\rho_c}\bigg|_{now}$$
$$= \frac{h^2 s}{\rho_c}\bigg|_{now} \frac{m_X n_X}{s}\bigg|_{now} . \tag{3.43}$$

If X forms the entirety of dark matter $(w_X = w_{DM})$, then using eq.(3.42), the annihilation rate and freeze-out temperature should be related with the cosmological parameters via

$$\frac{\langle \sigma_A v \rangle T_F}{m_X} = \frac{h^2 s}{\rho_c} \frac{1}{w_{DM}} \frac{1}{g_{*,F}^{1/2}} \frac{3.8}{M_P} \tag{3.44}$$

Let us first evaluate the left-hand side of this expression; considering a relic mass of $m_X \sim 100\text{GeV}$ with only weak scale interactions implies

$$\langle \sigma_A v \rangle \sim \frac{\alpha_w^2}{100^2 \text{GeV}^2}$$
$$\simeq 10^{-8} \text{GeV}^{-2} . \tag{3.45}$$

The freeze-out temperature also depends on the annihilation cross-section, though this time a more involved calculation is necessary; for weak scale interactions, the freeze-out temperature turns out to be $T_F \sim m_X/20$ (see [40] for details). Thus for our neutralino we obtain

$$\frac{\langle \sigma_A v \rangle T_F}{m_X} \simeq 5 \times 10^{-10} \text{GeV}^{-2} . \tag{3.46}$$

Using table 2.2 we can calculate the right-hand side of equation (3.44),

$$\frac{h^2 s}{\rho_c} \frac{3.8}{g_{*,F}^{1/2} M_P} \simeq 1 \times 10^{-10} \text{GeV}^{-2} . \tag{3.47}$$

with $g_{*,F} \sim 80$, corresponding to $T_F \sim m_X/20$. Thus as long as the assumptions we have considered hold, the neutralino (or any other weakly interacting massive particle, WIMP) 'naturally' has the correct relic density to be the dark matter. This result was obtained rather early in the development of the MSSM [40], and remains very important in the understanding of the dark matter question.

3.3.1 Mattergenesis revisited

As we have seen, in general the relic density of the neutralino LSP is of the same order than the observed dark matter density. If indeed the MSSM is an accurate description of Nature, and the neutralino is the LSP, than there is in general no need for mattergenesis. Any alternative scenario that involves a different dark matter candidate produced via a mattergenesis mechanism but that accepts the MSSM as an accurate description of Nature is confronted with the possibility of overclosure due to the relic LSP. For this reason it is important for our work to mention that although the result of the previous section holds in general, a number of special cases can alter it sizeably. For instance coannihilation [62] can occur when there exists a particle almost degenerate in mass with the candidate. If the candidate can convert into this new particle, and it has interactions much faster than the candidate, then it is the annihilation of the new particle that mainly determines the candidate's relic density. It is also possible for the candidate and quasi-degenerate particle to directly annihilate together, again modifying the candidate's relic density. This is a possibility for a neutralino of any composition, since we know little of the mass spectrum of the MSSM, but it is especially important in the case of a neutralino very largely composed of a higgsino, as in this case close-by charginos will induce coannihilations [11]. An analysis of the relic density of the neutralino as a function of its main component reveals that coannihilations can play an essential role and that both very small and very large relic densities can be achieved [63]. We will discuss this situation again in chapter 6, but for now it suffices to say that the results presented in the previous section should not be interpreted as a case against mattergenesis, but rather as an interesting observation that has often been used to argue for WIMP dark matter.

Chapter 4

Massive neutrinos

4.1 Evidence of neutrino masses

Over the recent years the existence of a non-zero mass for the neutrinos has been confirmed by a variety of experiments, involving solar, atmospheric, reactor and accelerator neutrino experiments [64]. These various experiments all make use of the fact that if the neutrinos have masses, then their mass and weak eigenstates need not be the same (just as is the case with quarks), and this mixing of states would cause neutrinos to change into one another as they propagate. The evidence for flavour changing in neutrinos is by now very strong [65]. The Super-Kamiokande experiment [66] studies neutrinos produced in cosmic rays, a source that is isotropic around the Earth. It has measured that neutrinos that come from above the experiment and neutrinos that enter the detector after having traversed the Earth do not however come in comparable numbers. This experiment has allowed to measure the oscillation of (what is best described as being) ν_μ to ν_τ, and obtain the corresponding mass square difference Δm^2_{atm} of (as cited in [64])[1]

$$\Delta m^2_{atm} = 2.2 \times 10^{-3} \text{eV}^2 .$$

(4.1)

---

[1]Here we should mention that by 'mass square difference' or 'mass square splitting' we mean generally $\Delta m^2_{1,2} = m^2_1 - m^2_2$. Hence a mass square splitting can be negative.

Here the index refers to 'atmospheric neutrinos' or neutrinos produced by cosmic rays within our atmosphere. The Super-Kamiokande data is well supported by the K2K experiment [67], that has measured the 'disappearance' (or oscillation to another species) of ν_μ's produced at the Kamioka accelerator.

The phenomenon of neutrino oscillation has also been observed in 'solar' neutrinos (neutrinos produced within the Sun). The Subdury Neutrino Observatory (SNO) [68, 69] has measured that the flux of ν_μ and ν_τ from the Sun is non-zero, despite the fact that the Sun only produces ν_e neutrinos; moreover the total amount of neutrinos (ν_e, ν_μ, ν_τ) from the Sun detected at SNO agrees with the calculations of (ν_e) neutrino production in the Sun. In other words, the amount of neutrinos received at SNO from the Sun is as expected, but the composition is not: the amount of ν_e is too small, but the missing quantity is made up of other types of neutrinos. This is very compelling evidence for neutrino oscillations, and in turn for the existence of neutrino mass. The best-fit mass square splittings difference in solar neutrinos (as obtained by combining the data from SNO and KamLAND [70, 71], which measures reactor ν_e) is obtained to be [64]

$$\Delta m^2_{Sun} = 8.1 \times 10^{-5} \text{eV}^2 .$$ (4.2)

The Los Alamos Liquid Scintillation Detector experiment (LSND) [72] also reports the apparition of $\bar{\nu}_e$ from another neutrino species, $\bar{\nu}_\mu$. LSND measures accelerator neutrinos produced in the decay $\mu^+ \rightarrow e^+\nu_e\bar{\nu}_\mu$. The corresponding mass square splitting is in this case [64]

$$\Delta m^2_{LSND} \sim 1\text{eV}^2 .$$ (4.3)

This result has not yet been confirmed by any other experiment. The MiniBooNE experiment [73] is designed to test the LSND results.

With three neutrinos in the SM it is not surprising that we would have three distinct mass splitting. These three mass splittings, however, have to be such that

$$\Delta m^2_{1-2} + \Delta m^2_{2-3} + \Delta m^2_{3-1} = 0$$ (4.4)

if there are indeed to be only three neutrino species involved. As we have seen, the atmospheric, solar and 'LSND' mass splitting are all of different orders of magnitude,

and for this reason it is impossible that eq.(4.4) be respected if LSND is confirmed. The simplest explanation for this situation is to include a fourth light neutrino in the analysis. As it is already well known that only three light neutrinos couple to the weak gauge bosons [21], this fourth neutrino would have to be sterile with respect to the weak interaction[2]. To understand the importance of this possibility, we need discuss the ways in which the neutrino mass can be included in the SM; the next section is concerned with this.

Before we go on however it is worth mentioning that although the experiments we have discussed up to now give no indications of the absolute mass scale of the neutrinos, it is not the case that we possess no clues as to what this scale might be. Considering the solar and atmospheric mass splittings to be involving the three SM neutrinos, three possible arrangements of the neutrinos emerge, as shown in fig.(4.1) [74].

If the neutrinos have non-degenerate masses, then the mass of the heaviest neutrino must be around $m_H \gtrsim \sqrt{\Delta m_{atm}^2} = 4.7 \times 10^{-2}$. If on the other hand they are degenerate, then a priori not much can be said on the absolute mass scale from the oscillation data. However cosmology gives some constraints on the absolute mass scale of the neutrinos as well. Indeed it is possible to obtain limits on the neutrino masses from the study of the power spectrum of matter on large scales [74]. For a three neutrinos model this implies [75]

$$\Sigma m_\nu < 1.01\text{eV} \tag{4.5}$$

and goes up to

$$\Sigma m_\nu < 2.12\text{eV} \tag{4.6}$$

for five neutrinos. Taking these along with the conclusions drawn from the mass splittings, we conclude that a reasonable guess for the scale of the neutrino masses

---

[2]If it is to explain a confirmed LSND result, this additional 'sterile' neutrino would still have to share *some* interaction with the SM neutrinos so as to, at the very least, allow mixing with one of them.

(a) (b)
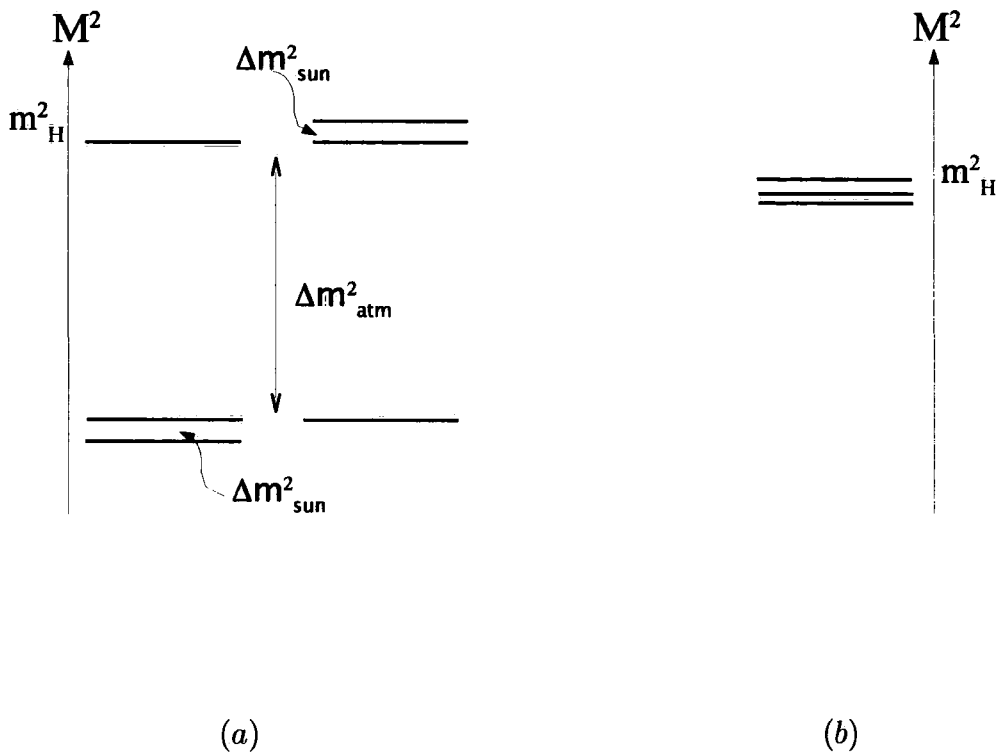
Figure 4.1: Possible neutrino masses configurations. Each line represents the mass square of a neutrino of the SM, and m_H stands for the mass of the heaviest neutrino. (a) Hierarchical and inverted hierarchy neutrinos. The exact emplacement of the zero of the mass square scale is unknown but close to the smallest neutrino mass square. In both cases $m_H \sim \sqrt{\Delta m_{atm}^2}$ (b) Degenerate neutrinos. The zero of the mass square scale is far below the neutrino masses square. Here $m_H \gg \sqrt{\Delta m_{atm}^2}$.

could be

$$m_\nu \sim O(10^{-2} - 10^{-1})\text{eV} . \tag{4.7}$$

This is the estimate we shall use throughout this work. Attempts at measuring neutrinos masses directly such as the KATRIN experiments [76] and others [77, 78] are under way. The KATRIN experiment is concerned with studying the energy spectrum of the electron produced in tritium decay,

$$^3H \rightarrow ^3He^+ + e^- + \bar{\nu}_u . \tag{4.8}$$

Although only the electron's energy spectrum is available, it depends on the neutrino mass. The careful study of the higher end of the spectrum (where neutrino mass

effects are relatively most significant) could lead to an absolute determination of the neutrino mass. As of now the limits on the total mass of the neutrinos involved in tritium decay (including mixing effects) obtained in this way are

$$\sqrt{\sum_i |U_{ie}|^2 m_{\nu,i}^2} \leq 2.3\text{eV}, \ 2.2\text{eV} \tag{4.9}$$

as obtained by [77] and [78], respectively, as cited in [38]. Here U_{ie} is a matrix element of the neutrino mass mixing matrix that relates the electron neutrino to any other it might mix with.

4.2 Dirac and Majorana masses

4.2.1 See-saw mechanism

In the Standard Model the neutrinos do not have mass at all, or equivalently there is no mass term that appears for them in the Lagrangian. As all the other SM particles evidently have mass in the SM, we already know a way of including a mass term for the neutrinos. Copying what already exists for the quarks and leptons, we can simply add to the SM a set of three right-handed neutrinos ν_R and in turn write down a new Dirac term in the Lagrangian [65]:

$$\mathcal{L}_D = -m_D \overline{\nu_L} \nu_R \tag{4.10}$$

where the mass parameter m_D is related to the Higgs *vev* v through the new neutrino Yukawa coupling λ_ν in the usual way,

$$m_D = \lambda_\nu v \ . \tag{4.11}$$

In models where the neutrino mass is constructed solely from a new Dirac term in the Lagrangian the neutrinos are said to be Dirac neutrinos.

Two very important questions arise from this simple analysis: first, eq.(4.11) tells us that the Yukawa coupling for the neutrinos should be of the order $\lambda_\nu \sim O(10^{-13})$, which is much smaller than the quarks Yukawa couplings (which only illustrates the smallness of the neutrino masses themselves compared to the masses of the quarks

and leptons)[3]. Second, this analysis overlooks a very specific aspect of the neutrinos, which is that contrary to the quarks and leptons, they do not have an electric charge. Because of their absence of electric charge, it is possible to write a Majorana mass term for the neutrinos:

$$\mathcal{L}_M = m_R \overline{\nu_R^c} \nu_R \ . \tag{4.12}$$

Such a mass term is forbidden for any other matter particle of the SM because it would not conserve electric charge. This term however does not conserve lepton number. But lepton number is an accidental symmetry in the SM: it is conserved solely because electric charge is conserved, and imposing electric charge conservation happens to also forbid lepton number violation.

The most popular theory of the neutrino mass links these two peculiarities of the neutrinos (the smallness of the mass and the absence of an electric charge). In the original see-saw mechanism [79–83], a Majorana mass term is added for the right-handed neutrinos and a Dirac mass term is added as well. The obtained 'Majorana neutrinos mass matrix' (in a basis of left-handed and right-handed neutrinos) is given by [38]:

$$\mathcal{M} = \begin{pmatrix} 0 & v\lambda_\nu \\ v\lambda_\nu & M_R \end{pmatrix} \ .$$

Considering very large Majorana masses, $M_R \gg v\lambda_\nu$ leads to the matrix having one eigenvector that is mainly composed of the left-handed neutrino of the original basis with an associated mass that is very small, $\frac{(v\lambda_\nu)^2}{M_R}$, and another eigenvector mainly composed of the right-handed neutrino of the original basis associated with a large mass M_R. Thus the observed left-handed neutrinos could have very small masses while having Yukawa couplings comparable to the ones of the charged leptons, say, due to the fact that there exists a large Majorana mass for the right-handed neutrinos. A Yukawa coupling of order $\lambda_\nu \sim 1$ leads to a mass scale for the unobserved right-handed neutrinos of $M_R \sim 10^{15}$GeV.

---

[3]Although it should be noted that even excluding the neutrino mass, within the quarks and leptons there already exist a large disparity of Yukawa couplings, from the top Yukawa, $\lambda_t \simeq 1$ to the up Yukawa, $\lambda_u \simeq 10^{-5}$ or the electron one, $\lambda_e \simeq 10^{-6}$.

This short introduction does not render justice to the many ramifications of the see-saw mechanism. Much work has been done to understand how a pattern such as eq.(4.2.1) can arise from higher energy theories such as GUT, or why the mixing angles observed between the various neutrinos are as they are (see for example [38]). In this work we wish to take a different route and consider the case of Dirac neutrinos. To better understand why, let us discuss the status of evidence regarding the nature of the neutrino mass.

4.2.2 Experimental status

Two important phenomenological differences appear between Dirac and Majorana neutrinos[4] as a result of the exclusion or inclusion of the Majorana mass term in the Lagrangian. When neutrinos are purely Dirac, both the left-handed and right-handed neutrinos are very light, as can be seen from eq.(4.10). This implies that we have now included in the particle zoo a certain number of new light particles, or 'right-handed neutrinos'. These will be completely sterile, however, as they have no charge at all under the SM symmetry group. In the see-saw Majorana case evidently the corresponding new particles are far from light. More generally when including a Majorana mass the additional degrees of freedom needn't be light; this is because there is a priori no expected scale for the Majorana mass as it is unrelated to the scale of the gauge symmetry breaking, unlike Dirac mass terms [84]. The second experimentally important difference between Dirac and Majorana neutrinos is the fact that Majorana neutrinos, no matter the relative size of their Dirac and Majorana mass terms, are their own anti-particle, meaning that $\nu = \bar{\nu}$ in the Majorana case[5]. Dirac neutrinos are not their own anti-particles, in the same way that none of the

---

[4]Here we use the name 'Majorana neutrinos' in a generic sense as being neutrinos that do have a Majorana mass term, as opposed to the special case of 'Dirac' neutrinos, or neutrinos that only have a Dirac mass term.

[5]This can be explained by the fact that the inclusion of a Majorana mass, no matter its size, causes non-conservation of the lepton number. As the lepton number is the only number that distinguishes neutrino and anti-neutrino, there is no sense in which Majorana neutrinos can be distinguished from their anti-particle.

charged leptons are. Both these differences are being exploited in the quest for determining experimentally the nature of neutrinos.

- LSND and MiniBooNE

We have already touched upon the possibility of the existence of an additional light degree of freedom. The simplest explanation for a confirmation of the LSND results would be to include at least one light sterile neutrino. Testing whether the LSND results can be confirmed is thus of high importance. At the moment various short baseline experiments (see references within [64]) have not measured the oscillation observed by LSND, although there is parameter space left for LSND still to be accurate. The MiniBooNE experiment [73] aims to test this possibility. It should not however be taken for granted that a confirmation of the LSND result straightforwardly implies the existence of exactly one light sterile neutrino. Indeed, fits of the LSND results combined with the global neutrino oscillations available data to four neutrino models yield poor results [64]. A five neutrinos model yields a better fit with the global data [85]. It should not be concluded either that a confirmation of the LSND result can only imply Dirac neutrinos - many interpretations might arise in this situation [86]. What is certain however is that a confirmation of the LSND result would yield an interpretation of the neutrino sector very different from the Majorana see-saw picture that is most widely studied at the moment.

- Neutrinoless double beta decay

Whether or not neutrinos are their own anti-particle might well be determined in the not-so-distant future by studying double beta decay. If a nucleus containing A nucleons, Z of which being protons, undergoes a double beta decay in which two protons turn into neutrons, then two anti-electrons and two neutrinos should be emitted to conserve charge and lepton number. If lepton number is not conserved, however, the two neutrinos needn't be there[6]. Thus

---

[6]Put another way the two emitted neutrinos could annihilate one another, being each other's anti-particle.

if neutrinos are Majorana particles neutrinoless double beta decay is possible, while if they are Dirac particle it is not. Although there might be many other sources of double beta decay than only the existence of a Majorana mass, it can be shown that the observation of double beta decay necessarily implies that at least one of the neutrinos is a Majorana particle [65]. Various experiments are under way to try and observe neutrinoless double beta decay in different nuclei (see [87] for a review).

Unless there is a clear neutrinoless double beta decay signal, determining the nature of the neutrino mass is unlikely to be straightforward, especially if it turns out neutrinos are Dirac particles. In such a case no signal will be seen at neutrinoless double beta decay experiments, and other experiments' results will be needed as well to decide whether there simply is no signal or whether the signal can still have eluded detection. Table (1) of [38] gives an overview of the possible outcomes of experiments. Moreover, it should be pointed that a refutation of the LSND result does not necessarily rule out the existence of light sterile neutrinos with smaller couplings to active neutrinos than required by LSND. Despite these difficulties, the key points for our work here are that first, from an experimental point of view the possibility of Dirac neutrinos is not yet excluded, and second the Dirac or Majorana nature of the neutrino mass might be elucidated in the coming years.

4.3 Dirac neutrinos

4.3.1 Constraints on Dirac neutrino models

Before turning to describing some Dirac neutrino models, let us first list the main questions they must address.

It is obvious that Dirac neutrino models can barely escape explaining the smallness of the neutrino mass, as the see-saw mechanism already does. In the case of Dirac models, the neutrino mass scale is directly related to the Yukawa scale (see eq. (4.11)). Thus the burden is to explain the size of the neutrino Yukawa coupling compared to the size of other fermions' couplings in the SM. We will see shortly that

indeed this is the very first question Dirac neutrino models assess, and that there exist a number of models that do so successfully[7].

Moreover, it is often argued that including a Majorana mass for the RH neutrino is more natural than excluding it, because there appears to be no need for reinforcing lepton-number conservation, which is only an accidental symmetry of the SM. It can also be argued, however, that since the inclusion of a Majorana mass breaks the lepton number symmetry that is not broken by a Dirac mass, a Majorana neutrino can be considered less natural than a Dirac neutrino. Moreover conservation of $B-L$ would be in line with, for example, ideas of quark-lepton symmetry. Quark-lepton symmetry is obviously not inherent to the SM, and taking it into account amounts to forbidding a Majorana mass via new physics; this is the road many models follow. To sum, Dirac neutrino mass models need tackle the question of why a Majorana mass for the RH neutrino does not appear in the new model, most probably by including a new symmetry that forbids it.

Finally the inclusion of new light degrees of freedom that is specific to Dirac models[8] incurs some additional cosmological constraints. The addition of new relativistic degrees of freedom in equilibrium at the time of BBN modifies the rate of expansion of the Universe and in turn the moment at which the weak interactions freeze-out, which can have important consequences on the abundances of primordial elements [88]. A careful study of this implies that only up to five 'effective' neutrinos can exist if BBN is to be kept safe [17]. This effectively constrains the mixing of light sterile neutrinos with the known active neutrinos. Thus, whether or not the new Dirac sterile neutrinos can be consistent with BBN is highly model-dependent.

---

[7]It could be said as well that some incarnations of the see-saw mechanism have been effective at explaining other aspects of neutrino physics than merely their mass [38]. This is unfortunately outside the scope of this work.

[8]Some versions of the see-saw mechanism can accommodate light right-handed neutrinos [38,88], but what we mean here is that specific to Dirac model is the *necessity* of some new light degrees of freedom.

4.3.2 Some Dirac neutrino models

There exist a number of Dirac neutrino models that address either all or most of the questions we have just mentioned. Let us survey some of the most popular possibilities for Dirac neutrinos (a short overview is given in [89]).

In theories with large extra dimensions, the SM particles propagate in the usual (3 + 1) dimensions while the added right-handed neutrinos propagate also in the added dimension(s). The resulting Yukawa coupling is suppressed due to the suppression of the overlap of the left-handed neutrino and Higgs wave functions and the right-handed neutrino wave function. The suppression factor is linked to the volume of the extra-dimensional space, and can be sufficiently small. Only (SM) gauge singlets can propagate in the bulk, hence the mass suppression of neutrinos alone. (See [38, 90] and references therein.)

Superstrings might also offer the possibility of models of small Dirac masses for neutrinos, as in [91]; see [38] for a discussion.

Some extensions of left-right symmetric models can produce small Dirac neutrino masses by having them vanish at tree level but arise at one or two loop levels [92] (and see [88] for an overview).

Finally SUGRA and SUSY breaking can provide a way to suppress the neutrino mass in the Dirac case, as was noted by [93, 94] and others. This is reminiscent of an idea suggested earlier by [95] in which instead it is the μ-term of the Higgses that is suppressed in this way. If the Dirac mass term of the neutrinos is, for some new symmetry reason, prevented from appearing in the superpotential, it might still be allowed to appear in the Kähler potential. The Kähler potential is an additional function of the chiral fields that appears within SUGRA. Within this potential the neutrinos could interact with the hidden fields that are responsible for SUSY-breaking; in fact the Yukawa term, present in the Kähler potential, could obtain its strength via this coupling to the SUSY-breaking field, and in such a case the effective Yukawa coupling should be suppressed by $m_{3/2}/M$, where M is the SUSY-breaking

scale and we recall that $m_{3/2}$ is the gravitino mass[9]. Especially interesting with this approach is the fact that no new scale is necessary, as opposed to the see-saw mechanism. Here the suppressing effect comes directly from SUSY-breaking, which is necessary for completely different reasons, as we have seen in section 3.2.

---

[9]We remind the reader that, from eq.(3.35), the gravitino mass is $m_{3/2} \sim \langle F \rangle / M_{Pl}$, which altogether means the neutrino mass would be suppressed by a factor $\langle F \rangle / (M M_{Pl})$. It would disappear either when gravity is neglected or when SUSY is restored, consistent with its absence from the superpotential.

Chapter 5

Dirac Right-Handed Sneutrinos in the MSSM

Let us now discuss the very model we shall be using for studying the Dirac right-handed neutrino, its cosmology and the possibility of leptogenesis. We wish to add to the MSSM and right-handed neutrino superfield, but by only adding a Dirac mass term and no Majorana mass. Here we discuss the superpotential that includes such a term, along with additional soft-breaking term. We also discuss the left-right mixing of the sneutrinos, the right-handed sneutrinos interactions, and its direct detection possibilities should it be the main component of dark matter.

5.1 Addition of the Dirac superfield to the MSSM

We add to the MSSM a RH neutrino superfield $\bar{N}$ which is given a Dirac mass term in the superpotential $\mathcal{W}$, so that the part of the superpotential that is of interest here is

$$\mathcal{W} \supset \lambda L^i \epsilon_{ij} h_u^j N_R^c - \lambda_e L^i \epsilon_{ij} h_d^j e_R^c + \mu h_u^i \epsilon_{ij} h_d^j , \qquad (5.1)$$

where L is the left-handed (LH) slepton doublet, h_u (resp. h_d) is the up-type (resp. down-type) Higgs field, and e_R^c is the right-handed selectron field. New terms ob-

tained from $\mathcal{W}$ and involving the RH sneutrino are:

$$
\begin{aligned}
\mathcal{L}_F &= -\sum_{i=L,H_u,N_R} \left| \frac{\partial W}{\partial \phi_i} \right|^2 - \sum_{i,j=L,H_u,N_R} \frac{\partial^2 W}{\partial \phi_i \phi_j} \psi_i \psi_j \\
&= -\lambda^2 \left(\tilde{e}_L \tilde{e}_L^* \tilde{\nu}_R^c \tilde{\nu}_R^{c*} + h_u^+ h_u^{+*} \tilde{\nu}_R^c \tilde{\nu}_R^{c*} + \tilde{\nu}_L \tilde{\nu}_L^* \tilde{\nu}_R^c \tilde{\nu}_R^{c*} + h_u^0 h_u^{0*} \tilde{\nu}_R^c \tilde{\nu}_R^{c*} \right) \\
&\quad + \lambda \left(\tilde{\nu}_R^c \tilde{H}_u^+ e_L - \tilde{\nu}_R^c \tilde{H}_u^0 \nu_L - \tilde{\nu}_L \tilde{H}^0 \nu_R^c \right) \\
&\quad - \mu \lambda \left(h_d^0 \tilde{\nu}_R^c \tilde{\nu}_L + h_d^- \tilde{\nu}_R^c \tilde{e}_L + h.c. \right) .
\end{aligned}
\tag{5.2}
$$

We are also adding new SUSY-breaking terms

$$
\mathcal{V}_{SB} = m_{\tilde{\nu}_L}^2 \tilde{\nu}_L^* \tilde{\nu}_L + m_{\tilde{\nu}_R}^2 \tilde{\nu}_R^{c*} \tilde{\nu}_R^c + \left(a\lambda \left(h_u^0 \tilde{\nu}_L \tilde{\nu}_R^c + h_u^+ \tilde{e}_L \tilde{\nu}_R^c + h.c. \right) \right)
\tag{5.3}
$$

where a is a mass dimension trilinear coupling.

5.2 Mass mixing of the sneutrinos

Because of the presence of both a Yukawa term and a trilinear term for the sneutrinos, left- and right-handed sneutrinos experience mass mixing, similarly to any other sfermion in the MSSM [57]. This mass mixing is unrelated to the mass mixing in the neutrino sector that would happen with the introduction of a Majorana mass. Here what we have is a purely SUSY-breaking effect which affects only the scalar neutrinos and occurs no matter what is the neutrino model used.

5.2.1 Parameterisation of the mixing

Let us consider what happens after the higgses have acquired vacuum expectation values (vev's). Considering the mass terms in the Lagrangian:

$$
\mathcal{L}_{mass} = -m_{\tilde{\nu}_R}^2 \tilde{\nu}_R^{c*} \tilde{\nu}_R^c - m_{\tilde{\nu}_L}^2 \tilde{\nu}_L^* \tilde{\nu}_L - \lambda v \left(a \sin\beta + \mu \cos\beta \right) \tilde{\nu}_L \tilde{\nu}_R^c + h.c.
\tag{5.4}
$$

where the higgses has been replaced by their vev's,

$$
\begin{aligned}
\left(\langle h_u^+ \rangle, \langle h_u^0 \rangle \right) &= (0, v\sin\beta) \\
\left(\langle h_d^0 \rangle, \langle h_d^- \rangle \right) &= (v\cos\beta, 0) .
\end{aligned}
\tag{5.5}
$$

For simplicity we will consider in the remainder of this work the case $\tan\beta \gg 1$ while $a \sim \mu$, and thus will drop the μ term. Reintroducing it is straightforward.

To study the mass mixing effect we need to diagonalise the following mass matrix

$$M = \begin{pmatrix} m_R^2 & a^*\lambda v \\ a\lambda v & m_L^2 \end{pmatrix} .$$

The mass eigenvalues are

$$m_\pm^2 = \left(\frac{m_L^2 + m_R^2}{2} \right) \pm \sqrt{\left(\frac{m_L^2 - m_R^2}{2} \right)^2 + |a|^2 \lambda^2 v^2} . \tag{5.6}$$

Defining

$$\begin{aligned} M^2 &= \left(\frac{m_L^2 + m_R^2}{2} \right) \\ m^2 &= \left(\frac{m_L^2 - m_R^2}{2} \right) \\ A^2 &= a\lambda v \end{aligned} \tag{5.7}$$

we have that in general the mass eigenvalues are

$$m_\pm^2 = M^2 \pm \sqrt{(m^2)^2 + (A^2)^2} . \tag{5.8}$$

From now on we deal with the μ-terms in the way mentioned in the previous section.

We are now left with obtaining the mass eigenstates; in the general case those are

$$\begin{aligned} \tilde{\nu}_+ &= \frac{1}{|\tilde{\nu}_+|} \left[A^2 \tilde{\nu}_R^c + \left(m^2 + \sqrt{(m^2)^2 + (A^2)^2} \right) \tilde{\nu}_L \right] \\ \tilde{\nu}_- &= \frac{1}{|\tilde{\nu}_-|} \left[\left(m^2 + \sqrt{(m^2)^2 + (A^2)^2} \right) \tilde{\nu}_R^c - A^2 \tilde{\nu}_L \right] \end{aligned} \tag{5.9}$$

with

$$|\tilde{\nu}_+|^2 = |\tilde{\nu}_-|^2 = \left(m^2 + \sqrt{(m^2)^2 + (A^2)^2} \right)^2 + (A^2)^2 . \tag{5.10}$$

We define the mixing angle θ such that

$$\begin{aligned} \cos\theta &= \frac{\left(m^2 + \sqrt{(m^2)^2 + (A^2)^2} \right)}{|\tilde{\nu}_+|} \\ \sin\theta &= \frac{A^2}{|\tilde{\nu}_+|} \end{aligned} \tag{5.11}$$

so that

$$\begin{aligned} \tilde{\nu}_+ &= \sin\theta \tilde{\nu}_R^c + \cos\theta \tilde{\nu}_L \\ \tilde{\nu}_- &= \cos\theta \tilde{\nu}_R^c - \sin\theta \tilde{\nu}_L \end{aligned} \tag{5.12}$$

and conversely

$$\tilde{\nu}_L = \cos\theta\tilde{\nu}_+ - \sin\theta\tilde{\nu}_-$$

$$\tilde{\nu}_R^c = \sin\theta\tilde{\nu}_+^* + \cos\theta\tilde{\nu}_- \ . \tag{5.13}$$

The mass eigenstate $\tilde{\nu}_-$ is taken to be the LSP; in the following we shall refer to it as either the LSP or the RH sneutrino[1]. In this parameterisation it is readily observed that the larger m^2 compared to A^2, the more sterile the LSP is; at the other extreme, the LSP becomes half right- and half left-handed sneutrino as A^2 becomes much larger than m^2. This allows us to identify two limiting cases:

1. $m^2 \gg A^2$, 'non-degenerate' sneutrinos;

2. $m^2 \ll A^2$, 'degenerate' sneutrinos.

Let us calculate the degree of degeneracy needed to reach the second case. Considering $\lambda = 10^{-13}$, $a = 100\text{GeV}$, we have that $A^2 \sim 10^{-9}\text{GeV}^2$. Indeed m_L and m_R have to be very degenerate for the second case to be reached. This is a very important observation for the remainder of this work, that it is phenomenologically natural for the sneutrinos to fall in the first category. A fair amount of fine-tuning is indeed necessary to obtain $m_L \neq m_R$ with the masses still falling in the second case. Another, perhaps more natural possibility, would be to have a mechanism that forces $m_L = m_R$. We shall come back to these questions later. For now, we look more closely at each case:

1. Non-degenerate sneutrinos, $m^2 \gg A^2$

   We should stress again that this is phenomenologically the most natural case.

   Masses:

$$m_\pm \simeq M^2 \pm m^2\left(1 + \left(\frac{A^2}{\sqrt{2}m^2}\right)^2\right)$$

$$= m_{L,R}^2 \pm \left(\frac{A^2}{\sqrt{2}m}\right)^2 \tag{5.14}$$

---

[1]Although strictly speaking it is a mixture of RH and a very small contribution of LH sneutrino.

Thus the left- and right-handed sneutrino masses are basically given by their SUSY-breaking masses and the left-right mixing makes a negligible contribution. Considering for example that $m_{L,R}$, a, v are all of order 10^2GeV, with $\lambda \sim 10^{-13}$, then the added $(A^2/\sqrt{2}m)^2$ term is completely negligible.

Mass eigenstates:

$$\begin{aligned} |\tilde{\nu}_+|^2 = |\tilde{\nu}_-|^2 &\simeq (2m^2)^2 + (A^2)^2, \\ \cos\theta &\simeq \frac{2m^2}{\sqrt{(2m^2)^2 + (A^2)^2}} \\ \sin\theta &\simeq \frac{A^2}{\sqrt{(2m^2)^2 + (A^2)^2}} \end{aligned} \tag{5.15}$$

and the LSP is dominantly right-handed, with only a small active component.

2. Degenerate sneutrinos, $m^2 \ll A^2$

Masses:

$$\begin{aligned} m_\pm^2 &\simeq M^2 \pm A^2 = m_L^2 - m^2 \pm A^2 \\ &\simeq m_L^2 \pm A^2 \end{aligned} \tag{5.16}$$

where in the first line we have used the definitions of M^2 and m^2. This shows that although we identified the mass degeneracy in the SUSY-breaking masses it translates directly to the physical masses of the sneutrinos.

Mass eigenstates:

$$\begin{aligned} |\tilde{\nu}_+|^2 = |\tilde{\nu}_-|^2 &\simeq 2(A^2)^2 + 2m^2A^2 \\ \cos\theta &\simeq \frac{m^2 + A^2}{\sqrt{2(A^2)^2 + 2m^2A^2}} \\ \sin\theta &\simeq \frac{A^2}{\sqrt{2(A^2)^2 + 2m^2A^2}} \, . \end{aligned} \tag{5.17}$$

As the SUSY-breaking masses become more degenerate, the mass eigenstates tend to maximal mixing.

5.2.2 Size of the mixing

As we have mentioned that the 'degenerate' sneutrinos case is not the most natural, we should also state what size of mixing is indeed natural in our model. The only mixing parameter we are leaving completely free is the mass degeneracy parameter, m^2. It is difficult to pinpoint a precise value for the sneutrino masses that would appear most natural or unexceptional, but let us consider for instance a RH sneutrino with mass 100GeV and a LH sneutrino with mass 150GeV. In such a case the mass degeneracy is

$$m^2 = \frac{150^2 - 100^2}{2} \text{GeV}^2 = 6250 \text{GeV}^2 \ . \tag{5.18}$$

Using again as a indicative value $A^2 = 10^{-9} \text{GeV}^2$, we obtain that the natural value for the mixing angle is a minute one (using eq.(5.15)):

$$\sin \theta = \frac{A^2}{\sqrt{(2m^2)^2 + (A^2)^2}} \simeq 8.0 \times 10^{-14} \ , \tag{5.19}$$

which is of the order of the Yukawa coupling (this can be seen directly from the definitions of A^2 and m^2 if we use $\sin \theta \sim A^2/2m^2$). So when we do not bias any of the parameters in any particular direction, we obtain that the RH sneutrino is almost completely sterile. For this reason we will often refer to our sneutrino model as one of *minimal mixing*, or of our RH sneutrino as a *minimally mixed* sneutrino. This is in comparison with models such as the one in [93]; indeed in this work trilinear couplings are not proportional to Yukawas[2].

5.2.3 A remark

We should mention before continuing that left-to-right transitions in sneutrinos could be in equilibrium before the higgses get *vevs* due for instance to four-point interactions. We will see in chapter 6 that all the interactions that interchange left- and right-handed sneutrinos are out of equilibrium before the electroweak phase

---

[2]See our discussion in section 3.2, which would be equivalent to using here $a\lambda \sim 100 \text{GeV}$ rather than simply $a \sim 100 \text{GeV}$. Evidently in this case large left-right mixing can appear even in the absence of lepton-number violation.

transition. This is similar, though not identical, to what was noted by [3], namely that Dirac neutrinos have a Yukawa coupling that is too small to allow left- and right-handed neutrinos to equilibrate. Here we have the supersymmetric equivalent of this statement. For the period before the electroweak phase transition, thus, we have that the weak eigenstates are the mass eigenstates:

$$
\begin{aligned}
\tilde{\nu}_+ &= \tilde{\nu}_L \\
\tilde{\nu}_- &= \tilde{\nu}_R^c \ .
\end{aligned}
\tag{5.20}
$$

5.3 Interactions of the (mass eigenstate) RH sneutrino

From the previous section we have the following interactions for the mass-eigenstate RH sneutrino:

5.3.1 Four-point interactions

As long as left-right mixing is out of equilibrium, four-point interactions for the mass RH sneutrino are directly obtained from the F-terms of eq.(5.2):

$$
\mathcal{L}_{4p} = -\lambda^2 \left(\tilde{e}_L \tilde{e}_L^* \tilde{\nu}_R^c \tilde{\nu}_R^{c*} + h_u^+ h_u^{+*} \tilde{\nu}_R^c \tilde{\nu}_R^{c*} + \tilde{\nu}_L \tilde{\nu}_L^* \tilde{\nu}_R^c \tilde{\nu}_R^{c*} + h_u^0 h_u^{0*} \tilde{\nu}_R^c \tilde{\nu}_R^{c*} \right) \ .
\tag{5.21}
$$

Once the mixing is effective every four-point term now accounts for three different interactions, only two of which involve the (mass) RH sneutrino . For instance the first term of eq.(5.2) is now

$$
\lambda^2 \tilde{e}_L \tilde{e}_L^* \tilde{\nu}_R^c \tilde{\nu}_R^{c*} =
$$

$$
\lambda^2 \left(\sin^2 \theta e_L e_L^* \tilde{\nu}_+^* \tilde{\nu}_+ + \cos^2 \theta e_L e_L^* \tilde{\nu}_-^* \tilde{\nu}_- + (\sin \theta \cos \theta e_L e_L^* \tilde{\nu}_- \tilde{\nu}_+ + h.c.) \right) (5.22)
$$

and so on for the other four-point terms.

5.3.2 Sneutrino-higgsino-lepton interactions

These again come from the F-terms; without mixing they are simply

$$
\mathcal{L}_{\tilde{H}} = \lambda \left(\tilde{\nu}_R \tilde{H}_u^{+} e_L - \tilde{\nu}_R \tilde{H}_u^{0} \nu_L \right) - \lambda \tilde{\nu}_L \tilde{H}_u^{0} \nu_R^c
\tag{5.23}
$$

while when mixing is active they become

$$
\begin{aligned}
\mathcal{L}_{\tilde{H},m} = \quad & \lambda \cos\theta \left(\tilde{\nu}_- \tilde{H}_u^{+} e_L - \tilde{\nu}_- \tilde{H}_u^{0} \nu_L - \tilde{\nu}_+ \tilde{H}_u^{0} \nu_R^c \right) \\
+ \quad & \lambda \sin\theta \left(\tilde{\nu}_+ \tilde{H}_u^{+} e_L - \tilde{\nu}_+ \tilde{H}_u^{0} \nu_L - \tilde{\nu}_- \tilde{H}_u^{0} \nu_R^c \right) .
\end{aligned}
\tag{5.24}
$$

5.3.3 Sneutrino-higgs-slepton interactions

These terms have two sources: the terms proportional to μ that appears in the F-terms and the SUSY-breaking terms (eq.(5.3)). Again, without mixing they can be read straightforwardly,

$$
\mathcal{L}_h = -\lambda \left(\left[\mu h_d^0 + a h_u^0 \right] \tilde{\nu}_R^c \tilde{\nu}_L + \left[\mu h_d^- + a h_u^+ \right] \tilde{\nu}_R^c \tilde{e}_L + h.c. \right)
\tag{5.25}
$$

while when mixing is turned on,

$$
\begin{aligned}
\mathcal{L}_{h,m} = \quad - \quad & \lambda \left(\left(\cos^2\theta - \sin^2\theta \right) \left[\mu h_d^0 + a h_u^0 \right] \tilde{\nu}_- \tilde{\nu}_+ - \sin\theta \cos\theta \left[\mu h_d^0 + a h_u^0 \right] \tilde{\nu}_- \tilde{\nu}_-^* \right) \\
- \quad & \lambda \cos\theta \left[\mu h_d^- + a h_u^+ \right] \tilde{\nu}_- \tilde{e}_L + h.c.
\end{aligned}
\tag{5.26}
$$

where we only kept terms involving $\tilde{\nu}_-$. Eq.(5.26) will be important when we consider the detection of the RH sneutrino LSP, as higgs exchange can be an important source of interaction between WIMPs and nuclei.

5.3.4 Interactions with gauge bosons and gauginos

When left-right mixing is in equilibrium the gauge interactions of the (weak) LH sneutrino are transferred in parts to the (mass) RH sneutrino. Following for instance [55], slepton-gaugino interactions are given by the following part of the full renormalisable, supersymmetric Lagrangian:

$$
\begin{aligned}
\mathcal{L}_{gaugino-slepton} = \quad & -\sqrt{2} g_2 \left[\left(\tilde{l}^* t_2^a l \right) \tilde{W}^a + \tilde{W}^{\dagger a} \left(l^\dagger t_2^a \tilde{l} \right) \right] \\
& -\sqrt{2} g_1 \left[\left(\tilde{l}^* l \right) \tilde{B} + \tilde{B}^\dagger \left(l^\dagger \tilde{l} \right) \right]
\end{aligned}
\tag{5.27}
$$

while the gauge-slepton interactions stem from the covariant derivatives of the matter fields:

$$
\begin{aligned}
\mathcal{L}_{cov.der.} &= -D^\mu \tilde{l}^* D_\mu \tilde{l} \\
&= -\left(\partial^\mu \tilde{l}^* - \frac{ig_2}{2} \vec{\sigma} \cdot \vec{W}^\mu \tilde{l}^* + \frac{ig_1}{2} B^\mu \tilde{l}^* \right) \\
&\quad \times \left(\partial_\mu \tilde{l}^* + \frac{ig_2}{2} \vec{\sigma} \cdot \vec{W}_\mu \tilde{l}^* - \frac{ig_1}{2} B_\mu \tilde{l}^* \right) .
\end{aligned}
\tag{5.28}
$$

Let us expand both eq.(5.27) and eq.(5.28) and extract the vertices involving the LH sneutrino. Gaugino interactions are

$$
\begin{aligned}
\mathcal{L}_{gaugino-\tilde{\nu}_L} &= -\sqrt{2} g_2 \left[\tilde{\nu}_L \nu_L \tilde{W}^0 + \tilde{\nu}_L^* e \tilde{W}^+ + h.c. \right] \\
&\quad -\sqrt{2} g_1 \left[\tilde{\nu}_L^* \nu_L \tilde{B} + h.c. \right] ,
\end{aligned}
\tag{5.29}
$$

which we can translate into interactions involving the (mass) RH sneutrino:

$$
\begin{aligned}
\mathcal{L}_{gaugino-\tilde{\nu}_-} &= \sqrt{2} g_2 \sin\theta \left[\tilde{\nu}_-^* \nu_L \tilde{W}^0 - \tilde{\nu}_- e \tilde{W}^+ + h.c. \right] \\
&\quad \sqrt{2} g_1 \sin\theta \left[\tilde{\nu}_- \nu_L \tilde{B} + h.c. \right] .
\end{aligned}
\tag{5.30}
$$

The gauge-slepton interactions stem from the following crossing terms:

$$
\begin{aligned}
\mathcal{L}_{gauge-slepton} &= -\frac{g_2}{2} \left[i\vec{\sigma} \cdot \vec{W}_\mu \tilde{l}^* \partial_\mu \tilde{l} + h.c. \right] + \frac{g_1}{2} \left[i\partial \tilde{l}^* B_\mu \tilde{l} + h.c. \right] \\
&= -\frac{ig_2}{2} \left[\sigma^+ W^{+,\mu} \tilde{l}^* \overleftrightarrow{\partial}_\mu \tilde{l} + \sigma^- W^{-,\mu} \tilde{l}^* \overleftrightarrow{\partial}_\mu \tilde{l} + \sigma^3 W^{3,\mu} \tilde{l}^* \overleftrightarrow{\partial}_\mu \tilde{l} \right] \\
&\quad + \frac{ig_1}{2} \left[B^\mu \tilde{l}^* \overleftrightarrow{\partial}_\mu \tilde{l} \right] .
\end{aligned}
\tag{5.31}
$$

After the electroweak symmetry breaking, gauge bosons mix such that

$$
\begin{pmatrix} W^3 \\ B \end{pmatrix} = \begin{pmatrix} \cos\theta_w & \sin\theta_w \\ -\sin\theta_w & \cos\theta_w \end{pmatrix} \begin{pmatrix} Z \\ A \end{pmatrix} ,
\tag{5.32}
$$

the coupling constants being related through

$$
e = g_2 \sin\theta_W = g_1 \cos\theta_W .
\tag{5.33}
$$

Expanding eq.(5.31) fully (we have dropped the summed μ indices for clarity),

$$
\begin{aligned}
\mathcal{L}_{gauge-slepton} &= -\frac{ig_2}{\sqrt{2}} \left(W^+ \tilde{\nu}_L^* \overleftrightarrow{\partial} \tilde{e} - W^- \tilde{e}^* \overleftrightarrow{\partial} \tilde{\nu}_L \right) \\
&\quad + \left(\frac{ig_2}{2\cos\theta_w} \right) \left(Z \tilde{e}^* \overleftrightarrow{\partial} \tilde{e} - Z \tilde{\nu}_L^* \overleftrightarrow{\partial} \tilde{\nu}_L \right) + ieA\tilde{e} \overleftrightarrow{\partial} \tilde{e} .
\end{aligned}
\tag{5.34}
$$

Finally, using

$$M_W = \frac{g_2 v}{2}, \quad M_Z = \frac{g_2 v}{2\cos\theta_w}$$

and keeping only terms involving the LH sneutrino,

$$
\begin{aligned}
\mathcal{L}_{gauge-\tilde{\nu}_L} &= -\frac{i\sqrt{2}M_W}{v}\left[W^+\tilde{\nu}_L^*\overleftrightarrow{\partial}\tilde{e} + W^-\tilde{e}^*\overleftrightarrow{\partial}\tilde{\nu}_L\right] \\
&\quad -\frac{iM_Z}{v}\left[Z\tilde{\nu}_L^*\overleftrightarrow{\partial}\tilde{\nu}_L\right] ,
\end{aligned}
\tag{5.35}
$$

which again will be transferred to the RH sneutrino when left-right contact is in equilibrium:

$$
\begin{aligned}
\mathcal{L}_{gauge-\tilde{\nu}_-} &= -\frac{i\sqrt{2}M_W}{v}\sin\theta\left[W^+\tilde{\nu}_-\overleftrightarrow{\partial}\tilde{e} + W^-\tilde{e}^*\overleftrightarrow{\partial}\tilde{\nu}_-^*\right] \\
&\quad -\frac{iM_Z}{v}\sin^2\theta\left[Z\tilde{\nu}_-\overleftrightarrow{\partial}\tilde{\nu}_-^*\right] \\
&\quad +\frac{iM_Z}{v}\sin\theta\cos\theta\left[Z\tilde{\nu}_-\overleftrightarrow{\partial}\tilde{\nu}_+ + Z\tilde{\nu}_-^*\overleftrightarrow{\partial}\tilde{\nu}_+^*\right] .
\end{aligned}
\tag{5.36}
$$

The interaction with the Z boson again will be important for direct detection as Z exchange can be a leading channel of WIMP-nucleus interaction.

5.4 Direct detection of the RH sneutrino LSP

As we have introduced it the RH sneutrino has many of the essential characteristics of a dark matter candidate. We will discuss this possibility further in chapter 6. As many dark matter direct detection experiments have now started releasing results [96–99], it is important to mention how our suggested dark matter candidate interacts with ordinary matter.

5.4.1 Experiment principles and recent results

Direct detection experiments are all based on the same basic idea: if the dark matter halo in our galaxy is a collection of WIMP's, then at any time the Earth should be showered by a large number of them. WIMP's are expected to interact with ordinary matter through elastic scattering with nuclei (or in fact quarks within the nucleon) with a very low interaction rate due to their very small cross-section with ordinary matter (hence their name - see chapter 2). Typical nuclear recoil energies

are expected to be around $1 - 100\text{GeV}$ [21], and typical rates around $10^{-4} - 1$ event per day per kilo of target material [11] (although see next paragraph). At such low recoil energies and rates, noise reduction becomes a major challenge. This is the reason why direct dark matter detection experiments are conducted underground. What differentiates the various experiments is the way in which they measure the nuclear recoil energy. CDMS-II [97] measures the change of temperature of a target germanium (Ge) crystal. It does so by gluing a superconducting material (tungsten) to the Ge crystal; the tungsten strip is kept just below its superconducting transition temperature, and when the Ge crystal 'heats up' due to the recoil of one of its nuclei, the temperature of the tungsten strip rises above the transition temperature and the tungsten stops being superconducting, thus causing a sudden change in its resistivity. The DAMA/NaI experiment [96] measure the ionization created by the nuclear recoil within an NaI scintillator; the ionization light is collected in photomultiplicators, and the signal is measured. Other experiments such as EDELWEISS or ZEPLIN use similar techniques or a blend of them [98, 99].

As pointed out, the direct detection experiments have released results already. Here we will use as a guideline the analysis of CDMS-II [97, 100], which gives experimental results as excluded regions in a WIMP-nucleon cross-section versus WIMP mass plan. As pointed out by DAMA [96] this analysis is model-dependent: indeed it requires modelling of the speed distribution of WIMP's in the halo and of the nuclear properties of the target. For our needs here however the advantage of this analysis is that it relates directly the parameters of the models to the experiments, thus allowing us to constrain the model. As we will see in the next subsections the interactions of RH sneutrino dark matter with nucleons is spin-independent as it goes through either vector or scalar interactions [21]. The most constraining results for WIMP-nucleon spin-independent cross-section at the moment come from CDMS (see fig.1 of [100], and fig.4 of [97]): for a WIMP mass of 100GeV the WIMP-nucleon cross-section is constrained to be below $\sim 8 \times 10^{-42}\text{cm}^2$, and this limit goes up to about $\sim 8 \times 10^{-40}\text{cm}^2$ for a WIMP mass of 10GeV. It is hoped that future upgrades of CDMS could lower this detection threshold to $1 \times 10^{-45}\text{cm}^2$ [101].

Because of crossing symmetry, we expect a WIMP with a small annihilation

rate to have a small detection rate via elastic scattering, and a WIMP with a large annihilation rate to have a large detection rate. The simple picture would be to expect a certain size of annihilation rate to produce an amount of relic WIMP corresponding to the observed dark matter, and from this annihilation rate deduce the expected detection rate [11] . In our work here we will deviate from this usual picture in two ways. On the one hand, it will not always be the case that the observed amount of dark matter will be equated with the relic density of our candidate. Indeed as we will observe in chapters 6, 7 in the model at play RH sneutrinos seem to be more naturally produced in the right amount when considering the possibility of mattergenesis as the source of dark matter. In such a case the relic density has to be low, either because the annihilation rate is very low or very large. We shall come back later to the size of the annihilation rate of the RH sneutrino, but it suffices for now to notice that once the constraint that the relic density must equate the observed dark matter density is abandoned, the usual expected detection rate also has to be given up. On the other hand, crossing symmetry only relates the annihilation rate to the elastic scattering detection rate. For certain WIMP candidates, and for the RH sneutrino in particular, it is unclear whether the assumption that elastic scattering dominates over inelastic scattering holds throughout the parameter space.

Hence what we want to do here is simply relate the scattering rate of the RH sneutrino off ordinary matter with the parameters of our model, without assuming any expected size for this rate.

5.4.2 Interaction with nucleon via higgs exchange

We take the general cross-section for an elastic scattering between the RH sneutrino LSP and a nucleon via the exchange of a Higgs to be given by [11, 102, 103]

$$\sigma_{h,\tilde{\nu}_-} \simeq m_{red}^2 \times \frac{1}{m_h^4} \times C_{\tilde{\nu}_-,h} \times C_{h,nucleon} \times \left(\frac{\mathcal{F}}{A_a^2} \right) \tag{5.37}$$

where

$m_{red} = \dfrac{m_N m_{\tilde{\nu}_-}}{(m_N + m_{\tilde{\nu}_-})}$	is the reduced mass of the RH sneutrino-nucleon system;
m_N	is the nucleon mass;
$\dfrac{1}{m_h^4}$	accounts for the higgs exchange;
$\mathcal{C}_{\tilde{\nu}_-,h}$	is the (dimensionless) higgs-RH sneutrino coupling;
$\mathcal{C}_{h,nucleon}$	is the (dimensionless) higgs-nucleon coupling;
$\mathcal{F} = \left((A_a - Z_a) - \left(1 - 4\sin^2\theta_W \right) Z_a \right)^2$	is the coherent interaction factor [102] which accounts for the structure of the nuclei as seen by the interaction;
A_a	is the atomic mass of the target nucleus;
Z_a	is the atomic number of the target nucleus.

We follow [102] in normalising the WIMP-*nucleus* cross-section with A_a^2 to obtain the WIMP-*nucleon* cross-section; this is to make our calculation comparable with experimental data (for example [97]) and other calculations in the literature (for instance [93]). This is valid for both scalar-type (which the higgs exchange is here) and vector-type interactions (which is the case for the Z exchange of the next subsection).

There is large uncertainty on the value of $\mathcal{C}_{h,nucleon}$ due mainly to the uncertainty in the quark content of the nucleon (see for example [104]). From [103,104] we have

$$\mathcal{C}_{h,nucleon} \simeq \frac{2}{\sqrt{2}} G_F \left\langle N | \Sigma_q m_q \bar{q}q | N \right\rangle^2 \simeq 10^{-7} \tag{5.38}$$

where we have included an indicative order of magnitude. In the model under discussion here the higgs-RH sneutrino coupling stems from the μ-term in the superpotential and from SUSY-breaking terms, as obtained in eq.(5.26). Reading from it we have that an elastic recoil via (up-type) higgs exchange has coupling

$$\begin{aligned} \mathcal{C}_{\tilde{\nu}_-,h} &= \frac{\lambda^2 a^2 \sin^2\theta \cos^2\theta}{m_{\tilde{\nu}_-}^2} \\ &= 10^{-26} \frac{a^2 \sin^2\theta \cos^2\theta}{m_{\tilde{\nu}_-}^2} \ . \end{aligned} \tag{5.39}$$

The value of λ is due to the fact that we are considering a model of Dirac neutrinos, and thus the Yukawa couplings need be small to explain the size of the neutrino mass. What this implies here is that direct detection via higgs exchange is impossible, no matter the size of the LSP mass or of the mass mixing. From eq.(5.37)

$$\sigma_{h,e} \simeq \frac{m_N^2 m_{\tilde{\nu}_-}^2}{\left(m_N + m_{\tilde{\nu}_-}\right)^2} \times \frac{1}{m_h^4} \times \frac{10^{-26} a^2 \sin^2\theta \cos^2\theta}{m_{\tilde{\nu}_-}^2} \times 10^{-7} \times \frac{\mathcal{F}}{A^2}$$

$$\lesssim 10^{-7} 10^{-26} \frac{m_N^2 a^2}{m_h^4 \left(m_N + m_{\tilde{\nu}_-}\right)^2}$$

$$\simeq 10^{-42} \text{GeV}^{-2} \left(\frac{m_N}{100 \text{GeV}}\right)^2 \left(\frac{a}{100 \text{GeV}}\right)^2 \left(\frac{100 \text{GeV}}{m_N + m_{\tilde{\nu}_-}}\right)^2 \left(\frac{10^3 \text{GeV}}{m_h}\right)^4$$

$$\simeq 4 \times 10^{-70} \text{cm}^2 \left(\frac{m_N}{100 \text{GeV}}\right)^2 \left(\frac{a}{100 \text{GeV}}\right)^2 \left(\frac{100 \text{GeV}}{m_N + m_{\tilde{\nu}_-}}\right)^2 \left(\frac{10^3 \text{GeV}}{m_h}\right)^4 \quad (5.40)$$

where we've taken in the second line $\mathcal{F}/A_a^2 \approx 10^{-1}$ as an indicative value (for germanium, $\mathcal{F}/A_a^2 \approx 0.3$). This situation is a first example of a case where large trilinear couplings would have important consequences. As was noted in [93] (which we mentioned in section 5.2), when considering trilinear couplings not suppressed by the Yukawa ($a\lambda \sim 100 \text{GeV}$), one obtains that the cross-section between RH sneutrino and matter via higgs exchange is just below threshold. This could be an interesting situation, although as we will see many of the interesting aspects of the cosmology of our RH sneutrino (chapters 6 and 7) will indeed depend on small left-right mixing.

5.4.3   Interaction with nucleus via Z exchange

The cross-section of our RH sneutrino with a nuclei via Z-exchange stems from terms in eq.(5.35); for an *unmixed* sneutrino it is given by four times the cross-section for a heavy neutrino-nuclei interaction via Z-exchange [11,105]:

$$\sigma_{Z,e} = 4 \times \frac{m_{red}^2}{64\pi} \times \left(\frac{4G_F}{\sqrt{2}}\right)^2 \left(\frac{\mathcal{F}}{A_a^2}\right) \quad (5.41)$$

where G_F and $\sin\theta_W$ are the usual Standard Model parameters and the other parameters are as before. Here the cross-section for RH sneutrino elastic scattering via Z exchange is simply the LH one with additional $\sin^4\theta$ suppression (eq.(5.36)):

$$\sigma_{Z,e} = \sin^4\theta \times \frac{m_{red}^2 G_F^2}{2\pi} \times \left(\frac{\mathcal{F}}{A_a^2}\right) \quad (5.42)$$

For small angles it is obvious that the suppression due to the mixing could reduce the cross-section down to a point where it becomes lower than detection limits. A RH sneutrino of mass $m_- = 100\mathrm{GeV}$ has a cross-section that falls just below the detection threshold of 8×10^{-42} if the mixing angle is of order 10^{-1}. As $\sin\theta$ is present at its fourth power, then a small change in mixing angle can rapidly render the RH sneutrino completely undetectable by the direct detection experiments. As we have mentioned in section (5.2.2), however, a natural mixing angle for this model is around $\sin\theta \sim 10^{-13}$, and as such we can expect that RH sneutrinos not too far below detection thresholds will hardly be a possibility. We will come back to this question in chapter 6.

Eq.(5.36) also allows for an inelastic scattering with the nucleus which is only suppressed by $\sin^2\theta$. The possibility of direct detection of mixed sneutrino dark matter via inelastic scattering has been suggested in [106] and studied further in [107]. From a kinematic point of view an inelastic scattering (in our case $\tilde{\nu}_- \rightarrow \tilde{\nu}_+$) can only occur if

$$\delta \equiv (m_+ - m_-) < \frac{\beta^2 m_- m_N}{2(m_- + m_N)}, \qquad (5.43)$$

where β is the velocity of the dark matter particle. This has two interesting consequences: an overall suppression of the signal as well as a difference in detection rate between different target nuclei. For a given target nuclei, let us call C_i the inelastic suppression factor. The cross-section for inelastic scattering of the RH sneutrino with the nucleon via Z-exchange can then be given by

$$\sigma_{Z,i,n} = \sin^2\theta \cos^2\theta \times C_i \times \frac{m_{red}^2 G_F^2}{2\pi} \times \left(\frac{\mathcal{F}}{A^2}\right). \qquad (5.44)$$

The relative importance of elastic and inelastic cross-sections is thus dependent upon the relative sizes of the mixing angle and the inelastic suppression factor, which in our model are related to one another. We will come back to discussing the detectability of RH sneutrino dark matter via elastic and inelastic Z exchange in chapter 6.

Inelastic scattering also causes different target nuclei to have different lower limits of detection. Let us compare CDMS and DAMA, as in [106]. The CDMS experiment uses germanium (Ge, $A_a = 73$, $Z_a = 32$) as target nuclei; thus for a WIMP of mass

$m_- = 100\text{GeV}$, an inelastic scattering is only possible if the mass splitting δ is smaller than 11keV. DAMA uses iodine as target material (I, $A_a = 127$, $Z_a = 53$) and so again for a WIMP of mass 100GeV the maximal mass splitting that allows for inelastic scattering is 15keV. For a mass splitting larger than 15keV, neither DAMA nor CDMS can see inelastic scattering; for a mass splitting smaller than 11keV, both can, although as the mass splitting is reduced to $\delta \ll$ 11keV the scattering becomes indistinguishable from an elastic scattering. If the mass splitting falls precisely between 11 and 15keV, then the both experiments obtain fairly different results [3]. Indeed this case is only interesting if at such a mass splitting, the inelastic detection cross-section is comparable to the current experimental limits. Again we will delay a discussion of this possibility to chapter 6.

---

[3]The precise analysis is somewhat more involved (it includes for instance the distribution of velocities found in the halo of the galaxy), but this simple calculation will be enough for our needs here.

Chapter 6

RH Sneutrino LSP in the Early Universe

We now turn to studying the behaviour of the newly introduced right-handed (RH) sneutrino in the early Universe. As we have seen in the previous chapter, the model we are studying is one of minimal mixing between the active and sterile sneutrinos. It is most likely then that the RH sneutrino will not attain thermal equilibrium. We will first study whether it is possible for the RH sneutrino to attain equilibrium, and if so, under which conditions. As we have discussed earlier, for mattergenesis purposes having a non-thermal dark matter candidate facilitates model building, and for this reason we want to verify how strongly non-thermal our candidate is, or in other words, how easily the parameters involved in the model respect the possible constraints arising from requiring the candidate to remain non-thermal.

Having settled this first question we can move to determining the relic density of our candidate, considering it to be the LSP. Again we have mentioned in chapter 2 that mattergenesis requires the presence of a low relic density for the candidate. While working on this thesis it was obtained by a different group [108] that indeed the relic density can be low, although the converse is also possible. Here we repeat this calculation and obtain compatible results. We discuss the constraints on the model arising from requiring the relic density to be low.

Finally within the constraints obtained we can discuss the possibility of direct detection of the RH sneutrino as our suggested dark matter candidate. Unsurpris-

ingly we will obtain that direct detection is not possible if the candidate is to respect the constraints of non-thermalicity and low relic density.

The results obtained in this chapter have been published in [2].

6.1 Thermalisation of the RH sneutrino

We recall from chapter 2 that an interaction is effective in the early Universe if it occurs with a rate Γ larger than the rate of expansion of the Universe, $H = T^2/M_P$ where T is the temperature of the Universe and M_P is the Planck mass [4]. Thus the RH sneutrino will reach equilibrium if at least one interaction of the type

$$\tilde{\nu}_- + \tilde{\nu}_-^* \rightarrow \text{anything} \tag{6.1}$$

happens at a rate larger than the rate of the expansion of the Universe . Hence to study thermalisation the criterion we will use here is simply that if a channel i of the type eq.(6.1) has a rate Γ_i such that

$$\Gamma_i < \frac{T^2}{M_P}, \tag{6.2}$$

then the channel does not allow thermalisation. Moreover if all possible channels of the type eq.(6.1) respect the condition in eq.(6.2), then the RH sneutrino is a non-thermal relic.

We will use the following simple assumptions to describe the conditions in the early Universe: before the electroweak phase transition but after reheating, temperatures run between the reheating temperature[1] $T_{RH} \sim 10^9 \text{GeV}$ and the electroweak phase transition temperature $T_{ewpt} \sim 300\text{GeV}$ [18]. During these times SM particles are massless while we consider all their superpartners to be massive. After the electroweak phase transition, the Universe cools down from $T_{ewpt} \sim 300\text{GeV}$ to the temperature it has today, $T_{now} \sim 3K \sim 2,58 \times 10^{-13}\text{GeV}$. We consider all SM

---

[1]We take as an indicative reheating temperature one that would be large enough to evade the gravitino problem [12–14]. Only reheating temperatures very much larger than this could alter our results; see table (6.1). This is not a possibility we shall consider further.

fermions to be 'suddenly' massive when $T < T_{ewpt}$ as for our needs this definition of the electroweak phase transition will be sufficient. We will also consider the RH sneutrino not to be degenerate in mass with any other particle enough to allow coannihilations to be important [62].

6.1.1 Left-right equilibration before the electroweak phase transition

Let us first decide whether the RH sneutrino is purely sterile or whether it has an active part due to its mixing with the LH sneutrino. Left-right mixing would be in equilibrium if at least one interaction of the type

$$\tilde{\nu}_R + \tilde{\nu}_L \rightarrow \text{anything} \tag{6.3}$$

had a rate $\Gamma > H$. Going back to section 5.3, we take in turn each of the interactions that can lead to left-right equilibration. Among the four-point interactions in section (5.3.1), we find one that mixes the left- and right-handed sneutrinos; for this interaction the rate is

$$\Gamma_{LR,4} \sim \lambda^4 T . \tag{6.4}$$

Imposing $\Gamma_{LR,4}$ to be smaller than the expansion rate means

$$\lambda^4 T < \frac{T^2}{M_P} \Rightarrow 10^{-33} \text{GeV} < T . \tag{6.5}$$

Evidently this is true throughout the period before the electroweak transition, but it is worth noticing straightaway that it is also true throughout the history of the Universe, as even the temperature now is larger than 10^{-33} GeV. This means that no four-point interaction can cause thermal equilibration.

The interaction of the sneutrinos with the higgsino (section (5.3.2)) is another channel that mixes the left- and right-handed sneutrinos. The left- and right-handed sneutrinos can exchange a neutral higgsino and become a pair of ordinary neutrinos. The rate of this interaction is

$$\Gamma_{LR,H} \sim \frac{\lambda^4 T^3}{m_{\tilde{H}_u^0}^2} ; \tag{6.6}$$

for $\Gamma_{LR,H}$ to be smaller than H requires

$$m_{\tilde{H}_u^0}^2 > 10^{-33}T .$$ (6.7)

This constraint is strongest when the temperature is at its highest. Before the electroweak phase transition the highest temperature we consider is the reheating temperature T_{RH}; at this temperature the constraint is

$$m_{\tilde{H}_u^0} > 10^{-12}\text{GeV}$$ (6.8)

which is evidently respected. So the higgsino exchange does not allow for left-right equilibration.

The last possible channel for left-right exchange comes from the sneutrino-higgs interaction of section (5.3.3); a left- and a right-handed sneutrino can turn into a higgs which can then produce a pair of SM particles. The rate for this is

$$\Gamma_{LR,h} \sim \frac{\lambda^2 a^2 \lambda_T^2}{T}$$ (6.9)

where λ_T is a 'typical' Yukawa coupling for an SM particle. Again imposing this rate to be smaller than H means that

$$a^2 < \frac{10^7 T^3}{\lambda_T^2}.$$ (6.10)

This is most constraining at a low temperature and large 'typical' Yukawa so let us consider the electroweak phase transition temperature, $T_{ewpt} \sim 300$ GeV and a Yukawa of $\lambda_T \sim 1$:

$$a < 1,6 \times 10^6 \text{GeV} .$$ (6.11)

As long as we are considering a trilinear coupling $\mathcal{A}$ proportional to the Yukawa with $a \sim m_{soft}$, it is clear that this constraint is always respected. Thus in our model left- and right-handed sneutrinos can never equilibrate before the electroweak phase transition. If we were considering a trilinear coupling not proportional to the Yukawa, then left-right mixing would fast reach equilibrium. Interestingly, it had been noticed earlier that left- and right-handed Dirac *neutrinos* cannot equilibrate before the electroweak phase transition due to their small Yukawa couplings [3];

here we note that this observation can be extended to the supersymmetric case as well, but is accommodated most easily by universal SUSY-breaking. We will make use of this observation in chapter 7, where we will suggest a leptogenesis (and mattergenesis) mechanism that is a supersymmetric extension of the model suggested in [3].

6.1.2 Thermalisation before the electroweak phase transition

Now that we have concluded that the RH sneutrino does not have a LH part before the electroweak phase transition, we know that the number of interactions that could allow for its thermalisation is very limited. Four-point interactions we already know are not effective. The exchange of a charged (resp. neutral) Higgsino between a RH sneutrino and an anti-RH sneutrino to form a pair of neutrinos (resp. a neutrino and an electron) has the same rate as in eq.(6.6), so again we already know that they cannot allow thermalisation. The only channel left to investigate stems from the sneutrino-higgs-slepton interaction. A RH sneutrino-anti-RH sneutrino pair can exchange a LH sneutrino to create a higgs-anti-higgs pair. The rate for this exchange is

$$\Gamma_{\tilde{\nu}_L} \sim \frac{\lambda^4 a^4 T}{m_{\tilde{\nu}_L}^4} \; .$$

(6.12)

It is smaller than the expansion rate if

$$T > 10^{-33}\text{GeV}\frac{a^4}{m_{\tilde{\nu}_L}^4}$$

(6.13)

which, at the electroweak phase transition temperature, is

$$\frac{a}{m_{\tilde{\nu}_L}} < 7.4 \times 10^8$$

(6.14)

which is certainly respected considering our previous comments.

Hence before the electroweak phase transition the RH sneutrino cannot thermalise, and this because the size of its Yukawa and of the trilinear coupling are both too small. More importantly perhaps, we also see that without mass mixing the RH sneutrino is unable to thermalise. The picture is fairly different when considering

mass mixing, and thus we do expect the mixing angle to play the major role in determining the thermalisation of the RH sneutrino.

6.1.3 Thermalisation after the electroweak phase transition

Again now we should take in turn each type of interaction listed in section (5.3), construct an interaction of the type eq.(6.1), then verify if the corresponding rate can be made larger than the rate of expansion of the Universe. We list the obtained constraints in table 6.1. For each channel mentioned we state the corresponding rate, then impose it to be smaller that H which turns into a temperature-dependent constraint; we finally use the most constraining temperature to obtain the constraints on the parameters. The Feynmann diagram that corresponds to each channel is shown in fig.(6.1)

Only few channels could allow for thermalisation. Constraints (a) through (f) are either trivially respected, or respected due to the size of the trilinear coupling we are using. This shows that indeed a very large trilinear coupling could make our dark matter candidate change from a relic that is most naturally non-thermal to one that would generally be thermal. Constraints (g) to (k) are the conditions we were looking for: indeed what is implied is that if the mixing angle $\sin\theta$ is not kept roughly of order $\sin\theta < 10^{-5}$, then despite having only the trilinear coupling as a mixing source the RH sneutrino would be mixed with its left-handed counterpart enough to (at some point after the electroweak phase transition) reach thermal equilibrium.

We have obtained in the previous chapter that mixing angles much smaller than $\sin\theta \sim 10^{-5}$ are to be expected in our model. For sneutrino masses of the order of m_{soft} but not degenerate, a mixing angle of the size of the Yukawa coupling is naturally obtained. Thus indeed the RH sneutrino in our model is most naturally non-thermal. Let us verify the amount of mass degeneracy and/or departure from a universal trilinear coupling this is needed to obtain a mixing angle of order 10^{-5}.

	Rate (Γ)	T-dependent constraint	T_c	Constraint
(a)	$\dfrac{\lambda^4 T^3}{m_{\tilde{H}_u}^2}$	$T < 10^{33}\text{GeV}^{-1} m_{\tilde{H}_u}^2$	T_{RH}	$m_{\tilde{H}_u} > 10^{-12}\text{GeV}$
(b)	$\dfrac{\lambda^4 a^4 T}{m_{\tilde{\nu}_L}^4}$	$T > 10^{-33}\text{GeV}\dfrac{a^4}{m_{\tilde{\nu}_L}^4}$	T_{ewpt}	$\dfrac{a}{m_{\tilde{\nu}_L}} < 7.4 \times 10^8$
(c)	$\dfrac{\lambda^4 c_\theta^4 T^3}{m_{\tilde{H}_u}^2}$	$T < 10^{33}\text{GeV}^{-1}\dfrac{m_{\tilde{H}_u}^2}{c_\theta^4}$	T_{ewpt}	$\dfrac{m_{\tilde{H}_u}}{c_\theta^2} > 5.5\times 10^{-16}\text{GeV}$
(d)	$\dfrac{\lambda^4 a^4 \left(c_\theta^2 - s_\theta^2\right)^4 T}{m_{\tilde{\nu}_L}^4}$	$T > 10^{-33}\text{GeV}\dfrac{a^4 \left(c_\theta^2 - s_\theta^2\right)^4}{m_{\tilde{\nu}_L}^4}$	T_{now}	$\dfrac{a\left(c_\theta^2 - s_\theta^2\right)}{m_{\tilde{\nu}_L}} < 1.3 \times 10^5$
(e)	$\dfrac{a^2\lambda^2 c_\theta^2 s_\theta^2 \lambda_t^2 T^3}{m_{h_u}^4}$	$T < 10^7\text{GeV}^{-1}\dfrac{m_{h_u}^4}{\lambda_t^2 a^2 c_\theta^2 s_\theta^2}$	T_{ewpt}	$a c_\theta s_\theta < 7.3 \times 10^6\text{GeV}$
(f)	$\dfrac{\lambda^4 a^4 c_\theta^4 T}{m_{\tilde{e}_L}^4}$	$T > 10^{-33}\text{GeV}\dfrac{a^4 c_\theta^4}{m_{\tilde{e}_L}^4}$	T_{now}	$\dfrac{a c_\theta}{m_{\tilde{e}_L}} < 1.3 \times 10^5$

	Rate (Γ)	T-dependent constraint	T_c	Constraint
(g)	$\dfrac{4g_2^4 s_\theta^4 T^3}{m_{\tilde{W}}^2}$	$T < 3.6 \times 10^{-20}\text{GeV}^{-1}\dfrac{m_{\tilde{W}}^2}{s_\theta^4}$	T_{ewpt}	$s_\theta < 7.4 \times 10^{-5}$
(h)	$\dfrac{4g_1^4 s_\theta^4 T^3}{m_{\tilde{B}}^2}$	$T < 5.0 \times 10^{-23}\text{GeV}^{-1}\dfrac{m_{\tilde{B}}^2}{s_\theta^4}$	T_{ewpt}	$s_\theta < 1.3 \times 10^{-4}$
(i)	$\dfrac{4m_W^4 s_\theta^4 T^5}{v^4 m_{\tilde{e}}^4}$	$T^3 < 5.7 \times 10^{-19}\text{GeV}^{-1}\dfrac{m_{\tilde{e}}^4}{s_\theta^4}$	T_{ewpt}	$s_\theta < 1.9 \times 10^{-4}$
(j)	$\left(\dfrac{m_Z}{v}\right)^2 \dfrac{s_\theta^4 g^2 T^5}{m_Z^4}$	$T^3 < \dfrac{3.2 \times 10^{-11}\text{GeV}^3}{s_\theta^4}$	T_{ewpt}	$s_\theta < 1.1 \times 10^{-5}$
(k)	$\dfrac{m_Z^4 s_\theta^4 c_\theta^4 T^5}{v^4 m_{\tilde{\nu}_L}^4}$	$T^3 < 1.4\times10^{-18}\text{GeV}^{-1}\dfrac{m_{\tilde{\nu}_L}^4}{s_\theta^4 c_\theta^4}$	T_{ewpt}	$s_\theta c_\theta < 5.4 \times 10^{-4}$

Table 6.1: Processes that contribute to the annihilation of RH sneutrinos. We impose each annihilation rate to be smaller than the expansion rate throughout the period when they apply. The letters listed in the first column refer to fig.(6.1). Four-points interactions are not included as they never allow thermalisation (see text). See text for temperatures; T_c stands for the most constraining temperature. The first two lines refer to the period before the electroweak phase transition; the rest of the table is for the period after the electroweak phase transition. $\cos\theta$ and $\sin\theta$ have been replaced by c_θ and s_θ respectively to lighten the table. In line (c) a $\sin\theta$ factor could have been used instead of the $\cos\theta$ one, but as the constraint is already always evaded with only a $\cos\theta$ factor, this is superfluous.
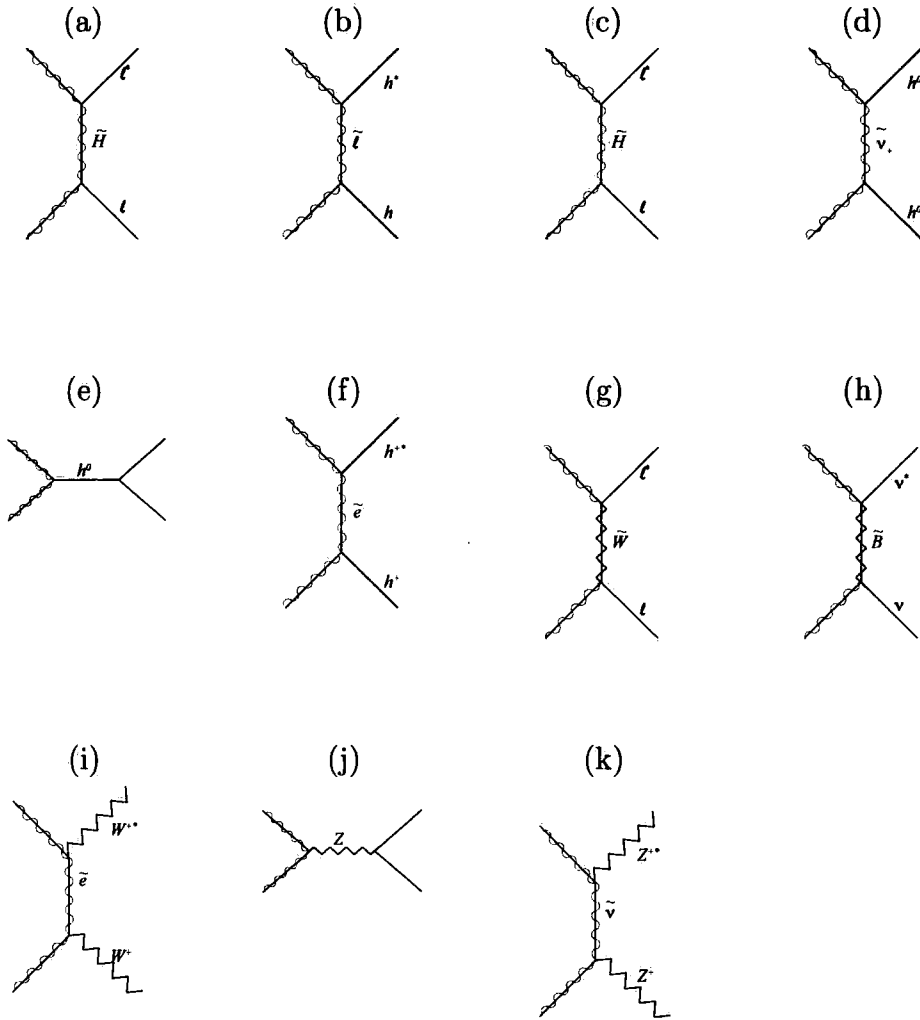
Figure 6.1: The annihilation channels of the RH sneutrino. Time runs from left to right; all incoming particles are pairs of RH sneutrino and anti-RH sneutrino. (a) is built from eq.(5.23); (b) from eq.(5.25); (c) from the 1st term of eq.(5.24); (d) from the 1st term of eq.(5.26); (e) from the 2nd term of eq.(5.26); (f) from the 3rd term of eq.(5.26); (g) from 1st term of eq.(5.30); (h) from the 2nd term of eq.(5.30); (i) from the 1st term of eq.(5.36); (j) from the 2nd term of eq.(5.36); (k) from the 3rd term of eq.(5.36).

We go back once more to the definition of the mixing angle (eq.(5.11)), :

$$\sin\theta = \frac{A^2}{\sqrt{\left(m^2 + \sqrt{(m^2)^2 + (A^2)^2}\right)^2 + (A^2)^2}}$$

$$\Rightarrow \frac{A^2}{m^2} = \frac{1}{2\left(s^{1/2} - s^{-1/2}\right)} \Rightarrow \frac{A^2}{m^2} \simeq 2\sin\theta \tag{6.15}$$

where $s = (1/\sin^2\theta - 1)$ and between the second and third line we have used that $\sin\theta \ll 1$. Hence a mixing angle of $\sin\theta \sim 10^{-5}$ can be obtained when parameters are such that

$$\frac{A^2}{m^2} \sim 2 \times 10^{-5} . \tag{6.16}$$

For a trilinear coupling such that $A^2 \sim 10^{-9}$ (see chapter 5), only very degenerate sneutrinos can give such a mixing angle. For a RH sneutrino of mass 100GeV, for instance, one would need a LH sneutrino of mass 100GeV + 5eV to create the right mixing angle. On the other hand, with non-degenerate sneutrinos of masses $m_- \simeq 100\text{GeV}$ and $m_+ \simeq 150\text{GeV}$, only a trilinear coupling of order $a \sim 10^{10}\text{GeV}$ would create this mixing angle. Interestingly, this shows again that for an overall trilinear coupling not proportional to the Yukawa, $a\lambda \sim 10^2\text{GeV}$, which corresponds here to $a \sim 10^{15}\text{GeV}$, then thermal equilibrium would most likely be attained.

Thus the RH sneutrino as defined in our model is a non-thermal relic, as the small interactions it possesses are too small to allow it to reach thermal equilibrium with the plasma. Natural values of the parameters create a RH sneutrino that lies very far from the mixing angle that would allow it to thermalise.

6.2 Relic density

Having settled that the RH sneutrino is non-thermal, we now turn to the calculation of its relic density, considering it is the LSP. As we have seen in chapter 3 the usual treatment (see for example [11]) assumes the dark matter candidate to be thermal and then obtains that the relic density is inversely proportional to the size of the annihilation cross-section. Here we find ourselves in a fairly different situation: our dark matter candidate being non-thermal, the annihilation processes do not decide of the relic density; rather it is the decay channels that take this role. For this reason, we start back from the Boltzmann equation and go on to solve it using numerical methods.

6.2.1 Boltzmann equation

Let us recall our comments in chapter 2 about the Boltzmann equation. The relic density of a particle species present in the early Universe is given by the Boltzmann equation in an expanding Universe [4, 109]. Consider particle 1 with a number density n which can only be changed via the interaction $1+2 \leftrightarrow 3+4$; the Boltzmann equation states that

$$
\begin{aligned}
\dot{n} + 3Hn = \quad & C \\
\equiv & \int \frac{d^3 p_1}{(2\pi)^3 2E_1} \int \frac{d^3 p_2}{(2\pi)^3 2E_2} \int \frac{d^3 p_3}{(2\pi)^3 2E_3} \int \frac{d^3 p_4}{(2\pi)^3 2E_4} \\
& \times (2\pi)^4 \, \delta^4 \, (p_1 + p_2 - p_3 - p_4) \\
& \times \left(|M_\leftarrow|^2 \, f_3 f_4 (1 \pm f_1)(1 \pm f_2) - |M_\rightarrow|^2 \, f_1 f_2 (1 \pm f_3)(1 \pm f_4) \right) (6.17)
\end{aligned}
$$

where $M_\leftarrow$ and $M_\rightarrow$ stand for the matrix element square for the processes $1+2 \leftarrow 3+4$ and $1 + 2 \rightarrow 3 + 4$, respectively, and the f_i are distribution functions. For particles in equilibrium one can use the Fermi-Dirac or Bose-Einstein distribution functions, respectively

$$
f = \frac{1}{e^{(E-\mu)/T} \pm 1} \, . \tag{6.18}
$$

The term involving the Hubble constant H takes into account the dilution of the number density coming from the Universe expansion. In the study of dark matter candidates the density parameter Ω is of more interest than the actual number density (see chapter 2). The density parameter can be expressed as

$$
\Omega \equiv \frac{\rho_{DM}/s}{\rho_{crit}/s} \, . \tag{6.19}
$$

To turn the Boltzmann equation from an equation on the number density to an equation on the density parameter, we use the yield variable Y (eg. [108])[2]. It is defined as

$$
Y \equiv \frac{n}{s} \tag{6.20}
$$

---

[2]A similar calculation was performed in [108], to which we will come back later. We use a formulation similar to the one used there to facilitate comparison (see section 6.2.3)

where $s \sim T^3$ is the total entropy density of the Universe. The density parameter can then be expressed as

$$\Omega_{DM} = \frac{m_{\tilde{\nu}_R} Y}{\rho_{crit}/s} \, , \tag{6.21}$$

where the critical density now is (see table 2.2)

$$\frac{\rho_{crit}}{s} = 3.6 h^2 \times 10^{-9} \text{GeV} \, . \tag{6.22}$$

Using that $H = -\dot{T}/T$, the Boltzmann equation can be turned into:

$$Y(T) = \int_T^{T_{max}} \frac{C}{sHT} dT \, . \tag{6.23}$$

This is the version of the Boltzmann equation that we shall use to obtain numerical results for the relic density.

6.2.2 Relic density of the RH sneutrino

The RH sneutrino is non-thermal because, as we have seen, its annihilation rate is always smaller than the rate of the expansion of the Universe. For this reason it is mainly decays and inverse decays that affect its relic density. Here 3-point decays $x \to y + \tilde{\nu}_R$, dominate largely (see sections (5.3) and (6.1); the 4-point interactions have rates only proportional to the fourth power of the Yukawa). Re-expressing the Boltzmann equation in this case, neglecting inverse decays:

$$Y(T) = \int_T^{T_{max}} \frac{\sum_i C_i}{sHT} dT \, , \tag{6.24}$$

$$C_i = \int \int \int \frac{d^3 p_x}{(2\pi)^3 2E_x} \frac{d^3 p_y}{(2\pi)^3 2E_y} \frac{d^3 p}{(2\pi)^3 2E} \\ (2\pi)^4 \delta^4 (p_x - p_y - p) |M_i|^2 (1 \pm f) (1 \pm f_y) f_x \tag{6.25}$$

For x and y we will use the Maxwell-Boltzmann approximation,

$$1 \pm f_y \simeq 1$$

$$f_x \simeq e^{-E_x/T} \, . \tag{6.26}$$

For relativistic species at equilibirum (which we will consider x and y to be for now; we will come back later to this assumption), this is straightforward and has only small quantitative effects (see [4]). For the RH sneutrino, we use

$$1 \pm f \; \simeq \; 1 \, . \tag{6.27}$$

since as a starting point we consider no RH sneutrinos to be present. Both this assumption and the neglect of inverse decays are consistent with the assumption that we start in a situation where no large amounts of RH sneutrinos exist. We will assume for now that inflation has erased any RH sneutrino relic density, much as is the case of gravitinos. We now need to rewrite the Boltzmann equation in a fashion that can more readily be integrated numerically. First, using the above approximations and integrating everything that can be integrated straightforwardly, we obtain for eq.(6.25)

$$
\begin{aligned}
C_i \; &= \; \frac{2}{(2\pi)^5} \iint \frac{d^3 p_x d^3 p}{E_x E \sqrt{|\vec{p_x} - \vec{p}|^2 + m_y^2}} \, |M_i|^2 \, f_x \\
&\quad \delta \left(E_x - E - \sqrt{|\vec{p_x} - \vec{p}|^2 + m_y^2} \right) \\
&= \; \frac{4}{(2\pi)^3} \iiint \frac{d\,(\cos\theta)\, d\,|\vec{p}|\, dE_x}{E_x E \sqrt{|\vec{p_x} - \vec{p}|^2 + m_y^2}} \, |M_i|^2 \, |\vec{p}|^2 \, |\vec{p_x}| \, f_x \\
&\quad \delta \left(E_x - E - \sqrt{|\vec{p_x} - \vec{p}|^2 + m_y^2} \right) \, .
\end{aligned}
\tag{6.28}
$$

In the first line we have integrated over p_y using the delta function over momenta; in the second line we have integrated over free angles and have changed one of the integration variables from $|\vec{p_x}|$ to E_x. What we are left to deal with now is the delta function over energies, which we should solve for either one of the integration variables and then use to integrate. Here we will integrate the $|\vec{p}|$ variable first. Let us determine the expression replacing $|\vec{p}|$ once the integral over it has been done

using the delta function over energies. $|\vec{p}|$ will be such that it respects [3]:

$$E_x - E - E_y = 0$$
$$E_x - E = E_y . \tag{6.29}$$

With a bit of algebra and using conservation of momentum, this can be rewritten as

$$p^2 \left(p_x^2 \cos^2 \theta - p_x^2 - m_x^2 \right) + p \left(cp_x \cos \theta \right) + \left(\frac{c^2}{4} - m^2 p_x^2 - m^2 m_x^2 \right) = 0 \tag{6.30}$$

where we have defined $c = m_x^2 + m^2 - m_y^2$. This allows us to solve for p as a function of p_x and $\cos\theta$:

$$p = \frac{-cp_x \cos\theta \pm \sqrt{c^2 p_x^2 \cos^2 \theta - 4 \left(\cos^2 \theta p_x^2 - p_x^2 - m_x^2 \right) \left(c^2/4 - m^2 p_x^2 - m^2 m_x^2 \right)}}{2p_x^2 \cos^2 \theta - p_x^2 - m_x^2} \tag{6.31}$$

Ensuring that the inside of the square root doesn't become negative relates the two remaining variables in the following way[4]. :

$$m_x < e_x < \frac{c}{2m}, \qquad 0 < \cos^2 \theta < 1$$

$$\frac{c}{2m} < e_x < \infty, \qquad \frac{4m^2 e_x - c^2}{4m^2 p_x^2} < \cos^2 \theta < 1 \tag{6.32}$$

where obviously $e_x^2 = p_x^2 + m_x^2$. This simply states that at very high incoming energies, the angle at which the right-handed sneutrino is emitted is focused along the line of incoming momentum.

Altogether the C_i terms are reduced to:

$$C_i = \frac{4}{(2\pi)^3} \int\int \frac{d \left(\cos\theta \right) dE_x \left| M_i \right|^2 \left| \vec{p} \right|^2 \left| \vec{p_x} \right| f_x}{E_x \sqrt{\left| \vec{p} \right|^2 + m^2} \sqrt{\left| p_x \right|^2 + \left| \vec{p} \right|^2 - 2 \left| \vec{p_x} \right| \left| \vec{p} \right| \cos\theta + m_y^2}} \tag{6.33}$$

where $|\vec{p}|$ is replaced everywhere by the expression in eq.(6.31) and p_x is related to E_x in the obvious way. With this now we are in a position to solve the Boltzmann equation for the relic density of the RH sneutrino. The channels that enter the Boltzmann equation are listed in fig. (6.2), along with their matrix element.

---

[3]In the following we will use p, p_x for $|\vec{p}|$, $|\vec{p_x}|$, as there can be no confusion that we are only dealing with 3-vectors lengths here and not 4-vectors.

[4]It is always possible for m_x to be greater than $c/2m$, in which case the first line of eq.(6.32) doesn't apply, and only the second line is relevant

$$|M|^2 = 4\lambda^2 \cos^2\theta \left(p_{\tilde{H}}p_l - m_{\tilde{H}}m_l\right) \qquad\qquad |M|^2 = \lambda^2 a^2 \cos^4\theta$$
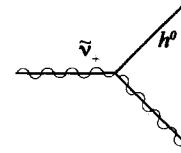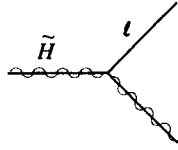
$$|M|^2 = 8g_2^2 \sin^2\theta \left(p_{\tilde{W},\tilde{B}} \cdot p_l - m_{\tilde{W},\tilde{B}}m_{\nu_l}\right) \qquad |M|^2 = \frac{2M_W^2\sin^2\theta}{v^2}\left[-\left(p_{\tilde{\nu}_R} + p_{\bar{l}}\right)\cdot\left(p_{\tilde{\nu}_R} + p_{\bar{l}}\right) \right.$$
$$\left. + \frac{1}{M_W^2}\left(p_{\tilde{\nu}_R} + p_{\bar{l}}\right)\cdot p_W \left(p_{\tilde{\nu}_R} + p_{\bar{l}}\right)\cdot p_W \right]$$
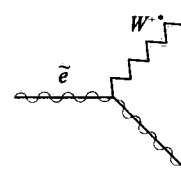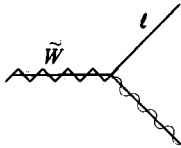
Figure 6.2: Decay channels that produce the RH sneutrino with their matrix element. In the second line we have only included one example of the channels that arise from equations (5.30) and (5.36) respectively.

6.2.3 Results of the numerical integration

We have solved eq.(6.24) with eq.(6.33) for a number of sets of parameters that respect the non-thermalisation constraints obtained in section 6.1. The results are presented in table (6.2). What we obtain is that if the RH sneutrino masses are not degenerate and/or if the trilinear coupling is not much larger than the soft scale, then the obtained relic density is much smaller than the observed dark matter density. It is possible with some degree of mass degeneracy, coupled with an increase in the trilinear coupling, to obtain a large relic density, and even overclose the Universe. This picture confirms results obtained by [108]. We should mention that [108] considered a model in which the electroweak phase transition is slowly 'turned-on', while we

a	$m_{\tilde{\nu}_L}$	$m_{\tilde{\nu}_R}$	$m_{\tilde{H}}$	$\sin\theta$	Ω_{relic}
100	150	100	1000	8.0×10^{-14}	2×10^{-2}
2000	300	1	1000	2.2×10^{-13}	3×10^{-3}
100	300	1	1000	1.1×10^{-14}	3×10^{-5}
100	100	1	1000	1.0×10^{-13}	2×10^{-4}
100	50	1	1000	4.0×10^{-13}	2×10^{-3}
100	300	100	1000	1.3×10^{-14}	3×10^{-3}
1000	300	100	1000	1.3×10^{-13}	8×10^{-1}
100	120	100	1000	2.3×10^{-13}	1×10^{-1}
300	120	100	1000	6.8×10^{-13}	1×10^{0}

Table 6.2: Various set of parameters and the relic density they generate. All masses are in GeV. We have also included the mixing angle corresponding to each set of parameters. In the first line are the parameters used to obtain the 'typical' mixing angle of section (5.2.2). The third line corresponds to the mattergenesis model that we will present in chapter 7.

have considered the transition to be completely sudden. They thus obtain slightly smaller relic densities throughout; for instance for sneutrino masses of $100, 120\text{GeV}$, they would need a trilinear coupling of 300GeV to obtain the observed dark matter density, while in our numerical simulation this set of parameters slightly overshoots this density. The same group has recently updated their numerical simulation to include additional thermal effects [110] and has obtained that they further reduce the relic density, rendering the parameter tuning necessary to obtain a sizeable relic density much finer.

We had obtained earlier that indeed the most natural case for the RH sneutrinos is to be non-thermal relics. Our conclusion concerning their relic density is not as clear-cut, although we observe that the tendency seems to be towards low relic densities; as we have just mentioned, this tendency seems to be further enhanced by the inclusion of additional thermal effects [110]. For the purpose of mattergenesis, this implies that there is a sizeable parameter space where mattergenesis remains a possibility.

6.3 Evolution after the MSSM-LSP freeze-out

We have considered up to now times when the other particles involved in creating the RH sneutrino relic density are in thermal equilibrium. They will eventually freeze-out, and since none of them is the LSP in our model, the next-to-lightest supersymmetric particle or NLSP (or *MSSM-LSP*) will also eventually decay into the RH sneutrino.

A few points need be considered in this picture. First we should verify if indeed it is the case that the particles involved remain in thermal equilibrium until the relic density of the RH sneutrino has reached its final value. We have plotted the evolution of the relic density for one of the models of table 6.2 in figure 6.3. Considering that a typical MSSM superpartner can be expected to freeze-out at around a temperature of $T \sim m/20$ (see chapter 3), then we see that indeed the simplifying approximation in the previous section (where we considered the other particles involved to be in equilibrium) is indeed valid. Thus we can also safely consider that indeed the
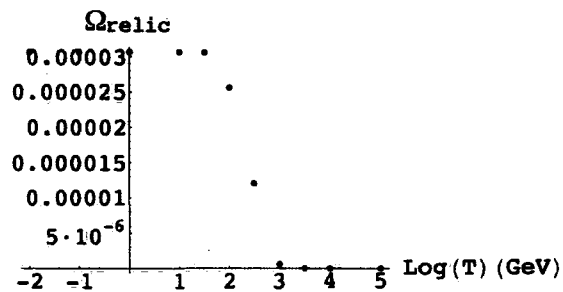
Figure 6.3: Evolution of the RH sneutrino relic density as a function of temperature (time running backwards). The parameters that have been used here are the ones in the sixth line of table 6.2. The next-to-LSP will freeze-out at around typically $m_{NLSP}/20$, at which point the RH sneutrino relic density has already reached its final value. Some time after the NLSP freeze-out the NLSP relic density will be 'dumped' into a RH sneutrino one, thus adding a 'step' to this plot (see text). This behaviour is also typical of other models in table 6.2 which yield low relic density.

additional RH sneutrino density coming from the MSSM-LSP will simply be added on top of what we have obtained in the previous section.

6.3.1   BBN constraints

Following this we need asking two more questions: when does the (out-of-equilibrium) decay of the MSSM-LSP to the RH sneutrino happens, and how much RH sneutrinos are created in this way. It turns out that these two questions are related. Let us evaluate the lifetime of a neutralino in our model; from eq.(5.30) we have that the rate for a neutral gaugino G (either a W^0 or a B^0, as they mix) to decay into a RH sneutrino and a neutrino is (see also [110])

$$\Gamma_G = \tau_G^{-1} \sim \frac{2g\sin^2\theta m_G}{32\pi} \tag{6.34}$$

where g is either g_1 or g_2 depending on the gaugino and the 32π factor is a kinematics factor. For a mixing angle of the order the Yukawa coupling the lifetime of the neutralino[5] is of the order $\tau_\chi \sim 10^2$sec. Thus the decay certainly happens long after the MSSM-LSP freeze-out which means the simple picture of the usual MSSM-LSP relic density being dumped into a RH sneutrino relic density can be used. What is more troubling however is that at this moment big-bang nucleosynthesis has already started, and thus we should make sure that we do not spoil its success. The effect of late decays on BBN is well documented in the literature [16, 111–118]. The abundances of the primordial elements as created by standard BBN could be modified by the decay products of the late decaying particle, either through the additional creation of elements or by their dissociation. Evidently if the unstable particle is in small enough number, then the effect of its late decay might be small enough not to be in conflict with standard BBN; hence in our model requiring BBN not to be modified can be effectively translated in a constraint on the relic density of the MSSM-LSP [16, 118]. Using eq.(6.34) we can see that the models we have been considering (table 6.2) generate lifetimes for the MSSM-LSP between approximately

---

[5]We remark that the coupling of the higgsino is proportional to the Yukawa coupling, eq.(5.24), and thus our order-of-magnitude estimate goes also for the higgsino part of the neutralino.

10 and 10^4sec. At these lifetimes the strongest constraint comes from the density of ^{6}Li [118]. It is evident that if we assume the MSSM-LSP to have a very small relic density compared to the observed dark matter density, then we are avoiding the BBN problem altogether. Although this is has the potential to be a fairly constraining assumption, it is the one we will make for the remainder of this work; to understand why we need go back to our previous comment on mattergenesis.

6.3.2 Small MSSM-LSP relic density

As we have mentioned many times, one of the necessary conditions for mattergenesis mechanisms to be possible is the absence of a sizeable relic density for the dark matter candidate. If we want the overall relic density to be kept small, as to allow for mattergenesis, we need for the additional RH sneutrinos coming from the decay of the out-of-equilibrium MSSM-LSP to come in small numbers. This is the one thing small Yukawas give no protection against: dumping of large amounts of RH sneutrino by the decay of a MSSM-LSP that would happen to have a relic density comparable to the observed dark matter density. More generally any mattergenesis scenario has to assess the question of MSSM-LSP dark matter, because if indeed the MSSM with R-parity is a reality, then the LSP is necessarily a source of dark matter. So, without considering BBN constraints, from a mattergenesis point of view the requirement of a small MSSM-LSP relic arises by itself. As it also happens to be one way of making the model consistent with BBN, it is the assumption we decide to take. The main differences between our study and the one suggested by [108,110] is that in [110] the goal is to obtain the correct amount of RH sneutrino dark matter directly from the relic density; for this reason they are investigating possibilities for a sizeable dumping of RH sneutrino from the MSSM-LSP, all within BBN constraints. This is the opposite goal to what we are pursuing.

In the common assumption of neutralino dark matter with a relic density corresponding to the observed dark matter one, parameter regions where the relic density is very low are considered 'forbidden' regions and are thus the focus of much less work than other parameter space regions. In such a case what we would need here is to study the MSSM parameter space regions where the MSSM-LSP has a very low

relic density, and verify whether these regions are consistent with universal SUSY-breaking, as we have been using, and whether in these regions a RH sneutrino as the overall LSP is possible. Such a study is unfortunately beyond the scope of this work. We should mention however that it has been noted previously that a neutralino with a low relic density is not ruled out, and might be natural in some regions of the parameter space [63]. Again, it remains to be verified whether these cases of small MSSM-LSP relic are compatible with our model. However such a thorough study would only be justified if in the first place a strong enough case is made for the RH sneutrino dark matter produced by mattergenesis; this is what this work is concerned with.

6.4 Direct detection prospects

We are now in a position to realistically evaluate the detection prospects of RH sneutrino dark matter through the direct detection channels mentioned in chapter 5. We have obtained in section (5.4.3) that any mixing angle smaller than $\sin \theta \sim 10^{-1}$ evades the present constraints coming from direct detection experiments, considering elastic scattering. From table (6.2) it is evident that the models we have studied lie far from the detection threshold, especially when we remember that the cross-section for an elastic scattering with the nucleus via Z-exchange depends on the fourth power of the mixing angle (eq.(5.42)). Considering a mixing angle that is twelve order of magnitudes smaller than the highest mixing angle allowed by experiment this means that we are looking at a cross-section 48 orders of magnitude smaller than the detection threshold. It is obvious as well that even if we were in a position where inelastic scattering were not suppressed (which is not the case) then even the $\sin^2 \theta$ suppression would be large enough to hide the RH sneutrino from any direct detection experiment. Definitely in the cases we have considered we are faced with a dark matter candidate that cannot be detected by direct detection experiments. A mixing angle of $\sin \theta \sim 10^{-1}$, we should also notice, creates large enough interactions to allow thermalisation of our candidate. Thus it is clear that a detectable RH position that is phenomenologically very much different from the

one we are studying here

6.5 Discussion

Let us dress an overview of what we have gathered about the RH sneutrino characteristics in the early Universe. First we have obtained that in our model it is a non-thermal relic. A departure from this result would mainly be allowed by very large (non-universal) trilinear coupling, which is a possibility we have decided to leave out of this work; some mention of this possibility has appeared in [93]. Next we have studied the relic density of this non-thermal relic, and have obtained that both large and negligible amounts can be obtained, though a small relic density is more generally obtained as it requires no tuning of the parameters. This result is seemingly enforced by the inclusion of thermal effects [110]. We have also obtained that indeed BBN adds a constraint on the model, and the means we have decided to use to avoid it is to assume a low relic density for the MSSM-LSP. This assumption also implies that if a small relic density is obtained by equilibrium decays, it is not enhanced by the out-of-equilibrium decay of the MSSM-LSP. With all this at hand we can conclude that the RN sneutrino is an interesting dark matter candidate especially within the context of mattergenesis. Adding to the study of this chapter, there are a number of open questions or additional points that it is interesting to discuss.

First, it is worth mentioning that within the MSSM, dark matter candidates with small relic density possibly exist, though they would not be most appropriate for mattergenesis. Depending on the exact mixture composing the neutralino, the obtained relic density can be small [63]. However such relics are evidently thermal; this would necessitate the use of a late-decay time of mattergenesis. In the MSSM there is in fact no candidate with weak enough interactions to be non-thermal, which in turn implies that mattergenesis might not be a possibility within the MSSM, except using a late-decay type of mechanim. Once we add a RH (s)neutrino superfield to the MSSM, we have seen that such a candidate arises and that in turn mattergenesis becomes very much a possibility. Moreover, adding this superfield does not create

the apparition of lepton-number violation, and no other, 'exotic' fields are added. If this model allows for mattergenesis, then we have a fairly minimal extension of the MSSM in which we have a tentative explanation for the ratio of matter densities. We will discuss such a possible model in the next chapter.

Let us now recall the assumptions we have made for obtaining the (small) relic density of our candidate. We have assumed that inflation has erased any amount of RH sneutrino, and in turn this has allowed us to assume that inverse decays are negligible and that indeed the distribution function is small $(1 \pm f \simeq 1$, section 6.2.2). Those assumptions evidently simplify the numerical calculations. With this we effectively obtain that the relic density in itself is not a sizeable source of RH sneutrinos and that the processes which usually affect most greatly the candidate density (annihilation and creation processes) are small. Two important notices are in order. First, it is most likely that, as is the case with the gravitino, it would be possible to erase the RH sneutrino during inflation, though it is possible that some parameters of the model might need to be constrained for this to happen. Secondly, once we are looking at adding externally (via mattergenesis) some amount of RH sneutrinos, knowing the relic density to be small and annihilation/creation processes to be inefficient means we are free to create large amounts without fearing overclosure or sizeable reprocessing. It is not impossible that the simplifying assumptions that inverse decays and the distribution function are small could need reconsidering once large amounts of dark matter are added, especially in the case of RH sneutrinos produced as coherent oscillations, which we will consider in chapter 7. This implies that some reprocessing might still happen. These questions, however, can only arise once we have determined that the relic density in itself is small, which we have just done, and once also a possible mattergenesis mechanism has been identified. The next chapter is concerned with introducing such a mechanism. A following chapter could have dealt with the questions we have just risen, but constraints of time force us to leave this to future work.

As a final remark let us discuss briefly the possibility of larger left-right sneutrino mixing. As we have seen a much larger trilinear coupling leads to potentially thermal sneutrinos. Strictly for dark matter purposes (outside mattergenesis) this can be

interesting, especially since in such a case the RH sneutrino might be detectable. The phenomenology of sneutrinos with large trilinear coupling has been studied in [93], where both the cases of Dirac and Majorana (s)neutrinos where discussed. A mattergenesis mechanism within this model has also been mentioned in [52]. Closer to our analysis would be the possibility of large left-right mixing due to mass degeneracy between left- and right-handed sneutrinos. Potentially interesting phenomenology could emerge: the RH sneutrino would be a thermal relic with a relic density very much dictated by coannihilations with the LH sneutrino, and direct detection would be conceivable, either via elastic or inelastic recoil. However the tuning of the masses necessary for this possibility appears unnaturally fine.

Chapter 7

Affleck-Dine neutrinogenesis

7.1 Leptogenesis, Neutrinogenesis and AD Mechanism

Within the context of any Dirac neutrino model such as the one we are studying here, the question of the origin of the baryon asymmetry is paramount. Indeed, as mentioned in the introduction, the popular leptogenesis scenario of [35] requires lepton-number violation. Let us review the argument. In the Standard Model the $B + L$ number is not conserved at the very high temperatures present in the early Universe [32]. At temperatures roughly higher than the electroweak phase transition temperature, $(B + L)$-violating anomalous 'sphalerons' transitions are indeed in equilibrium [18,32]. In the original leptogenesis scenario [35] (or 'Majorana leptogenesis' [38]), an added Majorana mass for the neutrinos is the source of lepton-number violation which allows for the creation of a net lepton number for the Universe (note that a similar baryon-number violation source is absent). In turn the sphalerons transfer the net lepton number into the observed baryon number of the Universe. Thus, when coupled with the see-saw mechanism, the possibility of Majorana leptogenesis offers an interesting picture for neutrinos and their link to early Universe physics.

This scenario obviously necessitates a source of lepton-number violation; indeed what it does is to transfer the problem of directly creating a net baryon number to

directly creating a net lepton number, and relating the two via sphalerons. Hence when considering Dirac neutrinos as we do here, one necessarily has to suggest an alternative to leptogenesis where it is possible to create the observed baryon number either without appealing to lepton number violation at all, or else by inventing a new source of lepton number violation[1]. As we have discussed in chapter 4, the conservation of lepton number even in the presence of neutrino masses is very much a possibility, and in that sense establishing that there exist leptogenesis models that function without lepton number violation is important. Here indeed we suggest a scenario that generates the baryon number of the Universe in the complete absence of lepton number violation.

7.1.1 Neutrinogenesis in the Standard Model and in the MSSM

A lepton-number conserving 'leptogenesis' mechanism was suggested a few years ago [3] within the SM+ Dirac neutrinos. The suggested alternative to creating a net lepton number relies on the observation that sphalerons only act on the left-handed sector of the SM, leaving the right-handed sector unaffected. Thus what really is necessary for a leptogenesis-type of mechanism is the creation of a lepton number in the left-handed sector; whether the left-handed lepton number is a net overall lepton number or whether it is compensated by an equivalent lepton number in the right-handed sector is of no importance. This distinction is however irrelevant for SM particles (and neutrinos with large Majorana masses), since left-right equilibration processes are in equilibrium for all of them in the early Universe. In [3], it was noticed that Dirac neutrinos with a Yukawa coupling λ_{SM} such that $\lambda_{SM} < 10^{-8}$ do not allow fast left-right equilibration, and indeed for pure Dirac neutrinos this condition is easily respected. This implies that if a 'left-right asymmetry' (or a net number of left-handed neutrinos compensated by an equal net number of anti-

---

[1]Although in such a case it would become fairly unnatural to have lepton number violation present somewhere in the model, yet absent in the neutrino sector.

right-handed neutrinos) can be created in the neutrino sector, then it will not be erased. Looking in the left-handed sector alone, as the sphalerons do, this would appear as a net lepton number, and then the usual course of leptogenesis would follow. The final ingredient is a way to create this asymmetry; in [3] this was done by adding to the SM a heavy Higgs-like doublet whose decay creates the asymmetry. The 'leptogenesis without lepton number violation' mechanism of [3] is sometimes referred to as *neutrinogenesis*, a term we will use in this work.
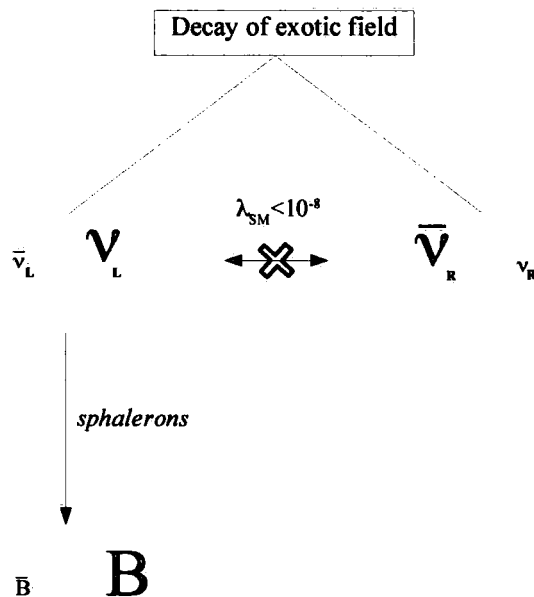
Figure 7.1: Overview of the neutrinogenesis mechanism suggested in [3]. As long as the Yukawa coupling of the Dirac neutrinos is small enough, the left- and right-handed neutrinos do not equilibrate, and thus the asymmetry created by the added field is not destroyed. The sphalerons see a net lepton number, as they are blind to the right-handed sector. As mentioned, a supersymmetrisation of this could possibly have dark matter on its right-handed side instead of right-handed neutrinos.

As we have seen in chapter 6, a Dirac RH sneutrino of the type we are study-

ing does not equilibrate with its left-handed counterpart, fulfilling the condition for neutrinogenesis to be possible[2]. It is interesting in turn to ask whether there exists a possible mechanism outside the straightforward supersymmetrisation of [3], and whether a SUSY version of [3] could allow a possibly more satisfying way of generating the left-right asymmetry than the addition of an exotic field. Specific to supersymmetric theories is the existence of flat directions, which can be used to generate net quantum numbers, as first propsed by Affleck and Dine for baryogenesis (the Affleck-Dine mechanism) [119]. This is the road we shall follow.

Let us outline the basics of the Affleck-Dine (AD) mechanism for baryogenesis. The AD mechanism makes use of the fact that supersymmetric theories such as the MSSM generally have a number of flat directions, which are directions in field space along which the supersymmetric scalar potential vanishes. When SUSY-breaking terms are added, the potential generally becomes non-zero, or as it is common to say, the flat direction is 'lifted'. Due to SUSY-breaking a minimum in the potential can develop, and can be far away from the origin, and the fields that make up the flat direction (or AD fields) can end up in such a minimum. During inflaton-matter domination and subsequently, the minimum of the potential evolves with time (for reasons that will become obvious shortly), and so do the AD fields. This evolution can lead to the AD field condensate acquiring a large quantum number; in the original work it is a baryon number, if the AD fields themselves carry a baryon charge. In the following we will use two flat directions of the MSSM+$\tilde{\nu}_R$, $\tilde{L}h_u$ and $\tilde{\nu}_R^c$, but will generate a left-right asymmetry in the sneutrino sector, in contrast to the original AD mechanism. As we go along the chapter we shall explain in more details the workings of the AD mechanism as we use it, and compare it to its more common version.

We should note that up to now we have not yet mentioned the creation of dark matter in (supersymmetric) neutrinogenesis. Indeed the creation of a large amount of RH sneutrinos will in some way come as a bonus in our suggested mechanism,

---

[2]Note that we are now talking of *s*neutrinos in the MSSM, while [3] is concerned with *n*eutrinos in the SM.

although we can see hints of such a thing happening already. Indeed in [3] the baryon number is compensated by a lepton number 'hidden' in Dirac neutrinos; once this is supersymmetrised, one can wonder about the fate of this lepton number, and whether the particles holding it 'hidden' could be related to dark matter in some way.

The rest of the chapter is as follows: first we will introduce the flat directions we shall be using, and investigate the potential that affects our chosen AD fields. Then in section 7.3 we study the dynamics of our fields and its relation to the generation of the left-right asymmetry. Finally we explain how the neutrinogenesis mechanism works as a whole, and how it can become a mattergenesis mechanism. In various places in this chapter we shall refer to the work of [120]; it is a general, non model-specific analysis of the AD mechanism with early Universe SUSY-breaking (which we will explain later).

7.2 Two flat directions of the MSSM+$\tilde{\nu}_R$: $\tilde{L}h_u$ and $\tilde{\nu}_R^c$

7.2.1 Flat directions in the MSSM

Flat directions are directions in scalar field space along which the scalar potential vanishes. Our first task is to identify flat directions in our superpotential that could be of use in generating an asymmetry in the sneutrino sector. Flat directions in the MSSM have been studied earlier [120] and [55] and a number of F- and D-flat directions have been identified[3]. Relevant to our work is the $\tilde{L}h_u$ direction, which involves the left-handed sneutrino. This direction is flat up to the contribution of the μ-term, which we have mentioned before. The μ parameter is however of the weak scale, as are the soft-breaking terms. As we will see shortly, the contribution to the scalar potential of the soft-breaking terms will play a very important part

---

[3]An F-flat (resp. D-flat) direction is a direction along which at least the F part (resp. D part) of the scalar potential vanishes.

in the mechanism. Since the μ-term contribution is at most as large as the soft-term contribution, and since we will keep track of their effects, we drop the μ term altogether, in line with the previous chapters.

As we have seen in chapter 3 the scalar potential is composed of F-terms and D-terms [55]:

$$V_S = -\sum_i \left| \frac{\partial W}{\partial \Phi_i} \right|^2 - \frac{1}{2} \sum_a g_a^2 \left(\Phi_i^* T^{a,ij} \Phi_j \right)^2 \tag{7.1}$$

where a runs over the three gauge groups and T^a are the gauge group generators. The MSSM superpotential, in terms of scalar fields, is given by [55, 56]

$$\mathcal{W}_{MSSM} = \lambda_u \tilde{u}_R^c \tilde{Q} h_u - \lambda_d \tilde{d}_R^c \tilde{Q} h_d - \lambda_e \tilde{e}_R^c \tilde{L} h_d + \mu h_d h_u \tag{7.2}$$

as we had mentioned in section 3.1.2. It is obvious from the superpotential that there exist many F-flat direction; we gain more interesting information by noticing what cannot be an F-flat direction. Notice for instance that since the LH squark, RH up squark and up-type higgs fields all appear together in one term, no two of them can be used at once to construct a flat direction, as the corresponding F-term would be non-zero. Indeed if the up-type higgs and LH squark fields are simultaneously non-zero, then

$$\frac{\partial W}{\partial \tilde{u}_R^c} \neq 0 \tag{7.3}$$

and thus the direction is not F-flat. Such a restriction does not apply to for example the up-type higgs and LH slepton both belonging to a flat direction [120]; indeed the direction $\tilde{L}h_u$, which we parametrise by

$$\tilde{L} = \frac{1}{\sqrt{2}} \begin{pmatrix} \phi \\ 0 \end{pmatrix},$$

$$h_u = \frac{1}{\sqrt{2}} \begin{pmatrix} 0 \\ \phi \end{pmatrix} \tag{7.4}$$

is F-flat in the MSSM up to the μ-term contribution[4]. Since the contracted $\tilde{L}h_u$

---

[4]We will from now on refer to $\tilde{L}h_u$ as an F-flat direction, and it is understood that this means the only contribution to F-terms is the μ-term one, or that the direction is flat when neglecting the μ-term.

forms a gauge invariant operator, then necessarily the gauge potential vanishes along this direction. Indeed flat directions are generally described by the gauge invariant operator that is formed by the contraction of the various fields that construct the flat direction[5]. $\tilde{L}h_u$ is such a gauge invariant operator and forms a flat direction by itself.

The superfield that involves the RH sneutrino is evidently absent from the MSSM. To be able to create the left-right asymmetry mentioned earlier without creating a net lepton number, we will need also the flat direction corresponding to this additional field. We turn to the effect of adding the RH sneutrino superfield in the next subsection.

7.2.2   Flat directions with added Dirac mass term for sneutrinos

In this work we are adding the RH sneutrino superfield through one term only, the Dirac mass term or Yukawa coupling; moreover we are not adding any other exotic fields. Thus we now have one additional term in the superpotential:

$$W \supset \lambda \tilde{L} h_u \tilde{\nu}_R^c \, , \tag{7.5}$$

where again we use the scalar field notation for the superpotential, as in eq.(7.2). Taken in itself we already know the right-handed (s)neutrino to be gauge invariant, and as such $\tilde{\nu}_R^c$ is a D-flat direction. The two D-flat directions we are using can thus be parameterised by

$$\tilde{L} = \frac{1}{\sqrt{2}} \begin{pmatrix} \phi \\ 0 \end{pmatrix} \, ,$$

$$h_u = \frac{1}{\sqrt{2}} \begin{pmatrix} 0 \\ \phi \end{pmatrix} \, ,$$

$$\tilde{\nu}_R^c = \tilde{\nu} \, . \tag{7.6}$$

---

[5]This means the fields that are non-zero along the direction.

As we have mentioned, in the MSSM the $\tilde{L}h_u$ flat direction is both F- and D-flat. Its D-flatness cannot be affected by the addition of the RH (s)neutrino superfield, but its F-flatness might, and indeed will. Recall that the only reason we could consider $\tilde{L}h_u$ to be an F-flat direction in the MSSM is because $\tilde{L}$ and h_u did not appear together in any term of the MSSM superpotential. Now we have added just such a term, which means that indeed $\tilde{L}h_u$ is not an F-flat direction anymore. Indeed, the F contribution of the Dirac mass term to the scalar potential along $\tilde{L}h_u$ and $\tilde{\nu}_R^c$ is:

$$\mathcal{V}_F \;=\; \left|\frac{\partial \mathcal{W}}{\partial \tilde{L}^i}\right|^2 + \left|\frac{\partial \mathcal{W}}{\partial h_u^j}\right|^2 + \left|\frac{\partial \mathcal{W}}{\partial \tilde{\nu}_R^c}\right|^2 \tag{7.7}$$

$$=\; \frac{|\lambda|^2}{4}\left|\phi^2\right|^2 + |\lambda|^2 \left|\tilde{\bar{\nu}}\phi\right|^2 \; . \tag{7.8}$$

As such our 'flat' directions are indeed not F-flat at the renormalisable level, but the F-term contribution they receive is necessarily very small as it is due solely to the (s)neutrino Yukawa coupling. Thus in our version of the AD mechanism, $\tilde{L}h_u$ and $\tilde{\nu}_R^c$ are the two 'almost flat' directions we will use.

Using 'flat' directions that are already slightly lifted at the renormalisable level is a departure from the conventional AD picture, where the flat directions are only lifted via higher-dimensional operators, or soft operators such as the SUSY-breaking soft terms. In the following we will confirm that the F-term contribution to the scalar potential along the 'flat' directions is small enough that the creation of a large asymmetry is not prevented. We note that if we were using larger Yukawas (as would be allowed in the presence of a see-saw mechanism), then the F-term contribution would become larger, eventually to the point where the chosen directions could simply not be considered flat at all, and obviously the AD mechanism would be ineffective. We shall not quantify here how large the Yukawa coupling can grow before stopping the AD mechanism, but it is worth noting that for example no flat direction of the MSSM includes both $\tilde{Q}$ and h_u (and other fields); this is because the Yukawa term for up quarks is large and thus any direction including both $\tilde{Q}$ and h_u is certainly neither flat nor 'almost flat'. Thus enlarging the neutrino Yukawa coupling to the size of other, 'typical' SM Yukawa couplings via the use of the see-saw mechanism would destroy our mechanism. As such it is a case of the smallness of the Yukawas enabling a specific baryon (and dark) matter production mechanism,

just as it was also creating the possibility of a non-thermal relic or a particle that has its left- and right-handed parts never in equilibrium.

7.2.3 Lifting of the flat directions

Despite having considered up to now only renormalisable contributions, our 'flat' directions are already lifted, but as we have mentioned it is only a very small effect, and a larger lifting is necessary if any sizeable asymmetry is to be created. Let us now include in our study the soft-breaking terms that we have listed in chapter 5, this time along the flat directions:

$$\mathcal{V}_{SB} = m_\phi^2 \, |\phi|^2 + m_\nu^2 \, \left|\bar{\tilde{\nu}}\right|^2 + (\lambda a \phi^2 \bar{\tilde{\nu}} + h.c.) \, . \tag{7.9}$$

In the early Universe, however, there exists yet another source of soft SUSY-breaking. Indeed during inflation the vacuum energy density is positive (or else inflation would simply not happen [4]). But as we have seen in the introduction, because of the way the SUSY and Hamiltonian operators are related, the presence of a positive vacuum energy necessitates and implies the spontaneous breaking of SUSY. Hence during inflation, and as long as the inflaton has not decayed, there exists 'early Universe SUSY-breaking' [58,120]. This SUSY-breaking contribution is crucial as it can create a minimum in the scalar potential far away from the origin, thus driving the AD fields out to large values during inflation. These additional SUSY-breaking terms are parameterised in terms of the (time-dependent) Hubble constant [58,120]

$$\mathcal{V}_H = -c_\phi H^2 \, |\phi|^2 - c_\nu \, \left|\bar{\tilde{\nu}}\right|^2 + (\lambda c_H H \phi^2 \bar{\tilde{\nu}} + h.c.) \, , \tag{7.10}$$

where c_ϕ, c_ν are real, order one constants. The overall potential for the scalar fields is thus

$$\begin{aligned}
\mathcal{V} &= \mathcal{V}_F + \mathcal{V}_{SB} + \mathcal{V}_H \\
&= (m_\phi^2 - c_\phi H^2) \, |\phi|^2 + (m_\nu^2 - c_\nu H^2) \, \left|\bar{\tilde{\nu}}\right|^2 + (\lambda(a + c_H H)\phi^2 \bar{\tilde{\nu}} + h.c.) \\
&\quad + \frac{|\lambda|^2}{4} \, \left|\phi^2\right|^2 + |\lambda|^2 \, \left|\bar{\tilde{\nu}}\phi\right|^2 \, .
\end{aligned} \tag{7.11}$$

A large vacuum expectation value for the AD fields can only develop if at least one of the fields' effective mass squared term is negative [120]; here we consider

$$(m_\phi^2 - c_\phi H^2) < 0 \, . \tag{7.12}$$

Thus the Hubble-induced terms in eq.(7.10) push the fields far from the origin. Moreover, because of their dependency on the Hubble 'constant' which is in turn time-dependent, the early Universe SUSY-breaking terms allow for a non-trivial evolution of the minimum in the potential. Let us see how the minimum first appears; we have to minimise[6]

$$\mathcal{V} = (m_\phi^2 - c_\phi H^2)\,|\phi|^2 + (m_\nu^2 - c_\nu H^2)\,|\tilde{\bar{\nu}}|^2 - 2\,|\lambda(a + c_H H)|\,|\phi|^2\,|\tilde{\bar{\nu}}|$$
$$+ \frac{|\lambda|^2}{4}\,|\phi^2|^2 + |\lambda|^2\,|\tilde{\bar{\nu}}\phi|^2 \ . \tag{7.13}$$

Taking the coefficient of $|\tilde{\bar{\nu}}|$ positive, and considering that for early times $|c_\nu|\,H^2 \gg m_\nu^2$ and $|c_\phi|\,H^2 \gg m_\phi^2$, the minimum of the potential is given by

$$|\phi|_{\min}(t) \simeq \sqrt{\frac{c_\phi}{2}}\frac{H(t)}{\lambda} \tag{7.14}$$

$$|\tilde{\bar{\nu}}|_{\min}(t) \simeq \begin{cases} \frac{-c_\phi}{2c_\nu - c_\phi}\frac{|a|}{|\lambda|}, & c_H H \ll |a|\,, \\ \frac{-c_\phi}{2c_\nu - c_\phi}\frac{|H(t)|}{|\lambda|}, & c_H H \gg |a|\,. \end{cases}$$

This shows that indeed the potential is minimal for large values of the AD fields, both because the Hubble constant is very large in the early Universe and the Yukawa is small throughout. This can be interestingly contrasted with the typical AD mechanism, where a very large Hubble constant is necessary for the creation of a large *vev*. Here the Yukawa coupling is also very much responsible for the large *vev*. Moreover, since the minimum evolves with the Hubble 'constant', as long as the AD fields sit in their minimum they also follow this evolution. This is a crucial aspect of the AD mechanism: if the quantum number of interest is related to the AD fields, then as these sit in the evolving minimum, this quantum number evolves as well, leading to the required baryon or lepton number with the appropriate choice of parameters. We will see in the next section that here indeed the left-right asymmetry in the lepton number of the sneutrino sector is related to our two AD fields, whose evolution we will study.

---

[6]This is exactly the same as eq.(7.11); we have only rewritten the third term using the generic result that $|c|\,e^{i\theta} + h.c. = 2\,|c|\cos\theta$, and used the minimal value for $\cos\theta$, $\cos\theta = -1$.

In the following we will take as a starting point that the fields' values lie in the minimum. In [120] two arguments are offered for this: that the fields cannot have *vev*'s much larger than the minimum or else their energy density would be larger than the inflaton energy density and prevent inflation from happening at all, and that if an AD field would start at some distance from its minimum, it would oscillate with an amplitude decreasing exponentially towards the minimum. Both arguments apply here in a straightforward fashion despite the peculiarities of our model. Moreover we will assume the fields' phases to be a constant over the Universe, but of a random value. Again, general arguments in favour of this assumption as presented in [120] apply directly here.

We have mentioned earlier that in the original AD mechanism the flat directions are lifted solely at the non-renormalisable level, which is not the case here. One known effect of the lifting at the renormalisable level is the fact that AD fields stop following the minimum closely [120]. Here the renormalisable F-term contributions are very small, but we can still expect the evolution of our AD fields not to reproduce precisely the behaviour of the original AD mechanism. In the next section we will track the evolution of the AD fields and the asymmetry in our scenario.

7.3   Dynamics of the fields and the left-right asymmetry

7.3.1   Left-right asymmetry in the sneutrino sector

What we have up to now is the hint of a non-trivial evolution of the AD fields throughout the early Universe. Before we explore this evolution, we should pause and recall that what we are looking for is a non-trivial evolution for the left-right asymmetry in the sneutrino sector, as this is what we need for neutrinogenesis. As we have chosen flat directions that involve the sneutrinos, we can expect these two quantities to be related; we make this relation explicit in this section. Let us first define the left-right asymmetry; we write the lepton number n_L as a sum of its

right-handed and left-handed parts:

$$n_L = n_L^{(L)} + n_L^{(R)} \tag{7.15}$$

with $n_L^{(L)}$ and $n_L^{(R)}$ being in terms of our scalar fields

$$\begin{aligned}
n_L^{(L)} &= \frac{i}{2}\left(\dot{\phi}^*\phi - \phi^*\dot{\phi}\right) \\
n_L^{(R)} &= -i\left(\dot{\tilde{\nu}}^*\tilde{\nu} - \tilde{\nu}^*\dot{\tilde{\nu}}\right) .
\end{aligned} \tag{7.16}$$

In these terms we can define the left-right asymmetry as

$$n_{LR} \equiv n_L^{(L)} - n_L^{(R)} . \tag{7.17}$$

Neutrinogenesis requires $n_{LR} \neq 0$. The evolution equation for the asymmetry is constructed from the ones of the AD fields. Indeed, the evolution equation for ϕ is:

$$\ddot{\phi} + 3H\dot{\phi} + \frac{\partial \mathcal{V}}{\partial \phi^*} = 0 \tag{7.18}$$

and analogously for $\tilde{\nu}$. Now using eq.(7.16) in eq.(7.18) and its conjugate, we find

$$\dot{n}_L^{(L)} + 3Hn_L^{(L)} = \mathrm{Im}\left(\frac{\partial \mathcal{V}}{\partial \phi}\phi\right), \tag{7.19}$$

and again analogously for $\tilde{\nu}$. From eq.(7.11) we see that the only imaginary terms are the a-terms and hence

$$\begin{aligned}
\dot{n}_L^{(L)} + 3Hn_L^{(L)} &= 2\mathrm{Im}\left(\lambda a\phi^2\bar{\tilde{\nu}}\right) \\
\dot{n}_L^{(R)} + 3Hn_L^{(R)} &= -2\mathrm{Im}\left(\lambda a\phi^2\bar{\tilde{\nu}}\right) .
\end{aligned} \tag{7.20}$$

From this we can deduce both the time evolution of the lepton number n_L and of the left-right asymmetry n_{LR}. As expected the lepton number is conserved throughout:

$$\dot{n}_L + 3Hn_L = \frac{d}{dt}\left(n_L^{(L)} + n_L^{(R)}\right) + 3H\left(n_L^{(L)} + n_L^{(R)}\right) = 0, \tag{7.21}$$

while the evolution of the left-right asymmetry is given by

$$\dot{n}_{LR} + 3Hn_{LR} = 4\mathrm{Im}\left(\lambda a\phi^2\bar{\tilde{\nu}}\right) . \tag{7.22}$$

We can see that the evolution is non-trivial if $|\phi| \neq 0$ and $|\tilde{\nu}| \neq 0$ and the combination of phases is not zero. This illustrates the necessity for both AD fields to

develop large expectation values, so that the driving term does not fall to zero. The requirement for the phases not to cancel is the necessity for some CP violation to be present, as is expected from the Sakharov's conditions [20].

Further insight into the creation of the net left-right asymmetry can be obtained by going back to eq.(7.16). In the more usual versions of the AD mechanism, only one flat direction is used, so let us first study the case of a quantum number, say the baryon number n_B, related to one AD field ϕ in the following way:

$$n_B = i \left(\dot{\phi}^* \phi - \phi^* \dot{\phi} \right) , \tag{7.23}$$

with

$$\phi = |\phi| \, e^{i\theta} \tag{7.24}$$

and $|\phi|, \theta \in \mathbb{R}$. This is obviously just a simplified version of our case. Let us relate the quantum number to the field parameters; we have

$$\begin{aligned} \dot{\phi} &= |\dot{\phi}| e^{i\theta} + i\dot{\theta} \, |\phi| \, e^{i\theta} \\ &= \phi \left(\frac{|\dot{\phi}|}{|\phi|} + i\dot{\theta} \right) \end{aligned} \tag{7.25}$$

so that the baryon number is

$$n_B = 2 \, |\phi|^2 \, \dot{\theta} . \tag{7.26}$$

The baryon number is thus dependent on the angular evolution of the AD field and on the (instantaneous) value of the field's *vev*. This exemplifies again the necessity for expectation values and CP violation, as mentioned earlier. Moreover it shows that a net baryon number would be created if the AD field's dynamics was that of regular oscillations.

In our scenario the left-right asymmetry is related to the two AD fields by eq.(7.16); in such a case the equivalent of eq.(7.26) is simply

$$n_{LR} = |\phi|^2 \, \dot{\theta} - 2 \, |\tilde{\nu}|^2 \, \dot{\theta}_\nu \tag{7.27}$$

where $\phi = |\phi| \, e^{i\theta}$, $\tilde{\nu} = |\tilde{\nu}| \, e^{i\theta_\nu}$, with all angles and lengths real. In the next subsection we study the time evolution of our AD fields; we shall obtain that this evolution indeed leads to regular oscillations, in turn creating a net left-right asymmetry.

7.3.2 Numerical evolution of the AD fields

We have used eq.(7.16) along with eq.(7.18) to obtain the time evolution of the AD fields numerically. The numerical evolution of the ϕ field is presented in figure 7.2. As is obvious from the figure, and as can be expected from the potential in eq.(7.11), there are different regimes of evolution for the fields, and in turn the asymmetry; the regular oscillations are obtained, but only for later times. In the following we sketch the various steps in the field evolution.
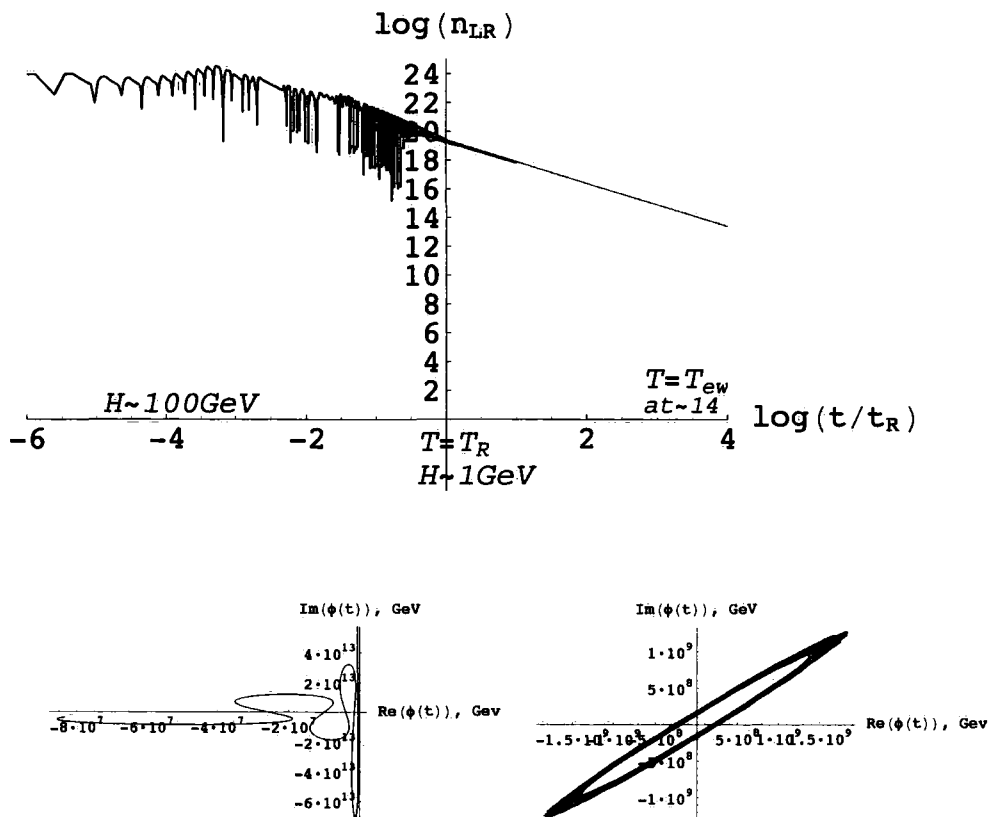
Figure 7.2: Time evolution of the generated LR asymmetry. Parameters and initial conditions are as follows: $m_\phi = 600$ GeV, $m_\nu = 500$ GeV, $a = e^{0.6i}100$ GeV, $c_\phi = 1$, $c_\nu = 0.8$, $c_H = 0$, $\lambda = 10^{-12}$, $\phi(t_{in}) = i\,|\phi|_{\min}\,(t_{in})$, $\tilde{\nu}(t_{in}) = |\tilde{\nu}|_{\min}\,(t_{in})$, $\dot{\phi} = \dot{\tilde{\nu}} = 0$, where the minima are given by the expressions in the text. The added line is matter evolution during radiation domination, $t^{-3/2}$. The behaviour of the ϕ field is also shown for early (shortly before $H \sim 100$GeV) and late (post-reheating) times.

7.3.3   Dynamical evolution of the AD fields: Hubble term domination era

As we have mentioned earlier during inflation the fields are drawn far away from the origin, and we take as a starting point that the fields lie in their minimum, with a certain phase. Exact values for each parameter are given in the legend of fig.(7.2).

Inflation is immediately followed by an era of inflaton oscillation, during which the Universe is (inflaton) matter-dominated. At this time the Hubble constant is very large, and the Hubble terms dominate the driving terms for the AD fields. During matter domination we have $H \sim 2/3t$, which in turn gives the time evolution of the minimum (eq.(7.14)). In the original AD mechanism, in the inflaton-matter era the AD fields followed the evolving minimum closely; however here it is not the case, as we will see shortly. It is clear from fig.(7.2) that indeed at this point the fields do not yet trace regular oscillations, and that the evolution of the left-right asymmetry is somewhat erratic on a short scale, yet fairly constant on larger scales. Let us try and understand the behaviour of the fields in this era. Considering the ϕ field, we recall that its evolution equation is given by

$$\ddot{\phi} + 3H\dot{\phi} + \frac{\partial \mathcal{V}}{\partial \phi^*} = 0 \tag{7.28}$$

with $\mathcal{V}$ given in eq.(7.11).

In the early times of the era we are considering, the Hubble constant is larger than the typical scale of the masses and the trilinear coupling,

$$H \gg m_\phi, m_{\tilde{\nu}_R}, a \tag{7.29}$$

so that we can approximate the potential as[7]

$$\begin{aligned}
\mathcal{V} &= -c_\phi H^2 |\phi|^2 - c_\nu H^2 |\bar{\tilde{\nu}}|^2 - 2\lambda c_H H |\phi|^2 |\bar{\tilde{\nu}}| + \frac{\lambda^2}{4} |\phi^2|^2 \\
&\quad + \lambda^2 |\bar{\tilde{\nu}}\phi|^2 ,
\end{aligned} \tag{7.30}$$

and the driving term for eq.(7.28) as

$$\frac{\partial \mathcal{V}}{\partial \phi^*} = \phi \left(-c_\phi H^2 + 2\lambda c_H H |\bar{\tilde{\nu}}| + \lambda^2 |\bar{\tilde{\nu}}|^2 \right) + \frac{\lambda^2}{2}\phi^2\phi^* . \tag{7.31}$$

---

[7]We have used our knowledge that λ is real and positive to alleviate some of the clutter.

Only the first term would be found in the usual AD mechanism; the second term translates the fact that we are using two coupled AD fields, while the third and fourth terms are due to flat direction lifting at the renormalisable level.

Let us define a new field μ that tracks the distance of ϕ to the minimum as defined in (7.14),

$$\phi = \mu \, |\phi|_{min} \, . \tag{7.32}$$

Replacing the Hubble constant by $H = 2/3t$ in both the evolution equation (7.28) and the minimum (7.14) we have the evolution equation for μ:

$$\ddot{\mu} + \frac{1}{|\phi|_{min}} \frac{\partial \mathcal{V}}{\partial \phi^*} = 0 \tag{7.33}$$

or

$$\ddot{\mu} + \mu \left(\frac{4c_\phi}{9t^2} + \frac{4\lambda c_H}{3t} |\tilde{\nu}| + \lambda^2 |\tilde{\nu}|^2 \right) + \frac{4c'^2}{18t^2}\mu^2\mu^* = 0 \, . \tag{7.34}$$

Now let us introduce a logarithmic time scale,

$$z \equiv \log t \tag{7.35}$$

which turns eq.(7.34) into

$$\ddot{\mu} - \dot{\mu} + \mu \left(\frac{4c_\phi}{9} + \frac{4\lambda c_H}{3}e^z + \lambda^2 |\tilde{\nu}|^2 e^{2z} \right) + \frac{4c'^2}{18}\mu^2\mu^* = 0 \tag{7.36}$$

where now dots stand for derivation with respect to z. With the AD field evolution equation in this form, we can see that the distance of the field to the minimum is described by an under-damped oscillator: thus the field does not follow the minimum, as would be the case in AD leptogenesis. This is in agreement with the observation of [120] that if the flat direction is lifted at the renormalisable level the field's oscillations about the minimum will not be damped[8]. To get a crude understanding of

---

[8]The under-damped oscillator solution can also be obtained from [120] if one uses $n = 3$ for the n variable that measures the level at which the flat direction is lifted. Here describing the solution as an oscillator might be a stretch due to the coupling terms, but they will not modify the damping term; as such eq.(7.36) is sufficient for the conclusions we want to draw.

the behaviour in this era, we can estimate the maximum amplitudes of the fields by assuming that the energy is constant in a co-moving volume: $R^3 H^2 \phi_{\text{max}}^2 = const$. This gives $\phi_{\text{max}} = const$ which in turn gives $n_{LR} = const$. This is good agreement with fig.(7.2).

7.3.4   Dynamical evolution of the AD fields: late times

During the matter domination era the important $H \sim m_{3/2}$ mark is reached. Below this point the Hubble induced terms in the effective potential become less and less relevant to the evolution, which instead becomes dominated by the mass terms, and the behaviour changes markedly. Going back to the evolution equation for ϕ, eq.(7.28) and neglecting the terms proportional to λ we have

$$\ddot{\phi} + 3H\dot{\phi} + \left(m_\phi^2 - c_\phi H^2\right)\phi = 0 . \tag{7.37}$$

As H drops below the mass scale and becomes more and more negligible, the evolution equation tends towards an oscillator about zero, with a damping term given by the Hubble constant: this means that at later times our AD fields *do* execute regular cycles, the behaviour required for the generation of our left-right asymmetry. This is confirmed by our numerical analysis. In this case then we can approximate the real and imaginary components of fields as $t^k \sin(m_\phi t)$. Neglecting terms in λ and writing H as $H = b/t$ we find

$$\frac{k(k-1)\sin(m_\phi t)}{t^2} + \frac{2km_\phi \cos(m_\phi t)}{t} + \frac{3bm_\phi \cos(m_\phi t)}{t} = 0, \tag{7.38}$$

and then neglecting $1/t^2$ terms we obtain $k = -3b/2$. This agrees with the constancy of energy in a comoving volume argument, which implies that $R^3 m_\phi^2 \phi_{\text{max}}^2 = const$. Again usin $H = b/t$ this then suggests

$$\phi_{\text{max}} \sim t^{-\frac{3b}{2}} . \tag{7.39}$$

We recall that the left-right asymmetry is related to the square of the AD fields and to their angular velocity (eq.(7.27)). When the fields reach the regular oscillation regime, their angle variation is a constant, thus the only variation in n_{LR} is due to the decline in the square of the AD field values; thus eq.(7.39) gives

$$n_{LR} \sim t^{-3b} . \tag{7.40}$$

In the matter domination era $b = 2/3$ so that n_{LR} drops as t^{-2}. This can be seen in fig.(7.2), at times shortly before reheating. We assume reheating happens at $T_R = 10^9$ GeV when the Hubble constant is $H \sim T_R^2/M_{Pl} \sim 1$ GeV. At that point the Universe becomes radiation dominated, and now $H = 1/2t$. In turn n_{LR} then drops as $t^{-3/2}$, which is plotted in fig.(7.2). The period immediately following $H \sim m_{3/2}$ is a transition period; as can be seen from fig.(7.2), the dynamics of the ϕ field shortly before this time is far from being regular. Thus it seems evident that the regime of regular cycles needs some time to be attained; this explains why the $n_{LR} \sim t^{-3b}$ regime is only reached some time after $H \sim m_{3/2}$, around $\log(t/t_R) \sim -2$ from our numerical simulation.

7.3.5   Size of the created asymmetry

What we finally need to determine is whether the correct amount of baryonic matter can be produced in this way. We have established that a left-right asymmetry is indeed created, but have yet to establish its order of magnitude. We need to evaluate

$$\frac{n_{LR}}{s} \sim \frac{n_\phi}{s}\Big|_{today} . \tag{7.41}$$

Since these oscillations behave like matter, their number density is constant in radiation domination (see introduction):

$$\begin{aligned}
\frac{n_\phi}{s}\Big|_{today} &= \frac{n_\phi}{s}\Big|_R \\
&= \frac{\rho_\phi}{m_\phi s}\Big|_R ,
\end{aligned} \tag{7.42}$$

where the subscript R stands for reheating time or temperature and where we have used $\rho_\phi = n_\phi m_\phi$. From our discussion of inflation in the introduction, we have that $T_R = \rho_I/s$, where the subscript I stands for the inflaton, so that in turn

$$\frac{n_\phi}{s}\Big|_{today} = \frac{\rho_\phi}{\rho_I}\Big|_R \frac{T_R}{m_\phi} . \tag{7.43}$$

The energy density stored in inflaton oscillations is

$$\rho_I \sim H^2 M_P^2 , \tag{7.44}$$

and they behave like matter. As we have seen, some time after $H \sim m_{3/2}$ the field's oscillations behave like matter as well; this means we can use the ratio of

$$\frac{\rho_\phi}{\rho_I}|_R = \frac{\rho_\phi}{\rho_I}|_{m_{3/2}} \tag{7.45}$$

where the subscript $m_{3/2}$ stands for a moment some time after $H \sim m_{3/2}$. In the case of the AD mechanism without the lifting of the flat direction at the renormalisable level, there would be no transition period after $H \sim m_{3/2}$; the fields would be oscillating from that point on, and their vev's could be automatically deduced from the minimum values. In that case eq.(7.45) could be directly related to the minimum of the fields and thus the model's parameters. Here we need to be more careful. We have shown that the AD fields do not follow their minimum closely in their early evolution. However we have also shown that the left-right asymmetry remains fairly constant on larger timescales, if one overlooks the complicated detailed evolution of the fields. Since we took as an assumption that the fields started close to their minimum, we will use the value of the minimum at $H \sim m_{3/2}$ as an approximation of the fields' vev's. From what we have just said this does not mean we assume that at $H = m_{3/2}$ the AD fields are executing regular oscillations and have a vev equal to the minimum at $H = m_{3/2}$; we are merely saying that sometime soon after $H \sim m_{3/2}$ the fields are executing regular oscillations and will have a vev of the order of the minimum at $H \sim m_{3/2}$. At this approximate moment we have that the fields are of order $\phi, \bar{\nu} \sim |a/\lambda|$ as in eq.(7.14), so that the energy density in their oscillations is of order $\rho_\phi \sim m_{3/2}^2 |a/\lambda|^2$ and behaves like matter. Hence eq.(7.45) becomes

$$\frac{\rho_\phi}{\rho_I}|_{m_{3/2}} \sim \frac{|a/\lambda|^2}{M_P^2} \tag{7.46}$$

and in turn the left-right asymmetry can be evaluated as

$$\begin{aligned}
\frac{n_{LR}}{s} &= \frac{\rho_\phi}{\rho_I}|_{m_{3/2}} \frac{T_R}{m_\phi} \\
&\sim \frac{|a/\lambda|^2}{M_P^2} \frac{T_R}{m_\phi} \\
&\sim 10^{-9} \left|\frac{a}{100\text{GeV}}\right|^2 \left|\frac{10^{-12}}{\lambda}\right|^2 \left(\frac{T_R}{1\text{TeV}}\right) \left(\frac{100\text{GeV}}{m_\phi}\right) .
\end{aligned} \tag{7.47}$$

A few comments are in order at this point. As one can notice to obtain the correct amount a reheating temperature lower than the one we used for our simulation is needed. From our discussions it is obvious that using this different reheating temperature would not alter the general behaviour of the mechanism. Moreover now is a good time to remark that, contrary to the situation in chapter 6, here the masses of the various fields are fairly unconstrained, and the only assumption we have used concerning them is that they are of order the gravitino mass, $m \sim m_{3/2}$, which is in any case one of the underlying assumptions of this work (as mentioned in chapter 3). From the various discussions of this section, it is clear that using masses different from the ones used for the numerical simulation that produced fig.(7.2) (but consistent with our general assumption on masses) would produce similar results. Moreover no assumption on which field is the LSP need be used. This is good news for the fate of our suggested mattergenesis mechanism, which we turn to in the next section.

It should be noted as well that AD neutrinogenesis (without a discussion of the possibility for creating dark matter at the same time) was proposed in ref. [121]. However in that work the AD field was considered to be an additional scalar field that was either Higgs-like, with $SU(2)$ number, or a singlet appearing in higher order non-renormalizable interactions. The implementation here using only the D-flat directions of the MSSM itself can be thought of as the minimal realisation of AD neutrinogenesis in the context of supersymmetry. Moreover some additional work related to the suggested mechanism has been published recently in [122] in which various thermal effects have been considered.

7.4 Mattergenesis mechanism

Now that we have created the left-right asymmetry we were after, there are a few steps missing before we have in hand a full mattergenesis mechanism. We have to explain how the left-right asymmetry is transferred to neutrinos, if we want to fall back on the leptogenesis mechanism of [3]; and we have to obtain the relationship between the final baryon density and the density of dark matter.
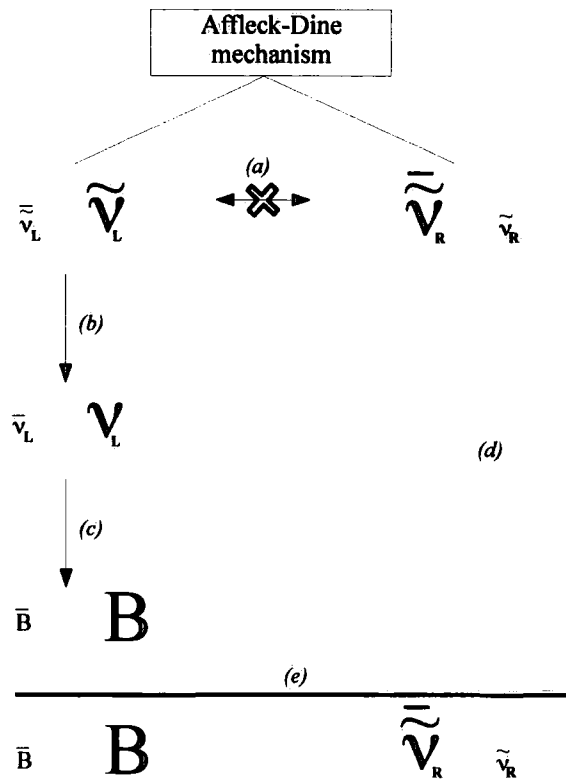
Figure 7.3: Overview of the suggested mattergenesis. The non-equilibration of left-right mixing processes (a) before the electroweak phase transition has been discussed in chapter 6. In (b) the LH sneutrinos are turned into LH neutrinos; this is in equilibrium (see text). Sphalerons turn the LH neutrinos in baryons (c), as in usual leptogenesis. On the RH side none of this happens (d), since the RH sneutrinos are out of equilibrium (see chapter 6) and sphalerons do not affect the RH sector. When the electroweak phase transition happens (e), the baryon number is frozen, and is related to the dark matter number as explained in section 7.4.

7.4.1 Left-handed sneutrinos and neutrinos

We need now to ensure that the conversion of LH sneutrinos to LH neutrinos is in equilibrium; if it is then we are back to the scenario first suggested by [3] (see fig.(7.1)). Unsurprisingly (LH (s)neutrinos being far from sterile) the LH sneutrinos are quickly turned into LH neutrinos through gaugino interactions. This can either

go by decay with $\Gamma \sim g_2^2 m_{\tilde{\nu}_R}$ or at high temperatures by a scattering whose rate is

$$\Gamma \sim \frac{g_2^4}{m_{\tilde{W},\tilde{B}}^4} T^5 \tag{7.48}$$

where the masses are understood to be thermal ones. All of the contributions are of the same order during the period we are considering when $T \sim M_W$ and so sneutrino$\leftrightarrow$neutrino conversion is in equilibrium. Then the sphaleron transitions can transfer the LH neutrino asymmetry into a baryon asymmetry as in the usual leptogenesis scenario. Above the electroweak phase transition this is essentially instantaneous (see chapter 2); after the electroweak transition the sphalerons are switched off and the non-zero baryon number is frozen in [18,19,32]. Throughout, the right-handed (s)neutrinos remain inert, as we have seen in chapter 6.

7.4.2 Baryon density and dark matter density

We need finally to establish the relation between our created baryon number and the dark matter density . The equilibrium ratio between lepton and baryon number under rapid sphaleron transitions was calculated for the SM in ref. [36] for an SM like structure and also in [123], where the same analysis was used in the MSSM, taking into account the additional Higgs. The results of these studies are that lepton and baryon numbers are related such that

$$\begin{aligned} B &= \frac{8N+4m}{22N+13m} & (B-L_e) & & T > T_{ewpt}, \\ B &= \frac{8N+4(m+2)}{24N+13(m+2)} & (B-L_e) & & T < T_{ewpt}, \end{aligned} \tag{7.49}$$

where N is the number of quark generations and m is the number of Higgs doublets. Here we have added the subscript 'e' to the lepton number, as only the lepton number attached to leptons *in equilibrium* is included in this calculation. Here the RH sneutrinos also hold a lepton number, which is given by $n_L^{(R)}$, but this lepton number is completely inert, and thus does not enter (or spoil) the results of [36,123]. As the overall $(B-L)$ number is not violated in our model, we need to have (excluding the sign, which refers to whether the number is held in sneutrinos or anti-sneutrinos)

$$n_L^{(R)} = (B-L_e) \tag{7.50}$$

and thus we have

$$
\begin{array}{llll}
B = \frac{8N+4m}{22N+13m} & n_L^{(R)} = \frac{8}{23}n_L^{(R)} & T > T_{ewpt}, \\
B = \frac{8N+4(m+2)}{24N+13(m+2)} & n_L^{(R)} = \frac{44}{137}n_L^{(R)} & T < T_{ewpt},
\end{array} \tag{7.51}
$$

where we have replaced[9] $N = 3$, $m = 2$. The correct relation between dark and baryonic matter densities would then be obtained for a RH sneutrino mass of order 1GeV:

$$
m_{DM} = \frac{8}{23}\frac{\Omega_{DM}}{\Omega_b}m_b. \tag{7.52}
$$

And thus indeed we have established a link between the amount of baryonic and dark matter present today in the Universe, by ensuring that they are both produced by a single encompassing mattergenesis mechanism. As we do not have strong constraints on the masses outside the RH sneutrino one, it is very much possible for this mattergenesis mechanism to be the main source of dark matter (see chapter 6), and as such eq.(7.52) can be used straightforwardly.

7.4.3 Discussion

An appealing aspect of this mattergenesis mechanism is the absence of exotic fields, outside the RH (s)neutrino superfield that is in any case required to generate a neutrino mass. All the ingredients necessary to produce dark and baryonic matter in this scenario are already present within the MSSM+$\tilde{\nu}_R$. Our scenario is also a simple illustration of the suggestion of [47] that dark and baryonic matter might have a single, common source, but that this primordial 'matter plasma' has been polarised in the early Universe, leading to the two apparently unrelated types of matter we observe today in the Universe. This we believe to be an interesting way to tackle the 'Ω_{DM}/Ω_b' problem mentioned in chapter 6. The absence of exotic fields also distinguishes this work from the work of [3] which first suggested leptogenesis without lepton number violation.

As mentioned what we have obtained here is a relation between the dark and baryonic number densities. We are free to adjust the ratio of mass densities by

---

[9]As there are 2 Higgs doublets in the MSSM.

choosing an appropriate mass for our dark matter candidate. An explanation of the origin of the mass of our dark matter candidate (and presumably of the other superpartners) would fully complete our mattergenesis explanation of the dark and baryonic matter densities ratio.

Lastly, it was observed before that the undetectability of a dark matter candidate produced via a mattergenesis mechanism might be generic [54], and indeed the dark matter candidate we have obtained is undetectable (see chapters 6). We in fact find ourselves in a situation where the very characteristic that makes the candidate undetectable is essential to the existence of the mechanism. Whether direct detection of dark matter is possible is still an open question, and perhaps the view that dark and baryonic matter are unrelated but both directly detectable might not hold.

Chapter 8

Discussion and conclusion

In this work we have discussed the addition to the MSSM of the right-handed neutrino as a Dirac particle, with a Yukawa coupling of order $\lambda \sim 10^{-12} - 10^{-13}$. As well as the right-handed neutrino we must include a right-handed sneutrino, which is a singlet of all gauge fields of the MSSM. We have studied its behaviour in the early Universe and have found it to be generally non-thermal and, in cases where it would be the LSP, to have a low relic density. We have also discussed its suitability as a dark matter candidate through mattergenesis mechanisms. We have presented a leptogenesis (and mattergenesis) mechanism within a lepton-number conserving model that achieves the correct baryonic density. Using an Affleck-Dine-inspired mechanism we have produced a left-right asymmetry in the sneutrino sector, which enabled the production of both baryons and dark matter without the introduction of either new fields or new mass scales.

Following this work some further avenues could be explored. As we have mentioned our suggested dark matter candidate is non-thermal, contrary to the common cold dark matter case. Structure formation within our model might thus be different from the neutralino dark matter case. Structure formation with superWIMP dark matter, or dark matter which has weaker interactions than WIMPs, has been studied in [124], where it was noticed that a better agreement with small scale structure observations might be obtained. However there the production mechanism for these superWIMPs was the late decay of a thermal WIMP after its freeze-out, and this in our model would be the equivalent of having the MSSM-LSP decay as the

main source of dark matter, contrary to our aim. It was also noticed that WIMPs produced non-thermally, either also by late decays (in [41,42]), or via the coupling with the inflaton (in [41]), could also lead to a good agreement with structure observations. So it seems very much a possibility that the non-thermal RH sneutrino, produced as we have presented, could be a dark matter candidate that respects constraints from structure formation. Studying the specific effect of an Affleck-Dine production of dark matter could prove interesting. Following this remark, we should notice that an interesting possibility would be that the RH sneutrino dark matter would have more than one source: it could have been produced in certain amounts via its coupling to the inflaton, by the suggested Affleck-Dine mechanism, and by the late decay of the MSSM-LSP. In such a case structure formation in this model would be at the cross-road of [41,42,124], possibly with an additional Affleck-Dine-specific effect. Interestingly, non-thermal (quasi-)sterile *neutrinos* produced resonantly have been shown before to allow consistent structure formation [125].

As the RH sneutrino takes the role of the LSP within our model, the MSSM-LSP would not have to respect the necessary constraints to be the dark matter, and for this reason it would not need to be the neutralino. Thus LHC phenomenology could be very much different from the neutralino-LSP case. Some aspects of LHC phenomenology with a RH sneutrino LSP and a stop MSSM-LSP [126] or a stau MSSM-LSP [127] have been recently published. In these cases the MSSM-LSP is charged and very long-lived, which would create a signature very much different from the neutralino-LSP case. The prospects for the indirect identification of the RH sneutrino LSP at the LHC thus appear to be in a much better position than the dark matter direct detection prospects. Gaining a better understanding of the sparticles mass spectrum through the LHC would also allow to better determine the relic density of the MSSM-LSP, and thus determine in turn whether its decay is a major source of RH sneutrino dark matter.

As crucial tests of supersymmetry and of the nature of neutrinos grow nearer, it is of utmost importance to keep in sight that there are indeed a variety of models that might well describe our Universe. As we have discussed here, even within supersymmetry the neutralino might not be the main dark matter candidate; the

relic density of the LSP might not have a role to play in the dark matter question; lepton number might not be violated, and the creation of a net baryon number in the Universe might well have been enabled by a very small Dirac neutrino mass. What has been said countless times before indeed appears as an appropriate conclusion for this thesis: the power of Nature to surprise us should never be underestimated.

Bibliography

[1] Steven Abel and Veronique Page. *JHEP*, 05:024, 2006. hep-ph/0601149.

[2] Veronique Page. *JHEP*, 04:021, 2007. hep-ph/0701266.

[3] K. Dick, M. Lindner, M. Ratz, and D. Wright. *Phys. Rev. Lett.*, 84:4039–4042, 2000. hep-ph/9907562.

[4] E. W. Kolb and Michael S. Turner. The early universe. Redwood City, USA: Addison-Wesley (1990) 547 p. (Frontiers in physics, 69).

[5] Sean M. Carroll. Lecture notes on general relativity. 1997. gr-qc/9712019.

[6] Sean M. Carroll. Spacetime and geometry: An introduction to general relativity. San Francisco, USA: Addison-Wesley (2004) 513 p.

[7] Gianfranco Bertone, Dan Hooper, and Joseph Silk. *Phys. Rept.*, 405:279–390, 2005. hep-ph/0404175.

[8] C. L. Bennett et al. *Astrophys. J.*, 583:1–23, 2003. astro-ph/0301158.

[9] D. N. Spergel et al. *Astrophys. J. Suppl.*, 148:175, 2003. astro-ph/0302209.

[10] D. N. Spergel et al. *Astrophys. J. Suppl.*, 170:377, 2007. astro-ph/0603449.

[11] Gerard Jungman, Marc Kamionkowski, and Kim Griest. *Phys. Rept.*, 267:195–373, 1996. hep-ph/9506380.

[12] John R. Ellis, Andrei D. Linde, and D. V. Nanopoulos. *Phys. Lett.*, B118:59, 1982.

[13] M. Yu. Khlopov and Andrei D. Linde. *Phys. Lett.*, B138:265–268, 1984.

[14] John R. Ellis, Jihn E. Kim, and D. V. Nanopoulos. *Phys. Lett.*, B145:181, 1984.

[15] G. Gamow. *Phys. Rev.*, 70:527, 1946.

[16] Masahiro Kawasaki, Kazunori Kohri, and Takeo Moroi. *Phys. Rev.*, D71:083502, 2005. astro-ph/0408426.

[17] Richard H. Cyburt, Brian D. Fields, and Keith A. Olive. *Phys. Lett.*, B567:227–234, 2003. astro-ph/0302431.

[18] A. Riotto and M. Trodden. *Ann. Rev. Nucl. Part. Sci.*, 49:35–75, 1999. hep-ph/9901362.

[19] A. G. Cohen, D. B. Kaplan, and A. E. Nelson. *Ann. Rev. Nucl. Part. Sci.*, 43:27–70, 1993. hep-ph/9302210.

[20] A. D. Sakharov. *Pisma Zh. Eksp. Teor. Fiz.*, 5:32–35, 1967.

[21] W. M. Yao et al. Review of particle physics. *J. Phys.*, G33:1–1232, 2006.

[22] J. H. Christenson, J. W. Cronin, V. L. Fitch, and R. Turlay. *Phys. Rev. Lett.*, 13:138–140, 1964.

[23] B. Aubert et al. *Phys. Rev. Lett.*, 87:091801, 2001. hep-ex/0107013.

[24] K. Abe et al. *Phys. Rev. Lett.*, 87:091802, 2001. hep-ex/0107061.

[25] C. Jarlskog. *Z. Phys*, C29:491–497, 1985.

[26] C. Jarlskog. *Phys. Rev. Lett.*, 55:1039, 1985.

[27] D. J. H. Chung et al. *Phys. Rept.*, 407:1–203, 2005. hep-ph/0312378.

[28] Mark Trodden. *Rev. Mod. Phys.*, 71:1463–1500, 1999. hep-ph/9803479.

[29] Stephen L. Adler. *Phys. Rev.*, 177:2426–2438, 1969.

[30] J. S. Bell and R. Jackiw. *Nuovo Cim.*, A60:47–61, 1969.

[31] Neil Turok. In G. L. Kane, editor, *Perspectives on Higgs physics*. 300, 1992.

[32] V.A. Kuzmin, V.A. Rubakov, and M.E. Shaposhnikov. *Phys.Lett.B*, 155(36), 1985.

[33] Marcela S. Carena, M. Quiros, and C. E. M. Wagner. *Phys.Lett.*, B380:81–91, 1996. hep-ph/9603420.

[34] Mark Trodden and Sean M. Carroll. Tasi lectures: Introduction to cosmology. 2004. astro-ph/0401547.

[35] M. Fukugita and T. Yanagida. *Phys. Lett.*, B174:45, 1986.

[36] J.A Harvey and M.S Turner. *Phys.Rev.D*, 42(10), 1990.

[37] F. Zwicky. *Helv. Phys. Acta*, 6:110–127, 1933.

[38] R. N. Mohapatra et al. *Rept. Prog. Phys.*, 70:1757–1867, 2007. hep-ph/0510213.

[39] H. Goldberg. *Phys. Rev. Lett.*, 50:1419, 1983.

[40] John R. Ellis, J. S. Hagelin, D. V. Nanopoulos, Keith A. Olive, and M. Srednicki. *Nucl. Phys.*, B238:453–476, 1984.

[41] W. B. Lin, D. H. Huang, X. Zhang, and Robert H. Brandenberger. *Phys. Rev. Lett.*, 86:954, 2001. astro-ph/0009003.

[42] Junji Hisano, Kazunori Kohri, and Mihoko M. Nojiri. *Phys. Lett.*, B505:169–176, 2001. hep-ph/0011216.

[43] S. M. Barr, R. S. Chivukula, and E. Farhi. *Phys. Lett.*, B241:387–391, 1990.

[44] S. M. Barr. *Phys. Rev.*, D44:3062–3066, 1991.

[45] D. B. Kaplan. *Phys. Rev. Lett.*, 68:741–743, 1992.

[46] S. D. Thomas. *Phys. Lett.*, B356:256–263, 1995. hep-ph/9506274.

[47] V. A. Kuzmin. *Phys. Part. Nucl.*, 29:257–265, 1998. hep-ph/9701269.

[48] Kari Enqvist and John McDonald. *Nucl. Phys.*, B538:321–350, 1999. hep-ph/9803380.

[49] A. Kusenko. 1998. Contributed to Conference on Particle Physics and the Early Universe (COSMO 98), Monterey, CA, 15-20 Nov 1998. hep-ph/9901353.

[50] G. R. Farrar and G. Zaharijas. 2004. hep-ph/0406281.

[51] R. Kitano and I. Low. *Phys. Rev.*, D71:023510, 2005. hep-ph/0411133.

[52] D. Hooper, J. March-Russell, and S. M. West. *Phys. Lett.*, B605:228–236, 2005. hep-ph/0410114.

[53] R. Kitano and I. Low. 2005. hep-ph/0503112.

[54] N. Cosme, L. Lopez Honorez, and M. H. G. Tytgat. *Phys. Rev.*, D72:043505, 2005. hep-ph/0506320.

[55] Stephen P. Martin. In Kane, G.L. (ed.): *Perspectives on supersymmetry*, 1-98, 1997. hep-ph/9709356.

[56] Manuel Drees. Lectures given at Inauguration Conference of the Asia Pacific Center for Theoretical Physics (APCTP), Seoul, Korea, 4-19 Jun 1996. hep-ph/9611409.

[57] Howard E. Haber and Gordon L. Kane. *Phys. Rept.*, 117:75, 1985.

[58] M. Dine, L. Randall, and S. Thomas. *Phys. Rev. Lett.*, 75:398–401, 1995. hep-ph/9503303.

[59] S. L. Glashow, J. Iliopoulos, and L. Maiani. *Phys. Rev.*, D2:1285–1292, 1970.

[60] P. Fayet and J. Iliopoulos. *Phys. Lett.*, B51:461–464, 1974.

[61] L. O'Raifeartaigh. *Nucl. Phys.*, B96:331, 1975.

[62] Kim Griest and David Seckel. *Phys. Rev.*, D43:3191–3203, 1991.

[63] N. Arkani-Hamed, A. Delgado, and G. F. Giudice. *Nucl. Phys.*, B741:108–130, 2006. hep-ph/0601041.

[64] M. Maltoni, T. Schwetz, M. A. Tortola, and J. W. F. Valle. *New J. Phys.*, 6:122, 2004. hep-ph/0405172.

[65] B. Kayser. in W. -M. Yao et al. Review of particle physics, J. Phys. G33:1-1232, 2006.

[66] Y. Fukuda et al. *Phys. Rev. Lett.*, 81:1562–1567, 1998. hep-ex/9807003.

[67] M. H. Ahn et al. *Phys. Rev. Lett.*, 90:041801, 2003. hep-ex/0212007.

[68] Q. R. Ahmad et al. *Phys. Rev. Lett.*, 87:071301, 2001. nucl-ex/0106015.

[69] Q. R. Ahmad et al. *Phys. Rev. Lett.*, 89:011301, 2002. nucl-ex/0204008.

[70] K. Eguchi et al. *Phys. Rev. Lett.*, 90:021802, 2003. hep-ex/0212021.

[71] T. Araki et al. *Phys. Rev. Lett.*, 94:081801, 2005. hep-ex/0406035.

[72] C. Athanassopoulos et al. *Phys. Rev. Lett.*, 77:3082–3085, 1996. nucl-ex/9605003.

[73] Andrew O. Bazarko. 1999. hep-ex/9906003.

[74] Steen Hannestad. *JCAP*, 0305:004, 2003. astro-ph/0303076.

[75] Steen Hannestad. *Eur. Phys. J.*, C33:s800–s804, 2004. hep-ph/0310220.

[76] A. Osipowicz et al. 2001. hep-ex/0109033.

[77] V. M. Lobashev et al. *Phys. Lett.*, B460:227–235, 1999.

[78] Ch. Kraus et al. *Eur. Phys. J.*, C40:447–468, 2005. hep-ex/0412056.

[79] M. Gell-Mann, M.P Ramond, and R. Slansky. In P. Van Nieuwenhuizen and D. Z. Freedman, editors, *Supergravity. Proceedings, Workshop at Stony Brook, 27-29 September 1979*. Amsterdam, Netherlands: North-holland (1979) 341p.

[80] T. Yanagida. In O. Sawada and A. Sugamoto, editors, *Proceedings of the Workshop on the Unified Theory and the Baryon Number in the Universe*. Tsukuba, Japan: Japan Natl Lab High Energy - KEK-79-18 (79,REC.JAN 80), 109p.

[81] S.L. Glashow. In M. Levy, J.-L. Basdevant, D. Speiser, J. Weyers, R. Gastmans, and M. Jacob, editors, *Proceedings of the 1979 Cargese Summer Institute on Quarks and Leptons*. Plenum Press, New York, 1980, pp. 687–713.

[82] R. N. Mohapatra and G. Senjanovic. *Phys. Rev. Lett.*, 44:912, 1980.

[83] Peter Minkowski. *Phys. Lett.*, B67:421, 1977.

[84] Raymond R. Volkas. *Prog. Part. Nucl. Phys.*, 48:161–174, 2002. hep-ph/0111326.

[85] Michel Sorel, Janet M. Conrad, and Michael Shaevitz. *Phys. Rev.*, D70:073004, 2004. hep-ph/0305255.

[86] Alessandro Strumia. *Phys. Lett.*, B539:91–101, 2002. hep-ph/0201134.

[87] Craig Aalseth et al. 2004. Part of the APS Neutrino Study. hep-ph/0412300.

[88] R. N. Mohapatra and P. B. Pal. Massive neutrinos in physics and astrophysics, third edition. *World Sci. Lect. Notes Phys.*, 72:1–451, 2004.

[89] Claudia Hagedorn and Werner Rodejohann. *JHEP*, 07:034, 2005. hep-ph/0503143.

[90] A. Yu. Smirnov. Talk given at SEESAW25: International Conference on the Seesaw Mechanism and the Neutrino Mass, Paris, France, 10-11 Jun 2004. hep-ph/0411194.

[91] Stefan Antusch, Oliver J. Eyton-Williams, and Steve F. King. *JHEP*, 08:103, 2005. hep-ph/0505140.

[92] Darwin Chang and Rabindra N. Mohapatra. *Phys. Rev. Lett.*, 58:1600, 1987.

[93] Nima Arkani-Hamed, Lawrence J. Hall, Hitoshi Murayama, David R. Smith, and Neal Weiner. *Phys. Rev.*, D64:115011, 2001. hep-ph/0006312.

[94] S. A. Abel, A. Dedes, and K. Tamvakis. *Phys. Rev.*, D71:033003, 2005. hep-ph/0402287.

[95] G. F. Giudice and A. Masiero. *Phys. Lett.*, B206:480–484, 1988.

[96] R. Bernabei et al. *Riv. Nuovo Cim.*, 26N1:1–73, 2003. astro-ph/0307403.

[97] D. S. Akerib et al. *Phys. Rev. Lett.*, 96:011302, 2006. astro-ph/0509259.

[98] Veronique Sanglard. *Nucl. Phys. Proc. Suppl.*, 173:99–103, 2007. astro-ph/0612207.

[99] G. J. Alner et al. *Astropart. Phys.*, 23:444–462, 2005.

[100] D. S. Akerib et al. *Nucl. Instrum. Meth.*, A559:390–392, 2006.

[101] D. S. Akerib et al. *Nucl. Phys. Proc. Suppl.*, 173:95–98, 2007. astro-ph/0609189.

[102] J. D. Lewin and P. F. Smith. *Astropart. Phys.*, 6:87–112, 1996.

[103] A. Bottino, F. Donato, N. Fornengo, and S. Scopel. *Astropart. Phys.*, 13:215–225, 2000. hep-ph/9909228.

[104] T. P. Cheng. *Phys. Rev.*, D38:2869, 1988.

[105] Mark W. Goodman and Edward Witten. *Phys. Rev.*, D31:3059, 1985.

[106] David R. Smith and Neal Weiner. *Phys. Rev.*, D64:043502, 2001. hep-ph/0101138.

[107] David Tucker-Smith and Neal Weiner. *Phys. Rev.*, D72:063509, 2005. hep-ph/0402065.

[108] Takehiko Asaka, Koji Ishiwata, and Takeo Moroi. *Phys. Rev.*, D73:051301, 2006. hep-ph/0512118.

[109] S. Dodelson. Modern cosmology. Amsterdam, Netherlands: Academic Pr. (2003) 440 p.

[110] Takehiko Asaka, Koji Ishiwata, and Takeo Moroi. *Phys. Rev.*, D75:065001, 2007. hep-ph/0612211.

[111] Savas Dimopoulos, Rahim Esmailzadeh, Lawrence J. Hall, and G. D. Starkman. *Nucl. Phys.*, B311:699, 1989.

[112] Savas Dimopoulos, Rahim Esmailzadeh, Lawrence J. Hall, and G. D. Starkman. *Astrophys. J.*, 330:545, 1988.

[113] John R. Ellis, G. B. Gelmini, Jorge L. Lopez, Dimitri V. Nanopoulos, and Subir Sarkar. *Nucl. Phys.*, B373:399–437, 1992.

[114] M. Kawasaki and T. Moroi. *Prog. Theor. Phys.*, 93:879–900, 1995. hep-ph/9403364.

[115] K. Jedamzik. *Phys. Rev. Lett.*, 84:3248, 2000. astro-ph/9909445.

[116] Richard H. Cyburt, John R. Ellis, Brian D. Fields, and Keith A. Olive. *Phys. Rev.*, D67:103521, 2003. astro-ph/0211258.

[117] Karsten Jedamzik. *Phys. Rev.*, D70:063524, 2004. astro-ph/0402344.

[118] Masahiro Kawasaki, Kazunori Kohri, and Takeo Moroi. *Phys. Lett.*, B625:7–12, 2005. astro-ph/0402490.

[119] Ian Affleck and Michael Dine. *Nucl. Phys.*, B249:361, 1985.

[120] M. Dine, L. Randall, and S. Thomas. *Nucl. Phys.*, B458:291–326, 1996. hep-ph/9507453.

[121] K. R. S. Balaji and R. H. Brandenberger. *Phys. Rev. Lett.*, 94:031301, 2005. hep-ph/0407090.

[122] Masato Senami and Tsutomu Takayama. *Phys. Rev.*, D75:105004, 2007. hep-ph/0701103.

[123] H. K. Dreiner and G. G. Ross. *Nucl. Phys.*, B410:188–216, 1993. hep-ph/9207221.

[124] Jose A. R. Cembranos, Jonathan L. Feng, Arvind Rajaraman, and Fumihiro Takayama. *Phys. Rev. Lett.*, 95:181301, 2005. hep-ph/0507150.

[125] Xiang-Dong Shi and George M. Fuller. *Phys. Rev. Lett.*, 82:2832–2835, 1999. astro-ph/9810076.

[126] Andre de Gouvea, Shrihari Gopalakrishna, and Werner Porod. *JHEP*, 11:050, 2006. hep-ph/0606296.

[127] Sudhir Kumar Gupta, Biswarup Mukhopadhyaya, and Santosh Kumar Rai. *Phys. Rev.*, D75:075007, 2007. hep-ph/0701063.